Inaugural dissertation

for

obtaining the doctoral degree

of the

Combined Faculty of Mathematics, Engineering and Natural Sciences

of the

Ruprecht - Karls - University

Heidelberg

Presented by

M.Sc. Klaudija Daugėlaitė

Born in: Kaunas, Lithuania

Oral examination: 11.11.2024

Regulation of hormonal stimulation and ageing
in female reproductive tract

Referees: Prof. Dr. Duncan T. Odom
Dr. Ângela Teresa Filimon Gonçalves
Prof. Dr. Ingrid Lohmann
Prof. Dr. Christof Niehrs

Zusammenfassung

In dieser Doktorandarbeit präsentiere ich vier wissenschaftliche Projekte, die ich im Laufe meiner Arbeit geleitet oder mitgeleitet habe. Jedes dieser Projekte befasst sich mit verschiedenen Aspekten der Regulation im weiblichen Reproduktionstrakt. Das erste Projekt adressiert mit entscheidende Wissenslücken im Verständnis der Interaktionen zwischen Oozyten und Granulosazellen innerhalb von Cumulus-Oozyten-Komplexen (COCs) im Kontext von Superovulation und Alterung. Hierbei habe ich entwicklungsbiologische Techniken angepasst, um präzise Vergleiche zwischen individuell verfolgten Oozyten-Granulosazell-Paaren und natürlich gealterten COCs zu ermöglichen. Zusätzlich habe ich ein prospektives Maus-IVF-Modell entworfen, um den Entwicklungsverlauf von Embryonen nicht-invasiv anhand von Granulosazelltranskriptomen vorherzusagen, wodurch die Einschränkungen retrospektiver Studien adressiert werden. Im zweiten Projekt wird die evolutionäre transkriptionelle Divergenz von Oozyten über verschiedene Mausspezien hinweg untersucht, was zu einem tieferen Verständnis der Evolution von Oozyten beiträgt – einem Forschungsgebiet, das bisher überwiegend auf männliche Gameten fokussiert war. Vorläufige Ergebnisse deuten auf differenzierte Muster transkriptioneller Divergenz zwischen den Arten hin. Im dritten Projekt habe ich experimentell zu einem größeren wissenschaftlichen Projekt beigetragen, das die Rolle von Fibroblasten bei der Bildung von Entzündungen und der Umgestaltung der extrazellulären Matrix im weiblichen Reproduktionstrakt während des Alterungsprozesses untersucht. Die Ergebnisse unterstreichen den Beitrag von Fibroblasten zur altersbedingten Fibrose und chronischen Gewebeentzündung. Schließlich beinhaltete das vierte Projekt die Sammlung umfangreicher Datensätze zur Einzelzell-RNA-Sequenzierung und räumlichen Transkriptomik bei Mäusen, um Einblicke in die Alterung des weiblichen Reproduktionstrakts nach wiederholten Hormonstimulationen zu gewinnen. Diese Datensätze wurden durch zusätzliche Experimente an Maus- und Humanproben ergänzt. Dieses Forschungsprojekt wird bedeutende Implikationen für das Verständnis der langfristigen Auswirkungen hormoneller Stimulation auf die Gesundheit des Reproduktionsgewebes und die übergeordneten Mechanismen der reproduktiven Alterung haben.

Summary

In this thesis, I present four scientific projects that I lead or co-lead during my thesis, each interrogating different aspects of regulation within the female reproductive tract. The first project addresses critical gaps in our understanding of oocyte and granulosa cell interactions within cumulus-oocyte complexes (COCs) in the context of superovulation and ageing. I adapted developmental biology techniques to enable precise comparisons between individually tracked oocyte-granulosa cell pairs and naturally aged COCs. Additionally, I designed a prospective mouse IVF model to non-invasively predict embryo development trajectory using granulosa cell transcriptomes, addressing limitations of retrospective studies. The second project explores the evolutionary transcriptional divergence of oocytes across different mouse species, contributing to our understanding of oocyte evolution - a field predominantly focused on male gametes. Preliminary results suggest nuanced patterns of transcriptional divergence among species. In the third project, I contributed experimentally to a larger scientific project that investigates of the role of fibroblasts in shaping inflammation and extracellular matrix remodelling in the female reproductive tract during ageing. The results emphasize the contribution of fibroblasts to age-related fibrosis and chronic tissue inflammation. Finally, the last project involved collecting extensive datasets of mouse single cell RNA sequencing and spatial transcriptomics data to provide insights into female reproductive tract ageing after repeated hormonal stimulations, complemented by additional experiments in mouse and human. This research project will have significant implications for understanding the long-term effects of hormonal stimulation on reproductive tissue health and the broader mechanisms of reproductive ageing.

Table of contents

Zusammenfassung 1

Summary 2

Table Of Contents 3

List Of Figures 6

List Of Tables 8

List Of Abbreviations 9

Introduction 11

1. Overview Of The Field 11
1.1. The Developmental Genomics 11
1.2. Latest Advancements Of Omics 11
1.3. Future Directions Of The Field 12
2. Mouse As A Model Organism For Developmental Genomics 13
2.1. Mouse Genetics And Evolution 13
2.2. Speciation And Reproductive Barriers 13
2.4. Mouse Comparison To Human In Developmental Genomics 15
3. Development And Function Of Female Reproductive Tract And Oocytes 16
3.1. Early Development Of Reproductive Tract 16
3.2. Function, Morphology And Histology Of Frt In Adulthood 17
3.2.1. Ovaries 17
3.2.2. Oviducts 18
3.2.3. Uterus 19
3.2.4. Cervix And Vagina 20
3.3. Ovarian Folliculogenesis And Oocyte Maturation 20
3.4. Oocyte And Granulosa Cell Bi-Directional Communication 23
3.5. Fertilization And Zygotic Genome Activation 25
3.6. Evolution Of Gametes 25
4. Ageing Of Reproductive Tissues And Oocytes 27
4.1. Reproductive Tissue Ageing 27
4.2. Oocyte Ageing 28
5. Assisted Reproductive Technologies 29
5.1. Hormonal Stimulation (Superovulation) 29
5.2. Developments Of Reproductive Technologies And Their Limitations 30

Overview Of Result Chapters 32

Chapter 1 33

Transcriptomic Insights Into Superovulation And Ageing Of COCs And Predicting Early Embryo Developmental Potential 33

1. Results 35

1.1. Transcriptomic Insights Into Superovulation And Ageing Of COC 35
1.1.1. Study Design 35
1.1.2. Superovulation Perturbs COC Gene Expression 37
1.1.3. Superovulation Deregulates Key COC Maturation Pathways 38
1.1.4. Superovulation And Ageing Induce Similar Gene Expression Changes 41
1.1.5. Transcriptional Effects Of Superovulation And Ageing Are Not Cumulative 43
1.1.6. COC Ageing Is Modestly Conserved Between Mouse And Human 45
1.2. Predicting Early Embryo Developmental Potential 46
1.2.1. Superovulation Perturbs Oocyte-Granulosa Communication 46
1.2.2. Transcription Factor Activity Disruptions After Superovulation Reveal Granulosa Cell Heterogeneity 49
1.2.3. Development Of Targeted IVF Experiment 51
1.2.4. Granulosa Cells Can Predict Early Embryo Trajectory 53
Discussion 56

Chapter 2 58

Coc Evolution In Closely Related Mice Species 58

2. Results 59

2.1. Study Design 59
2.2. Reproduction Characteristics Of Exotic Mice 59
2.3. Female Gametes Drive Reproductive Evolution 60
Discussion And Outlook 62

Chapter 3 63

Ovarian Cyclicity And Ageing Increase Inflammation In Lower Reproductive Tract Organs 63

3. Results 64

3.1. Study Design 64
3.2. Inflammatory Fibroblasts As Primary Source Of Inflammatory Niches In Ovaries And Uteri 65
3.3. Age-Related Increase In Fibroblast Inflammation 67
3.4. Both Cycling And Ageing Contribute To Fibrosis Development In FRT 67
Discussion 70

Chapter 4 71

FRT TRANSCRIPTIONAL REGULATION AND AGEING AFTER REPEATED SUPEROVULATION....71

4. Results....72

4.1. STUDY DESIGN....72
4.2. AGEING-ASSOCIATED CHANGES IN OVARIAN MORPHOLOGY AND TRANSCRIPTOME....73
4.3. MORPHOLOGY, PHYSIOLOGY AND TRANSCRIPTOMICS OF TISSUE AGEING AFTER REPEATED SUPEROVULATION....75
4.4. UNCOUPLING HORMONE DOSE AND AGE....76
DISCUSSION AND OUTLOOK....77

General Conclusions....78

Materials And Methods....79

EXPERIMENTAL METHODS....79
MICE COLONIES....79
NATURAL OVULATION AND SUPEROVULATION....80
REPEATED SUPEROVULATION....81
COC COLLECTION....81
IN VITRO FERTILISATION ASSAY....81
OOCYTE, GRANULOSA CELL AND EMBRYO SAMPLE SEQUENCING (SMART-SEQ2)....82
TOTAL RNA SEQUENCING FOR OOCYTES....82
QPCR FOR CLASSIFIER MARKER GENES IN GRANULOSA CELLS....83
VAGINAL SMEARS FOR ESTROUS CYCLE STAGING....84
SINGLE CELL RNA SEQUENCING FOR MOUSE FRT....84
VCD TREATMENT....84
FIBROSIS STAINING AND QUANTIFICATION....85
SPATIAL TRANSCRIPTOMICS FOR MOUSE FRT....85
GDNA EXTRACTION AND DNA METHYLATION MICROARRAYS FOR MOUSE OVARIES....86
BULK RNA SEQUENCING OF HUMAN GRANULOSA CELLS....86
BIOINFORMATICS METHODS (COLLABORATION)....87
QUALITY CONTROL FOR SEQUENCED SAMPLES....87
DIFFERENTIAL GENE EXPRESSION (DGE)....87
OVERREPRESENTATION ANALYSIS....87
CELL-CELL COMMUNICATION ANALYSIS....88
TRANSCRIPTION FACTOR ACTIVITY ANALYSIS....88
PATHWAY ACTIVITY SCORING....89
TRANSCRIPTIONAL HETEROGENEITY ANALYSIS....89
IVF ANALYSIS....90
EMBRYONIC PSEUDOTIME ANALYSIS....91
TOTAL RNA-SEQ ANALYSIS....91
HUMAN GRANULOSA CELL DATA ANALYSIS....92
SPATIAL TRANSCRIPTOMICS ANALYSIS....92
DATA AND CODE AVAILABILITY....93

Reference List....94

List of figures

Introduction:

Figure 1. Hormonal regulation of female reproductive tract.

Figure 2. Female reproductive tract with focus on structures in ovary and uterus.

Figure 3. Folliculogenesis and oocyte maturation.

Figure 4. Summary of chapters in this thesis.

Results Chapter 1:

Figure 1. Study design for COC isolation after superovulation and ageing.

Figure 2. Gene expression comparison between young naturally ovulated and superovulated COCs.

Figure 3. Superovulation perturbations of specific pathways involved in COC maturation.

Figure 4. Comparison of COC gene expression after superovulation and ageing.

Figure 5. Relative impacts of superovulation and ageing effects.

Figure 6. COC ageing comparison between human and mice.

Figure 7. Cell-cell communication patterns after natural ovulation and superovulation.

Figure 8. Transcription factor activity after natural and superovulation.

Figure 9. Targeted IVF assay and full embryonic dataset.

Figure 10. Embryo developmental trajectory prediction from its granulosa cells.

Results Chapter 2:

Figure 1. Oocyte and granulosa cell diversion in four closely related mice species.

Results Chapter 3:

Figure 1. Graphical representation of experimental datasets used for analyses in Chapter 3.

Figure 2. Fibroblast contribution to inflammation and ECM remodelling.

Figure 3. Ageing of FRT: fibroblast inflammation and fibrosis.

Results Chapter 4:

Figure 1. Core dataset of FRT healthy ageing and repeated superovulation.

Figure 2. Morphology and transcriptional regulation during normal ovarian ageing.

Figure 3. Schematic drawing of dose-response experiments in mice and human.

List of tables

Results Chapter 2:

Table 1. Ovulation rates and litters of four mice species.

Table 2. Number of oocytes and granulosa cells that passed quality control.

Methods:

Methods Table 1. Ovulation timing after superovulation.

Methods Table 2. Natural ovulation methodology and timing for 4 mouse species.

Methods Table 3. qPCR primer sequences.

List of abbreviations

AMH - Anti-Müllerian Hormone

APC – Antigen-Presenting Cell

ART - Assisted Reproductive Technology

cAMP - Cyclic Adenosine Monophosphate

cGMP - Cyclic Guanosine Monophosphate

CL - Corpus Luteum

CNV - Copy Number Variation

COC - Cumulus-Oocyte Complex

E2 - Estradiol

ECM - Extracellular Matrix

FSH - Follicle-Stimulating Hormone

FRT - Female Reproductive Tract

GC - Granulosa Cell(s)

GJ - Gap Junction

GnRH - Gonadotropin-Releasing Hormone

GV - Germinal Vesicle

GVBD - Germinal Vesicle Breakdown

hCG - Human Chorionic Gonadotropin

HPG - Hypothalamic-Pituitary-Gonadal (Axis)

H&E - Hematoxylin and Eosin

ICSI - Intracytoplasmic Sperm Injection

IGF-1 - Insulin-Like Growth Factor 1

IU - International Unit

IVF - In Vitro Fertilization

IVM - In Vitro Maturation

Kit - Proto-Oncogene Kit

KitL - Kit Ligand

LH - Luteinizing Hormone

LHR - Luteinizing Hormone Receptor

MAPK - Mitogen-Activated Protein Kinase

M - Months

mRNA - Messenger RNA

MZT - Maternal-Zygotic Transition

MYA - Million Years Ago

NEBD - Nuclear Envelope Breakdown

NO - Naturally Ovulated Old

NPPC - Natriuretic Peptide Precursor C

NPR2 - Natriuretic Peptide Receptor 2

NSN - Non-Surrounded Nucleolus

NY - Naturally Ovulated Young

O - Old

OC - Oocyte

OHSS - Ovarian Hyperstimulation Syndrome

ORA - Overrepresentation Analysis

PCA - Principal Component Analysis

PCG - Primordial Germ Cell

PCOS - Polycystic Ovary Syndrome

PDE3A - Phosphodiesterase 3A

PGT - Preimplantation Genetic Testing

PKB/Akt - Protein Kinase B (Signalling)

PI3K - Phosphoinositide 3-Kinase

PMSG - Pregnant Mare Serum Gonadotropin

qPCR - Quantitative Polymerase Chain Reaction

RNA - Ribonucleic Acid

ROS - Reactive Oxygen Species

RSO - Repeated Superovulation

S - Superovulated

SAC - Spindle Assembly Checkpoint

SC - Stromal Cells

scRNA-seq - Single-cell RNA Sequencing

SN - Surrounded Nucleolus

SO - Superovulated Old

SY - Superovulated Young

TGFβ - Transforming Growth Factor Beta

TF - Transcription Factor

TZP - Transzonal Projections

VCD - 4-Vinylcyclohexene Diepoxide

Y - Young

ZGA - Zygotic Genome Activation

ZP - Zona Pellucida

Introduction

1. Overview of the field

Developmental genetics is a relatively new definition for merging scientific questions and research tools of developmental biology and genetics - it was first introduced as a separate discipline after Second World War. In this section, I will discuss the short history, development and future directions of the field.

1.1. The developmental genomics

Around 1800's embryology became a discipline and focused on comparing development in vertebrate embryos. From 1860s the Darwinists were using embryology for proof of common descent (1) and, in parallel, Mendel started working on the principles of inheritance (2). In the late 19th century, the experimentalists focused mostly on physiological development excluding evolutionary questions. The anatomical and pathological focus in search of potential medical benefits persisted until the end of 1940s when developmental biology started to be in direct competition with quickly expanding field of genetics (3).

In post-war years, developmental biology changed direction, grew and diversified to include more topics from physiology to oncology, and by the 1970s was well funded in the United States. However, the evolution was not included as the subject until the birth of evo-devo at the end of 70's (4,5). At this time, reproductive biologists worked somewhat separately, reaching their success with the first live human birth from *in vitro* fertilization (IVF) in 1978 (6). In the 80s' and 90s' animals - from flies and worms to mice – became model organisms that offered flexibility for genetic engineering and contributed to many exciting discoveries (7). Since 2000s very rapidly growing fields of genetics and stem cell biology overshadowed developmental biology, ending its golden age. What we are observing now, is the renaissance of developmental biology, marked by a marvellous union of developmental questions with novel genomics technologies (8).

1.2. Latest advancements of omics

Recently, omics has overtaken most of the traditional single gene approaches (9). Omics is an umbrella term for genomics, transcriptomics, proteomics, metabolomics, epigenomics and other -omics. The term comes from the Greek word "ome", which means "all" and is used to tackle biological questions via large-scale data collection and analysis, taking a systems biology approach to study biological questions from a global perspective. Attempts to better understand dynamic processes gave rise to

temporal, including single cell RNA sequencing (scRNA-seq) and spatial -omics, where collected data extends across species, timescales and morphology (10,11). Omics provide high-throughput methods for data generation that contribute to an integrated understanding of complex biological processes and physiology, including disease marker discovery and better understanding the responses to treatment.

The challenge of such data is the need for sophisticated bioinformatics tools and computational power to integrate and analyse large datasets. Current large bioinformatics developments include cell-cell communication tools for single-cell transcriptomics (over 30 new methods since 2019), cell segmentation and automated tissue structure recognition for spatial transcriptomics. AI-driven, especially machine learning, methods are rapidly gaining popularity (12,13).

1.3. Future directions of the field

In the context of this thesis, the more efficient embryo selection and innovation in assisted reproductive technologies will redefine the best practices in reproductive medicine (7) to satisfy the demand for faster, cheaper and more efficient procedures, including improved outcomes for older IVF patients. In the ageing society, it is important to better understand basic molecular mechanisms that act in adult female reproductive tract to design better health management strategies and continuously improve life quality in advanced age (3).

From a different perspective, it is intriguing to ask the basic questions about the evolution of reproductive cells using comparative genomics. In the light of warming environment, it is imperative to know more about how gametes evolve in closely related species that live in different environmental conditions.

More generally, developmental biology did not have a technological breakthrough, such as in -omics or stem-cell research until the creation of synthetic embryos and their *ex-utero* culture system (14) which may lead to a new direction in this field. The spatial omics technologies will stay attractive over coming years and many other genomics technologies will arise. The societal demand for more research on women's health is now pressuring to revise how developmental biology and reproductive medicine should be funded, which will likely lead to a sharp increase in future funding (15).

2. Mouse as a model organism for developmental genomics

Studying human development is ethically and practically difficult, accentuating the need for a comparable and pragmatic alternative. It comes to no surprise that mouse is an attractive model organism for developmental genomics. It offers very well studied development and reproduction, intact hormonal system and accessible developmental and genetic tools, all within mammalian context with similar interindividual genetic backgrounds.

2.1. Mouse genetics and evolution

Mouse is one of the most studied model organisms in biology, especially in genetics, development and reproduction. First high-quality mouse genome was assembled in 2002 (16). Mouse has 20 chromosomes, containing ~48 000 genes (17). The mouse reference genome is based on the common mouse (*Mus musculus)*, however, other inbred mice strains and wild-derived inbred species have a varying number of Single Nucleotide Polymorphisms (SNPs) (18). Most of the wild-derived strains are largely subspecies of wild mice trapped in various locations, where origin of *Mus musculus castaneus* is from Southeast Asia, *Mus spretus* from Mediterranean basin, and *Mus caroli* from a trapped mouse in Thailand. These species share a proportion of orthologous genes that have evolved from a common ancestor through speciation and retain the same function in different species (see section 2.2.). Wild-derived inbred mice are a valuable tool for evolutionary developmental biology, especially for studying how gene expression in reproductive cells or organs evolved. Changes in non-coding regulatory elements are important in driving the evolution of gene expression through *cis* and *trans* regulatory mechanisms. *Cis* effects are mechanisms that affect gene expression only on the same chromosomal allele, while *trans* effects act equally on both alleles. An example of *trans* effect would be transcription factors (TFs) (19). In mice, most changes in gene expression arise from a combination of *cis* and *trans* effects (20).

2.2. Speciation and reproductive barriers

Speciation is an evolution of reproductive barriers, leading to reproductive isolation and formation of new species. The reproductive system and gametes thus play a central role in determining reproductive permissiveness and fitness. Though most instinctive and basic reproductive barrier is behavioural, the post-mating reproductive isolation through gamete genetic incompatibility seems pose the largest barrier. The biological knowledge of cell biology of reproductive incompatibility is limited (21). A study of Dr. Lydia Wooldridge in Jackson Laboratory will explore specific molecular mechanisms in more detail (not published yet). This genetic incompatibility between

two species creates reproductive isolation and overrides attempts to create hybrids (22). For example, mice chimeras can be created only post-fertilization, if the embryos are fused together (23). Membrane surface proteins play an important role in oocyte-sperm recognition to guard species-specificity (24). In oocytes, meiosis is a straightforward target for establishing such genetic incompatibility, as recently shown in *Mus musculus domesticus* and *Mus spretus* hybrids (25). Other post-mating reproductive barriers include female reproductive tract (FRT) environment and its bilateral interaction with seminal proteins (26–28), sperm capacitation capacity in FRT (29,30), incompatibility of oocyte surface proteins (24), among other molecular mechanisms.

2.3. Mouse reproduction and hormonal regulation

The female reproductive cycle is a set of recurrent physiological changes, known as estrous cycle in rodents or menstrual cycle in human. The 4-5-day estrous cycle in rodents is comprised of 4 prominent phases: proestrus, estrus, metestrus and diestrus (31,32). In human, menstrual cycle is divided into proliferative, secretory, and menstrual phases. In estrus and at the end of proliferative phase, the pre-ovulatory luteinizing hormone (LH) surge induces the ovulation, a release of oocytes into the reproductive tract (33) (Figure 1A). The cycle is controlled by negative feedback loop in hypothalamic-pituitary-gonadal axis (HPG axis). The gonadotropin releasing hormone (GnRH) produced in the hypothalamus stimulate gonadotrophs in the anterior pituitary gland that release follicle stimulating hormone (FSH) and LH. The FSH stimulates the growth and maturation of ovarian follicles until pre-ovulatory stage. The LH stimulates the secretion of estrogen and progesterone in the ovary that successively inhibits the secretion of GnRH (34) (Figure 1B).

The gestation period of standard laboratory mouse is 19-21 days. A few days after birth female mice reach puberty, which is marked by vaginal opening. Mice should reach the sexual maturity by the age of 6-8 weeks but should be used in fertility studies around 10-16 weeks of age, when they have completed sexual maturation (35). Mice are non-seasonal breeders, meaning that the ovulation does not need to be induced. Reproductive behaviour depends on estrous cycle phase and mating usually takes place during the dark light cycle (at night). In mice, the circadian rhythm regulated by light-dark cycle is particularly important for successful reproductive function (36).

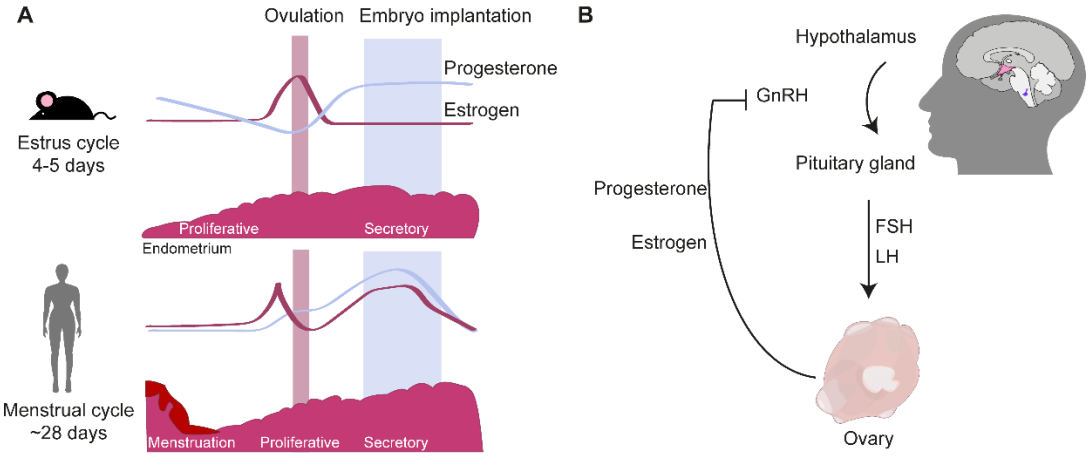

Figure 1. Hormonal regulation of female reproductive tract.

(A) Comparison of reproductive cyclicity events in mouse and human, showing hormonal peaks at ovulation and implantation. (B) The hypothalamic-pituitary-gonadal (HPG) axis feedback loop between the brain and the ovaries.

2.4. Mouse comparison to human in developmental genomics

Around 90% of mouse genome shares conserved regions with human (17). Mice and human protein-coding genes are direct orthologs in ~16 000 protein-coding genes that are the main focus of transcriptomic studies (17). Generally, average gene expression levels correlate well, meaning highly expressed genes in humans are generally highly expressed in mice too. Also, even if the sequence of regulatory regions diverge, gene expression stays largely conserved between mice and human. It could be that compensatory mechanisms are in place, for example, a TF could activate the same gene in both species without binding to exactly the same regulatory sequence (17).

However, while human and mouse share many fundamental biological processes and genetic components, significant divergences exist, including distinct phenotypes, genetic variation and tissue-specific transcriptomic regulation (37). Importantly, most of basic sex hormone regulation is shared between rodents and human (38). Gametes are also morphologically very similar, with some timing differences during early embryo development. Reproductive organ development sometimes is similar (e.g. oviduct), or can lead to different morphologies, for example, single uterus in humans and duplex uteri in mice (38). The reproductive cycle dynamics are comparable with specific differences, for example, humans attained decidualization of endometrium and menstruation within each cycle and mice did not (decidualization must be induced). Age-comparison between mouse and human has been proposed to be non-linear, especially after reproductive senescence (39), but mice spend similar duration of lifespan in ‘oopause’ compared to humans (40). In addition, they have comparable total number of reproductive cycles per lifetime.

Overall, it is important to consider these diverging features when comparing data from mice and human.

3. Development and function of female reproductive tract and oocytes

Female reproductive tract (FRT) consists of five organs: ovary, oviduct, uterus, cervix and vagina. They vary in function, morphology, and regulation during development and adult life. This section explores the development and main molecular mechanisms in these organs, with particular focus on the ovary and oocytes. It will also take you through a voyage to oocyte's maturation - folliculogenesis. Embedded into ovarian follicles, oocyte undergoes nuclear and cytoplasmic maturation, which are highly coordinated events, crucial for successful fertilization and embryo development.

3.1. Early development of reproductive tract

In mammals, gonadal development undergoes two distinct phases. The first phase involves the formation of bipotential gonad, known as the genital ridge, on the surface of the mesonephros (derived from intermediate mesoderm). The second phase is the formation of either testis or ovaries, depending on sex-determining region Y (*Sry*) gene expression.

The genital ridge is composed of primordial germ cells (PGCs) and somatic precursor cells that can adopt either testis or ovary fate (41). In mice, germ cell precursors segregate from somatic lineages in the primitive streak around embryonic day 7.25 (E7.25) and migrate to the genital ridge around E10.5 (41). In the female (XX) embryos, supporting cells differentiate into pre-granulosa cells, which arise from two different waves (42,43). The first wave pre-granulosa cells are located in the medulla and express *Runx1* in comparison to XY gonads and at E12 start expressing *Foxl2*. The second wave pre-granulosa cells start forming at E12.5 from ovarian surface epithelium cells marked by *Lgr5* expression. After birth, *Lgr5* expression is lost and second wave pre-granulosa cells start expressing *Foxl2* (44). PGCs proliferate and at E13.5 reach ~25 000 population. At this stage, they arrest the meiosis at the prophase I (45,46). The final ovary development is achieved postnatally when primordial follicles are formed from single oocytes and theca cells are recruited from ovarian stroma and the mesonephros to surround the larger follicles (47).

Both male and female duct systems originate from mesonephros. Precursors to the female system, the Müllerian ducts, form through invagination of a tube from the mesonephric surface epithelium, and run parallel to the precursors to the male system, Wolffian ducts, in embryos of both sexes (41). In the absence of testosterone, Wolffian ducts regress under exposure to anti-Müllerian hormone (AMH) and the Müllerian ducts develop into the oviduct, uterus, and upper part of the vagina (48).

3.2. Function, morphology and histology of FRT in adulthood

Female reproductive organs facilitate various stages of reproduction, from the production and release of oocytes to the development of a fertilized oocyte into an embryo, implantation and birth. Female reproductive tract can be divided into upper (ovaries and oviducts) and lower (uterus, cervix, vagina) (Figure 2A). Each organ has a unique function and cellular composition.

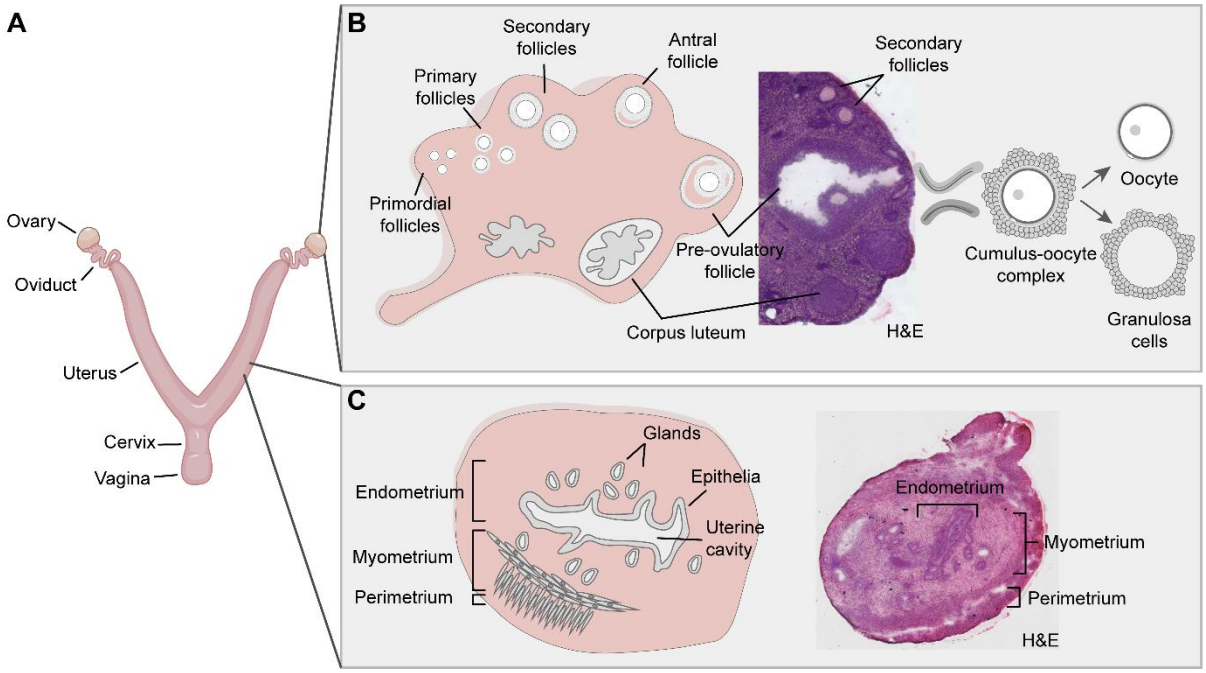

Figure 2. Female reproductive tract with focus on structures in ovary and uterus.

(A) Mouse female reproductive tract, consisting of ovary, oviduct, uterus, cervix and vagina. (B) Ovarian cross-section in schematic drawing and H&E staining. After ovulation, cumulus-oocyte complexes are expelled from the ovary. (C) Uterine cross-section in schematic drawing and H&E staining. H&E stainings were generated during spatial transcriptomics experiments.

3.2.1. Ovaries

Ovaries are paired organs that produce oocytes and hormones, including estrogen and progesterone. Oogenesis occurs in the embryo as described in the section above, and constitutes a finite pool of primordial oocytes, called the ovarian reserve. Once primordial follicles are activated, oocytes and granulosa cells form follicles that go through distinct developmental stages, called folliculogenesis (see section 3.3.). Folliculogenesis is not only cyclic but also non-synchronized. Many follicles can grow, degenerate or ovulate at the same time. Rodents are multiparous species; hence, many oocytes can be released into FRT at the same time. The ovulation rate, that is, how many oocytes will be released is genetically determined and depends on the

species (49,50). Humans usually have singleton births, meaning that their ovulation is more controlled. Several waves of follicles are recruited for folliculogenesis in each cycle, however, only one dominant follicle is destined for ovulation. The precise mechanisms of how dominant follicle becomes most competitive are not fully understood, but it's growth is associated with intra-follicular regulation of estradiol-17β (estradiol, E2) and estrogen production, greater gonadotrophin responsiveness as well as increased paracrine signalling (51).

Besides the oocyte, other major cell types in ovaries are granulosa, theca, luteal, epithelial cells, immune cells and fibroblasts.

Two transcriptomically different granulosa cell types are mural and cumulus granulosa cells (52), where mural granulosa cells outline the follicles and cumulus surround the oocytes. Cumulus cells appear only after antrum formation and serve as a first contact with the environment through bi-directional communication, passing nutrients, autocrine and paracrine signals and small molecules (see section 3.3.). Mural granulosa cells convert androgens through aromatase to produce E2, and also produces inhibin B which is important for steroid production in response to gonadotropin stimulation (53). In turn, theca cells surround the growing follicles and produce androgens in response to LH, which will be used by granulosa cells to produce estradiol (54). E2 and inhibin then reduce the FSH secretion to suppress further follicle growth. In parallel, the granulosa cells of the dominant follicle acquire LH receptors and follicle becomes dependant on the LH. Ovulation is then triggered by the LH surge (55).

After ovulation, residual granulosa cells undergo luteinisation to transform into luteal cells to form endocrine structure called corpus luteum (CL) (Figure 2B). It is the largest hormone-producing structure in the ovary, responsible for the main progesterone production, but in case of pregnancy also produces prolactin. It is degraded in following reproductive cycles if fertilization does not occur. Macrophages accumulate around CL, regulate its development and play a role in sustaining CL for successful implantation (56).

Together, these folliculogenesis events shape ovarian morphology into a heterogenous landscape that changes depending on estrous/menstrual cycle. In addition to follicles, ovarian stroma consists of stromal cells, fibroblasts and blood vessels. The outer layer of single epithelial cells makes up ovarian surface epithelium to outline the ovaries. The surface epithelia is considered as a potential ovarian cancer initiation place (see section 3.2.2.).

3.2.2. Oviducts

Oviducts in mice, or fallopian tubes in human, are thin tubes that connect the ovaries to the uterus and have four morphologically distinct segments: infundibulum, ampulla, isthmus, and uterotubal junction (ovary towards uterus) (57). Main function of oviducts

is to transport oocytes from the ovaries to the uterus, and to facilitate fertilization by providing nutrients to the oocytes, embryos and accommodating sperm.

Infundibulum have fimbriae that pick up the ovulated COCs to transport them into ampulla. Interestingly, there is a constant forward-and-back movement of COC clump in the ampulla and the amount of cumulus granulosa surrounding the oocyte reduce once oocytes move to lower ampulla (58). Fertilization takes place in the ampulla and the embryos are then pushed through isthmus and uterotubal junction until uterus.

Ciliated and non-ciliated epithelial cells outline the oviduct. Ciliated cells facilitate the movement of the oocyte or embryo from the ovary toward the uterus through rhythmic beating. Tubulin and acetylated alpha-tubulin can be used as markers to highlight cilia, for example, *Foxj1* may show differentiated ciliated cells. Non-ciliated cells are secretory cells that secrete glycoproteins and fluids to provide nourishment and protection to the oocyte or embryo. *Pax2*, *Pax8*, *Ovgp1*, *Muc1* can be used as gene expression markers for identifying non-ciliated cells (57,59,60), however, the *Ovgp1* is the only truly organ-specific marker.

Oviduct is a stipulated place for ovarian cancer initiation. There are two running hypotheses of how ovarian cancer arises (61). First concerns the epithelial origin of ovarian cancer, stating that the area at the oviduct-ovary transition is vulnerable to malignant transformation. Second defines oviduct as an origin of malignancy. Briefly, during ovulation, secretory epithelial cells from the fimbriae in the oviduct implant on the denuded surface of the ovary, resulting in the formation of inclusion cysts that become transformed in the ovarian microenvironment. It is, however, not understood how exactly the ovary is colonized by oviduct cells and when it happens.

3.2.3. Uterus

Uterus is a muscular organ, essential for female reproductive health, embryo implantation, development and birth. Uterus is composed of three distinct layers: the endometrium, myometrium, and perimetrium (Figure 2C).

Endometrium is the inner surface of the uterus, formed from epithelial cells, and is the place for implantation. Just underneath, stromal cells provide structural support for implantation and respond to hormonal changes. Between the stromal cells, glandular cells are interspersed and secrete glycoproteins, lipids, and enzymes into the uterine cavity. Immune cells regulate the remodelling of endometrium during reproductive cycle stages and participate in defence against infections. Smooth muscle cells form myometrium or uterine wall, which is necessary for contractions during menstruation and labour. The outermost layer, the perimetrium, is a serous membrane that provides a protective cover and reduces friction with surrounding pelvic organs (62).

When embryo attaches to the luminal epithelium, stromal cells differentiate and endothelial cells proliferate as part of a process known as decidualization.

Decidualization is dependent on steroid hormones, and it has been shown that stromal cells participate in local *de novo* synthesis of estrogen (63).

The structure of uterus is different between humans and rodents. Mice have bicornuate uteri (two-horned) where fertilized embryos can implant in both horns at multiple implantation sites, but humans have a pyriform uterus that usually accommodates 1-2 embryos. The myometrium muscle layers are clearly defined in mice but in human they are mixed (64).

3.2.4. Cervix and vagina

Cervix is a narrow lower part of the uterus that connects it to the vagina, that can be divided into endocervix and the ectocervix. The endocervix is lined with a single layer of mucus-producing columnar epithelial cells that form the endocervical glands, contributing to the prevention of ascending infections by microbial pathogens. Cervical mucus is also important for sperm penetrance, which depends mucus microstructure (65). The ectocervix is covered by stratified squamous epithelium, which is more resilient to physical stress and microbial exposure. The transformation zone, where the columnar epithelium of the endocervix transitions to the squamous epithelium of the ectocervix, is a critical area for the development of cervical pathologies (66). The underlying stroma of the cervix is composed of dense connective tissue with a substantial amount of collagen and elastic fibres, providing structural support. This region also contains smooth muscle fibres, blood vessels, and immune cells, which play roles in cervical function and response to injury or infection. Antigen-presenting cells (APCs), mononuclear cells and macrophages make up the most of immune populations in cervix (67).

The vagina is a fibromuscular tube that connects the cervix to the external genitals. The stratified squamous epithelium that outlines the vagina provides protection against friction and microbial infections. Beneath the epithelium lies the lamina propria, a connective tissue layer rich in elastic fibres, blood vessels, and immune cells, predominantly CD8+ T cells, but also macrophages, and dendritic cells, and others (67). The immune cells play crucial roles in maintaining mucosal immunity and protecting against infections. The muscular layer consists of smooth muscle fibres arranged in circular and longitudinal layers, which contribute to the vagina's elasticity and ability to stretch during intercourse and childbirth.

3.3. Ovarian folliculogenesis and oocyte maturation

In the adult ovary, the pool of non-growing primordial follicles, arrested at prophase I, make up the ovarian reserve which is going to be used in a cyclic manner throughout life. Oocyte maturation is a complex process, which occurs concomitantly with the

development of ovarian follicles. The ovarian follicles undergo distinct stages of development: primordial, primary, secondary, antral, and pre-ovulatory. The primordial to secondary phases is often re-grouped into pre-antral phase of folliculogenesis and the factors regulating it are still largely unknown.

Primordial follicles are around 40μm in diameter and contain diplotene oocytes surrounded by flat, single layer of granulosa cells (Figure 2B). They stay dormant until primordial follicular activation (68). The precise mechanisms triggering the activation of primordial follicles and how hormones are involved in primordial follicle activation remain elusive. Several pathways that are known to regulate the activation of primordial follicles are PI3K–Akt–FOXO3 and mTOR signalling pathways, including *Foxl2*, *Nobox*, *Gdf-9*, *Bmp4*, *Bmp7*, *Amh* and others (69).

Once the follicle is committed, the developmental trajectory is unidirectional and irreversible. After activation, its granulosa cells transform into a cuboidal layer, differentiate and start expressing FSH receptor, the oocyte starts growing and actively transcribing ribonucleic acid (RNA). This primary follicle now measures around 100μm. Recent study from Richard et al. (70) challenges the idea that primary follicles develop at a constant rate and shows that there are limited and accelerated growth rates instead.

The secondary follicle growths further to reach around 200μm diameter, with multiplying layers of granulosa cells (Figure 2B). There is much confusion about whether FSH is involved in pre-antral follicle development. The debate is well summarized by Morton et al. (71) who then defines the pre-antral stage follicles as responsive but not dependent on FSH (Figure 3A). Other studies suggest that gene expression of oocytes and granulosa cells can be altered even by minor FSH fluctuations in follicles as early as secondary stage (72).

Transition from secondary to antral follicles is marked by theca cell layer formation, which envelopes the oocyte and granulosa cells (68). The blood vessels now connect this follicle and the ovary. At the end of secondary phase, the antrum, liquid filled cavity, starts to form. Granulosa cells start forming into two distinct types: mural – outlining the follicle – and cumulus – enclosing the oocyte (Figure 2B). Now, this follicle starts to be dependent on gonadotropins and paracrine signalling for further follicle growth, granulosa cell differentiation and antrum expansion (Figure 3A). FSH induces the expression of *Cyp19a1*, which promotes E2 synthesis in granulosa cells (73). Once E2 synthesis starts, it will stimulate granulosa cell proliferation and luteinizing hormone receptor (LHR) expression.

As the follicle progresses from the pre-antral to antral stages, the oocyte progressively gains the ability to initiate meiotic resumption. When oocyte grows, it is at germinal vesicle (GV) stage, blocked at meiosis I, prophase I. During growth stage, it undergoes chromatin conformation changes. The chromatin first has a non-surrounded-nucleolus (NSN) conformation that is characterized by expanded chromatin and is considered as incompetent for further development. During the final growth stages of the antral follicle, oocyte's chromatin condenses into a compact ring around the nucleolus that is called the surrounded-nucleolus (SN). Oocytes that have this type of chromatin

conformation are considered developmentally competent (74). When oocyte reaches SN chromatin conformation, transcriptional activity gradually stops (75) (Figure 3B).

Antrum expands further to form the pre-ovulatory follicle, with now very well defined cavity and a cumulus-oocyte-complex (COC) which clearly separates from mural granulosa cells (Figure 2B). Now, the LH surge is triggered the E2 synthesized by granulosa cells. Following the surge of LH, GV-stage oocytes undergo germinal vesicle breakdown (GVBD), a process involving nuclear envelope breakdown (NEBD) and the release of chromosomes into the cytoplasm. Here, the cytoplasmic maturation is critically important - meiosis can be re-initiated through natriuretic peptide type C/ natriuretic peptide receptor 2 (NPPC/NPR2) signalling cascade (Figure 3C, see section 3.4.) and the prophase I block is released. In prometaphase I, microtubule-based spindle fibres attach to chromosome centromeres and the chromatin keeps condensing (76). At metaphase I, chromosomes align in the centre of the cell, at the metaphase plate. At anaphase I, the spindle fibres pull chromosomes to opposite cell poles and divide the chromosomes into two cells (Telophase I), creating haploid, 2-chromatid containing cells (Cytokinesis I). The oocyte that completed the meiosis I should extrude a polar body containing a set of chromosomes. The correct segregation of chromosomes is assured by chromosome assembly checkpoint (SAC) that scans for potential errors of microtubule to chromosome attachment prior to anaphase. SAC proteins are capable of delaying anaphase onset until all attachment errors are corrected. Therefore, a weak SAC signal may lead to chromosome segregation errors (77) (see also section 4.2.).

Concurrently to nuclear events, accumulated maternal RNA transcripts are post-transcriptionally modified during meiosis I (Figure 3B). Generally, initiated during meiosis I, the translation intensifies during meiosis II. Transcript remodelling takes place through degradation, de-polyadenylation, and re-polyadenylation of maternal transcripts (78,79). Master regulators of these processes include *Dazl*, *Cpeb1*, *Btg4, Cnot6* and others.

DAZL accumulates during oocyte maturation and is needed for the translational regulation of maternal messenger ribonucleic acids (mRNAs). If its accumulation is disrupted, oocytes cannot progress to MII. DAZL acts as both a repressor and activator of translation, where a signal in the oocyte at GVBD causes a shift from repressor to activator (80). It also cooperates with CPEB1 to regulate translation of a subset of mRNAs (80,81). At the onset of oocyte maturation, CPEB1 phosphorylation and degradation is triggered by MAPK cascade (82). The MAPK pathway also triggers *Btg4*, another important factor in maternal mRNA decay, translation in fully grown oocytes (83).

CNOT6L-mediated decay of specific maternal mRNAs during oocyte maturation is essential for meiosis resumption. In oocytes, the deletion of *Cnot6l* leads to impaired de-adenylation and degradation of selected maternal transcripts and subfertility, including defects in SAC, microtubules, and meiotic cell cycle arrest at prometaphase (84). FSH regulates the transcription and translation of *Cnot6* and *Cnot6l* in granulosa cells, facilitating the clearance of specific transcripts during the transition from pre-

antral to antral follicles. This indicates that FSH influences granulosa cell function by promoting selective mRNA translation and degradation of existing mRNAs and can initiate *de novo* transcription (85).

As the oocyte in the pre-ovulatory follicle has now undergone the cytoplasmic and nuclear maturation, it is ready to be ovulated (Figure 2B). The pressure in the follicle increases, rupturing it and pushing the oocyte into the oviduct/fallopian tube. Noteworthy, even though LH surge is known to trigger the ovulation, the precise molecular mechanisms of ovulation are still not fully understood (86). After ovulation, the oocyte is blocked in the metaphase II, awaiting fertilization in the ampulla.

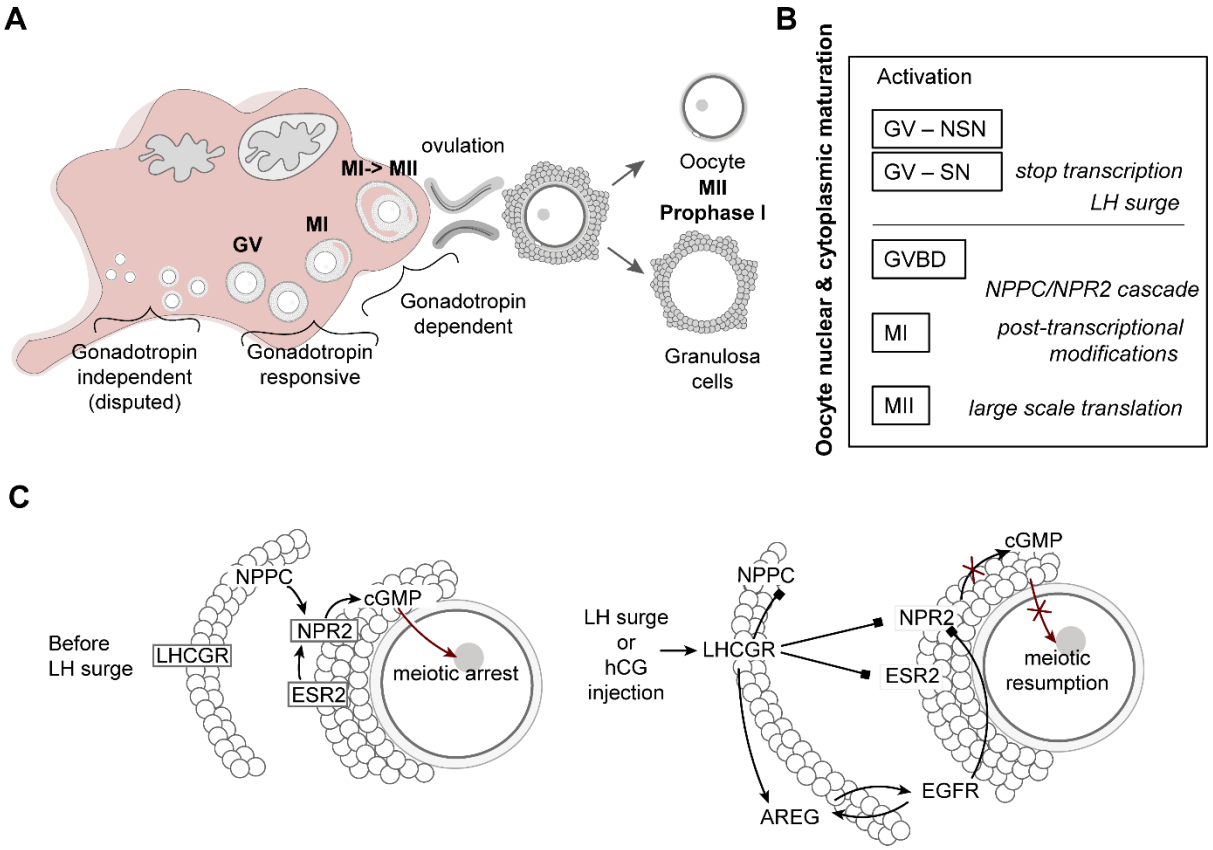

Figure 3. Folliculogenesis and oocyte maturation.

(A) Gonadotropin-dependency of maturing follicles and their oocyte meiosis state. (B) Summary of oocyte nuclear and cytoplasmic maturation events, in context of oocyte meiosis. (C) NPPC/NPR2 signalling before the LH surge and after.

3.4. Oocyte and granulosa cell bi-directional communication

Cell-cell communication plays a major role in oocyte maturation through physical contacts, paracrine signalling cascades, and granulosa cell remodelling.

Granulosa cells and oocytes establish a direct physical contact through gap junctions (GJs) and transzonal projections (TZPs). The GJs between oocytes and granulosa cells are predominantly made of Connexin-37 proteins, and the GJs between granulosa cells themselves are made of Connexin-43. The GJs allow small molecule transport, including ions, metabolites, amino acids, and signalling molecules. This includes two important small weight molecules that are involved in oocyte maturation – calcium and cyclic adenosine monophosphate (cAMP) (87). During follicle maturation, the GJs progressively reduce until nearly gone (88). The transzonal projections protrude from granulosa cells into the oocyte membrane and once their number reduces, the oocyte matrix integrity is perturbed. Around 40% of TZP-deprived oocytes arrest at meiosis I, suggesting that the lack of physical contact directly affects oocyte maturation (89).

Paracrine signalling is another way of exchanging signals between oocytes and granulosa cells, necessary for regulating steroidogenesis and mitogenesis in granulosa cells and the maturation of the oocyte.

One of the best studied signalling loops between oocyte and granulosa cells is through oocyte-derived paracrine factors *Gdf9* and *Bmp15*, which both belong to the transforming growth factor β (TGFβ) superfamily. Before the LH surge, GDF9 and BMP15 inhibit FSH-stimulated expression of luteinizing hormone/choriogonadotropin receptor (*Lhcgr*) mRNA in granulosa cells. After the LH surge, these proteins stimulate cumulus expansion. BMP15 and GDF9 signals in cumulus granulosa cells are mediated by phosphorylation of SMAD1/5/8 and SMAD2/3, respectively (90).

One of the first ligand-receptor systems identified in the ovarian follicle is Kit Ligand (KitL) expressed in granulosa cells and its receptor tyrosine kinase (Kit) expressed in all developmental stages of oocytes. Interactions between KitL and Kit are important for initiating follicular growth from the primordial pool, controlling further follicle growth including theca cell differentiation, and protecting pre-antral follicles from apoptosis. Additionally, this signalling pathway is essential for antral cavity formation, cytoplasmic maturation of the oocyte, and maximizing thecal androgen output (91). During follicular development, binding of KitL to the Kit receptor activates the receptor's kinase domain, leading to activation of signalling pathways that regulate apoptosis via Ras, Raf, MAPK, protein kinase B (PKB/Akt). KitL also activates phosphatidylinositol (PI) 3-kinase (PI3K), which is essential for mitogenesis and cell survival (92). FSH promotes proliferation and differentiation of pre-antral follicles through insulin-like growth factor-1 (IGF-1) and activin. It also regulates Bmp15 expression in a dose-dependent manner through Kit signalling (92,93). In fully grown oocytes, GDF9 suppresses *KitL* mRNA expression (94).

Meiotic arrest in oocytes is maintained through NPPC/NPR2 system that keeps elevated cAMP levels in immature oocytes (Figure 3C). Before the LH surge, cAMP phosphodiesterase (PDE3A) activity in cumulus granulosa cells inhibited by cyclic guanosine monophosphate (cGMP) from both cumulus and mural granulosa. Following the LH surge, NPR2 in granulosa cells gets activated through NPPC and converts guanosine triphosphate to cGMP, which is further transported into the oocyte

through GJs. The activation of PDE3A in oocyte lowers cAMP levels, initiating GVBD (95). The expression of *Npr2* is regulated by estradiol (96).

3.5. Fertilization and zygotic genome activation

Fertilization is a complex process that results in formation of a zygote. Sperm migrates through FRT where it undergoes capacitation, biochemical compositional changes that lead to increased mobility and penetrability. In parallel, ovulated COCs are pushed through the oviduct. At sperm-oocyte encounter, sperm uses lysosomal enzymes from the acrosome to digest hyaluronic acid around the oocyte and then, acrosin in the inner membrane, to digest oocyte's zona pellucida (ZP), a protective glycoprotein layer. Fusion of acrosome and ZP increases calcium concentration and oocyte modifies the extracellular matrix to protect itself from detrimental polyspermy (97). Once the membranes fuse, the oocyte can finalize the meiosis II by extruding the second polar body. Oocyte and sperm independently form a pronucleus which both move towards each other and fuse to create a diploid cell. In mice, pronucleus forms 3-6h post-fertilization and after around 24h the zygote achieves its first mitotic division when 2-cell stage embryo can be observed.

Maternal transcript degradation is a crucial preparatory phase for successful fertilization and early embryo development, until it will be capable to transcribe its own transcripts, and is called the maternal-zygotic transition (MZT). Meiotic maturation triggers the first wave of maternal transcript degradation in an oocyte, then fertilization triggers a second wave of transcript degradation in the zygote, and once the zygotic genome is activated after the 2-cell stage, the third wave degrades the remaining maternal mRNAs in the embryo (98). In the second part of MZT, zygotic genome undergoes activation (ZGA). Historically, two ZGA waves were described as the major at 2-cell stage and a minor at 4-cell stage in mice, but it is more likely to represent dynamics of gradual transcriptional activation (99).

3.6. Evolution of gametes

Sexual reproduction is almost universally present in eukaryotes. Due to its widespread occurrence and common fundamental characteristics, it may have originated once in the last common ancestor of all eukaryotes. The proposed evolutionary adaptations involve reduction of ploidy through meiosis, production of haploid gametes that are different but complementary (oocytes and sperm), and uniparental organelle inheritance (e.g. mitochondria) (100). More generally, the biological processes of sexual reproduction include meiosis, fertilization, sex determination, and speciation.

It is currently deduced that meiosis evolved from mitosis. Both processes share many common features but meiosis is more complex, suggesting that it is a derivative from mitosis. Meiosis probably arose once because of high similarity between taxonomic

groups, with specific chromosomal events evolving gradually, first, homolog synapsis and later synaptonemal complexes and the recombination (101).

Generally, reproductive proteins evolve faster than non-reproductive in many species (102). More specifically, in mammals, genes involved in sperm development and maturation evolve fast (103,104), and X-chromosome evolves faster than autosomes (105). Most studies in mammalian oocytes focus on ZP proteins that also evolve rapidly but a larger-scale experimental data on gene expression is currently lacking.

4. Ageing of reproductive tissues and oocytes

End of reproductive life is not the end of organismal life for most vertebrates (40). An intriguing but little explored topic is how reproductive organs age and what changes during post-cyclic/post-menopausal period. Numerous biological processes are recognized as hallmarks of ageing across mammalian species, such as genomic instability, epigenetic modifications, telomere attrition, mitochondrial dysfunction, cellular senescence, stem cell depletion, and altered cell-cell communication (106). Female reproductive ageing is unique in terms of its apparent disconnection with the onset of ageing processes in the non-reproductive organs. Ovaries are the first to show age-related decline when ovarian reserve starts diminishing in late 30s and gets exhausted around the age of 50 (107,108). In this section, I will describe major mechanisms of FRT and oocyte ageing.

4.1. Reproductive tissue ageing

The FRT organs exhibit varying levels of susceptibility to age-related pathologies.

Ovary is the most studied organ in terms of FRT ageing. Ovarian reserve sharply decreases, resulting in ovarian follicle depletion and cessation of ovarian cycling (107). Ovarian production of estrogen and other hormones reduces, which in turn causes a deregulation of HPG axis, and gonadotropin levels stay constantly higher in older individuals (109). These lower estrogen levels also negatively affect oocyte quality (110). During ageing, LH levels also drop and CL size reduces (111).

The incessant ovulation model hypothesizes that throughout reproductive lifespan ovarian tissue damage accumulates at each cycle of recurrent ovulation. During normal folliculogenesis, inflammation is resolved with each cycle and ovarian stroma remodelling facilitates ovulation. During tissue repair, cytokines interact to facilitate extracellular matrix (ECM) deposition and lead to fibrosis (112). However, this constant repetitive inflammation and wound healing cycle could become more difficult to resolve during ageing because chronic inflammation is associated with fibrosis development in other organs (113). In addition, reduced ovulation frequency, such as oral contraception or parity history, is predicted to have a protective effect against reproductive senescence, and especially against reproductive system cancers (114). On a cellular level, ovulation suppression reduces oocyte aneuploidy by preserving centromeric cohesion (115).

There is much less data about oviduct ageing. Oviduct epithelial tissue may look disorganized in older animals (110). It is known that the ciliated cells accumulate autolysosomes and vacuoles but retain their cilia in addition to affected ECM (111). In the old secretory cells, the secretory granules nearly disappear (116).

Ageing in uterus shows through structural and immune changes. Uteri undergo cellular senescence and are prone to inflammation. Collagen accumulates in the endometrium

and response to oxytocin reduces. Stromal cells may lose estrogen receptors while myometrium weakens and has shorter contractions (117). Uteri of old rodents exhibit a reduced decidual response compared to younger animals, which is important in uterine-embryo crosstalk (118).

There is extremely little information about cervix and vagina ageing as studies tend to primarily focus on microbiota, HPV infections and cervical cancers.

As in most other organs, cancer incidence increases with age in all FRT organs (119).

4.2. Oocyte ageing

Successful fertilization and embryo development depends on the release of high-quality oocytes. During ageing, humans and other animals experience a significant decline in fertility due to reduced oocyte numbers (107,120) and lower oocyte quality (121), accompanied by dysregulated gene expression (122) and/or maturation (123). Research on biomarkers of ovarian reserve in women conceiving naturally suggests that the age-associated decline in female fertility is primarily due to a decrease in oocyte quality, rather than quantity (124). Oocytes from older mice have higher rates of aneuploidy (125), dysregulated gene expression patterns (126,127), and worse developmental outcomes (128).

Aneuploidy results from a two-step process involving, first, the presence of a chromosome prone to mis-segregation, and second, the failure of the SAC to respond appropriately to this error. In meiosis I, homologous chromosomes segregate to opposite spindle poles, where each homolog consists of replicated sister chromatids. Their kinetochores must achieve mono-orientation, attaching to the same pole. During prometaphase of meiosis I, bivalents align and attach kinetochores to spindle microtubules, forming kinetochore fibres. Tension from chiasmata between homologs stabilizes the fibres. The SAC monitors these attachments and regulates the transition from metaphase to anaphase. Once the SAC is satisfied, the cell divides, and homologs are distributed to different daughter cells (129).

Old oocytes are known to be prone to chromosome segregation errors due to progressive loss of cohesion (125), generating an important fraction of aneuploid oocytes during anaphase of MI. Key proteins in SAC response pathway drive the SAC integrity deterioration with age (130). Even when SAC is intact, aneuploidy can arise from changes in cortical tension that impacts oocyte's cytoskeleton through myosin-II (131). Interestingly, if the cytoskeleton is affected through actin complex, the oocyte's development is perturbed without SAC defects or aneuploidy (132). Lagging chromosomes have recently been attributed to two mechanistically different classes where the class-I results in aneuploid oocytes and class-II is generally benign (133), depending on the cell cycle prolongation in class-I oocytes.

Gene expression changes are also observed during oocyte ageing. In mouse and human oocytes, the processes deregulated during ageing include genes regulating

cell cycle, especially chromosome alignment and separation, DNA stability, mitochondria as well as genes involved in fertility and embryo development (122,127).

Mitochondria are essential for oocyte and embryo development. The removal of damaged mitochondria via autophagy is called mitophagy, that may be perturbed during oocyte ageing. In both mouse and human, oocytes from older individuals have less mitochondria and reduced mitochondrial function (134). Oocytes use oxidative phosphorylation for high energy needs, especially during meiosis and early embryo development. However, the electron transport chain produces the reactive oxygen species (ROS) as a by-product which is the main source of mitochondrial damage during ageing (135). In addition, mitophagy might be related to erroneous spindles in old oocytes because anti-oxidative treatments partially restore not only the mitochondrial function, but also the spindle assembly (134,136).

Noteworthy, the vast majority of studies that investigate oocyte ageing use oocytes from superovulated mice because naturally ovulated oocytes are difficult to obtain. In human, natural ovulation is not a standard IVF protocol, hence only oocytes after hormonal treatment are available for studies.

5. Assisted reproductive technologies

Infertility is a global problem, affecting approximately 8–12% of reproductive-aged couples worldwide (137). In high-income countries, female infertility is a growing health issue, where later pregnancy is becoming a more common choice. Biologically, common causes of female infertility include ovulatory disorders, for example, polycystic ovarian syndrome (PCOS), blocked fallopian tubes, endometriosis, and uterine abnormalities as well as idiopathic causes. Systemic disease, such as infections or auto-immune disease, and lifestyle choices also play a role in fertility (137).

Assisted reproductive technologies (ART) were first adapted in animals and then mastered to overcome infertility in patients (138). Despite large number of ART procedures per year, the live birth ratios are still around 30% in Europe and the United States, and much lower for older women (139–141). ART are also used in animal husbandry and, increasingly, in species preservation programmes.

In this chapter, I will cover the crucial part of ART – hormonal stimulation - and common ART practises alongside their limitations.

5.1. Hormonal stimulation (superovulation)

During IVF, hormonal stimulation is used to induce the development of multiple follicles to increase the number of retrievable oocytes and enhance the chances of successful fertilization and embryo implantation. However, too mild stimulation may yield

insufficient amount of retrieved oocytes and an excess may lead to decreased live birth rates (142) or ovarian hyper-stimulation syndrome (OHSS), which is a consequence of fluid accumulation in surrounding tissues due to impaired blood vessels in and around the ovary (143). Each patient has a varying response to hormonal stimulation, and they can generally be categorized into normal and poor responders. The fine balance in hormonal stimulation is not evident and an active debate about dosage is still ongoing (144).

Main hormones used for hormonal stimulation are gonadotropins: FSH to stimulate the ovaries to produce multiple follicles and LH to promote follicular growth, GnRH agonists and antagonists are also used. GnRH agonists initially increase and then suppress the natural hormone production, preventing premature ovulation. GnRH antagonists directly suppress the release of LH and FSH to prevent premature ovulation. Human Chorionic Gonadotropin (hCG) is used in all protocols to trigger final oocyte maturation and ovulation. Progesterone and estrogen are sometimes used to support the endometrium but are not part of stimulation itself as they are administered after oocyte retrieval.

There are three main IVF protocols: long, short and antagonist (145). In the long protocol GnRH agonists are used to suppress natural hormone production. Once suppression is confirmed, ovaries are stimulated by gonadotropins and hCG is given when follicles are mature, followed by oocyte retrieval 34-36 hours later. In the short protocol, ovaries are stimulated using gonadotropins in the beginning of the menstrual cycle without prior suppression. Then, GnRH antagonists are added mid-cycle to prevent premature ovulation. Finally, ovulation is triggered by hCG. Antagonist protocol is very similar to short protocol, except that antagonists are introduced later in the cycle.

In animals, similar hormonal stimulations based on gonadotropins are used for superovulation. Superovulation is often used in animal husbandry to improve farm animal quality through faster selection of traits, in research for genetically engineered animals, improving ART procedures, and studying reproductive physiology, as well as for species conservation programs for endangered species preservation. Specifically, in mice, two gonadotropins are used. First hormone is Pregnant Mare Serum Gonadotropin (PMSG), which mimics the effects of FSH, is administered to stimulate the development of multiple ovarian follicles. 48 hours later, hCG, which acts similarly to LH, is administered to trigger ovulation (146). As in humans, superovulation efficiency in mice strongly depends on age, hormone dose, and timing.

5.2. Developments of reproductive technologies and their limitations

After hormonal stimulation, *in vitro* fertilization or intracytoplasmic sperm injection (ICSI) is used to fertilize retrieved oocytes. Following successful fertilization, embryos can be transferred into uterus, further cultured or frozen for storage. One of the challenges in ART is to choose embryos with the highest developmental potential for

implantation. Currently, to evaluate embryo quality, the embryos are observed and graded by their morphology by an embryologist. Though most important morphological features seem to correlate with better embryo development outcomes, some worse-looking embryos also have a chance for correct development (147). To test for chromosomal abnormalities, clinics may use an embryo-invasive testing, called preimplantation genetic testing (PGT), where a biopsy is taken from a blastocyst. This increases the risk of embryo wastage, lacks accuracy, prolongs already lengthy IVF procedure, and may have negative consequences for placenta development (148).

There are numerous attempts for non-invasive embryo screening. For morphology, AI-based technologies recently started to be developed to provide embryo grading using images taken through time-lapse imaging (149). The biophysical properties are also explored as markers for fertilization success (150). Many studies are looking for biomarkers that have a potential for more accurate prediction that physical-property based methods, including granulosa cells that have emerged as such non-invasive target (151). The advantage of profiling granulosa cell transcriptomes is that the oocyte will not be disturbed. Despite extensive efforts to find a consistent transcriptomic signature linking granulosa cells to embryo developmental potential, it is challenging because of variations in IVF procedures and analyses, the pooling of COCs, small sample sizes, and the lack of reproducibility across different studies (152,153). Therefore, currently there is no consensus on granulosa cell markers.

Most often, one cycle of IVF is not enough for getting pregnant (154), hence, the majority of patients undergo a few IVF cycles. How repeated hormonal stimulation affects hormone balance and reproductive organ health in long-term is unknown because studies tend to focus on successful pregnancy outcomes and neonate health after IVF. In addition, current cohort of women who received IVF treatments is not old and large enough yet to estimate effects in older age. Several animal studies showed increased risks for general health, like decreased bone density and heart ejection fraction, reduced fertility (155), increased oxidative stress in the ovaries (156) and even disrupted methylation patterns in embryos from oocytes after repeated superovulation (157). How transcription in cells and reproductive organs is affected by multiple rounds of superovulation is not yet clear, especially, in the context of ageing. Whether hormonal stimulations contribute to increased reproductive cancer risk in older age is also unclear. In addition to still young IVF patient cohort, there is a general lack of clinical study depth, and regularization of information about specific drugs and IVF protocols used (158).

In conclusion, there are many developing technologies around IVF but some basic molecular mechanisms of how excessive amount of exogenous gonadotropins affects reproductive tissues remain unanswered. It is also important to note that ART can overcome some infertility issues in younger women but it does not counteract the age-related decline in fertility (141).

Overview of Result Chapters

Results chapters span four different research projects that I undertook during my thesis. The collective aim of these projects is to investigate various aspects of hormonal stimulation and ageing in the FRT tissues and cells (Figure 4).

- Chapter 1 will cover how superovulation and ageing affect COC transcriptomes and cell-cell communication. It will show how to predict embryo developmental trajectories from granulosa cells.

- Chapter 2 will cover preliminary results on how COCs evolved in mice and speculate about further work.

- Chapter 3 will transition to the tissues of the reproductive tract and show how reproductive cycle and ageing can influence tissue composition and gene expression throughout FRT, with focus on fibroblasts.

- Chapter 4 will go into more detail about FRT ageing and how it is affected by repeated hormonal stimulations.

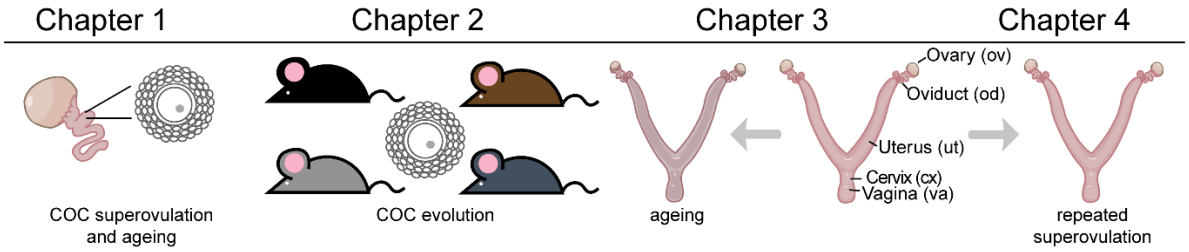

Figure 4. Summary of chapters in this thesis.

Chapter 1

Transcriptomic Insights into Superovulation and Ageing of COCs and Predicting Early Embryo Developmental Potential

Advancements in reproductive biology have led to a deeper understanding of the intricate interactions between oocytes and granulosa cells within the COC. However, there is a knowledge gap about how oocytes and granulosa cells interact within individual COCs in mammals, especially, in the context of superovulation and ageing.

This research project focuses on decoupling the individual COC interactions, as well as their individual and combined reactions to superovulation or ageing. Historically, it was practically very hard to retrieve COCs from aged mice, more so, trying to ovulate them naturally. It was thought that this difficulty comes from diminished ovarian reserve when animals age. During my thesis, I newly adapted developmental biology methods and animal husbandry techniques to allow comparisons of individually tracked oocyte-granulosa cell pairs and comparisons to naturally aged old COCs.

The idea of using granulosa cell transcriptomes for non-invasive prediction of early embryo quality has been explored in clinical studies without an agreement about which markers could predict embryo development best. It is due to multiple complex variables in human studies, but also retrospective designs in both animal, and human studies. In this thesis, I modified standard mouse IVF to design a prospective single embryo-based approach to predict embryo development.

This project is now completed and the presented results are final.

Klaudija Daugelaite#, Perrine Lacour#, Ivana Winkler#, Marie-Luise Koch, Anja Schneider, Nina Schneider, Francesca Coraggio, Alexander Tolkachov, Xuan Phuoc Nguyen, Adriana Vilkaite, Julia Rehnitz, Duncan T. Odom*, Angela Goncalves*

"Granulosa cell transcription is similarly impacted by superovulation and aging and predicts early embryonic trajectories" - Manuscript in 3rd round of reviews at *Nature Communications.* Currently on BioRxiv: bioRxiv 2023.10.30.563978;
doi: https://doi.org/10.1101/2023.10.30.563978

I presented this project in following meetings and conferences:

PhD Poster Presentation at DKFZ

Heidelberg, Germany | November 2023

Poster "*Superovulation and aging perturb oocyte-granulosa cell communication*"

FSP-B department meeting at DKFZ

Heidelberg, Germany | September 2023

Talk *"Decoupling the effects of superovulation and aging in oocytes and granulosa cells"*

Fertilization and Activation of Development Gordon Research Seminar & Conference

Holderness School, New Hampshire, United States | July 2023

Poster *"Decoupling the Effects of Superovulation and Aging on Oocyte-Granulosa Cell Transcriptomes and Communication"*

24th EMBL PhD Symposium

Heidelberg, Germany | December 2022

Poster *"Superovulation and ageing perturb transcriptional regulation in mouse oocytes and granulosa cells"*

Contribution acknowledgement

Perrine Lacour and Dr. Ivana Winkler performed all bioinformatics analyses.

Marie-Luise Koch and Dr. Francesca Coraggio assisted with technical handling and sperm preparation for IVF experiments.

Anja Schneider prepared oocyte libraries for total RNA sequencing.

Dr. Julia Rehnitz and Ulrike Bender have kindly provided extracted RNA from human granulosa cells.

Nina Schneider prepared bulk RNA sequencing libraries for human granulosa cells.

Animal caretakers checked vaginal plugs for naturally ovulated mice.

Dr. Frank van der Hoeven and Larissa Ziegler vasectomized male mice and provided frozen sperm for IVF experiments.

1. Results

1.1. Transcriptomic Insights into Superovulation and Ageing of COC

The first part of this study focuses on effects of superovulation and ageing on COC transcriptomes. Some of the questions asked are simple, yet relevant, for example, how does the gene expression change in reproductive and somatic cells after hormonal overdose? Is that relevant for developmental outcomes? How does this compare with physiological ageing of COCs? Whether and how older naturally obtained cell transcriptomes differ from superovulated ones?

1.1.1. Study design

To investigate COCs after superovulation and organismal ageing, I first established natural and superovulation protocols for young (3 months old) and old (12 months old) mice (Methods, Figure 1A). Briefly, I mated females with vasectomized males to track when natural ovulation occurs. In case of ovulation, female mice mated and presented a vaginal plug in the morning. For superovulation, I used standard dose of 5 international units (IU) of PMSG and hCG for all ages. This yielded on average 7.5 COCs after natural ovulation and 15 COCs after superovulation. I used the idea that natural ovulation is slower in old mice from Ishikawa and Endo (1996) to postpone the COC collection by only a few hours for old naturally and superovulated mice. This proved successful to retrieve on average 9 natural COCs and 11 superovulated COCs per mouse. Old mice with FRT pathologies did not ovulate at all, even if these were small lesions on oviducts (~50% of mice).

Next, to be able to study individual COC transcriptomes, I adapted standard COC collection protocols to manually isolate oocyte and its granulosa cells while keeping their *in vivo* pairing information (Methods, Figure 1B). Contrary to standard research and clinical practises, here, granulosa cells are also collected. Two main changes to standard procedure is a very gentle hyaluronic acid digestion to keep COC units intact while being able to separate them from each other, and using Accutase to further separate OC and GCs in their individual drops.

I then collected COCs from mice in four conditions: naturally-ovulated young (NY), superovulated young (SY), naturally-ovulated old (NO), and superovulated old (SO) (Figure 1C). I used full-length transcript protocol SMART-seq2 to sequence each OC as a single cell and its GCs as a small bulk (Methods). I collected COCs from 3-4 mice in each condition, totalling 15-31 samples per condition. In 72% of these samples both OCs and GCs successfully passed quality control; in cases where analyses were done without pairing information, all available OCs and GCs were used.

The OCs and GCs clearly separated in transcriptional space after dimensionality reduction (Figure 1D). There was no cross-contamination when comparing oocyte and granulosa cell-specific markers (Figure 1E, bold). In addition to known markers (159–162), multiple novel markers with polarized gene expression were found (Figure 1E, not bold). The heatmaps of Top100 variable genes for OCs and GCs (Figure 1F and 1G, respectively) showed some clustering but no striking patterns.

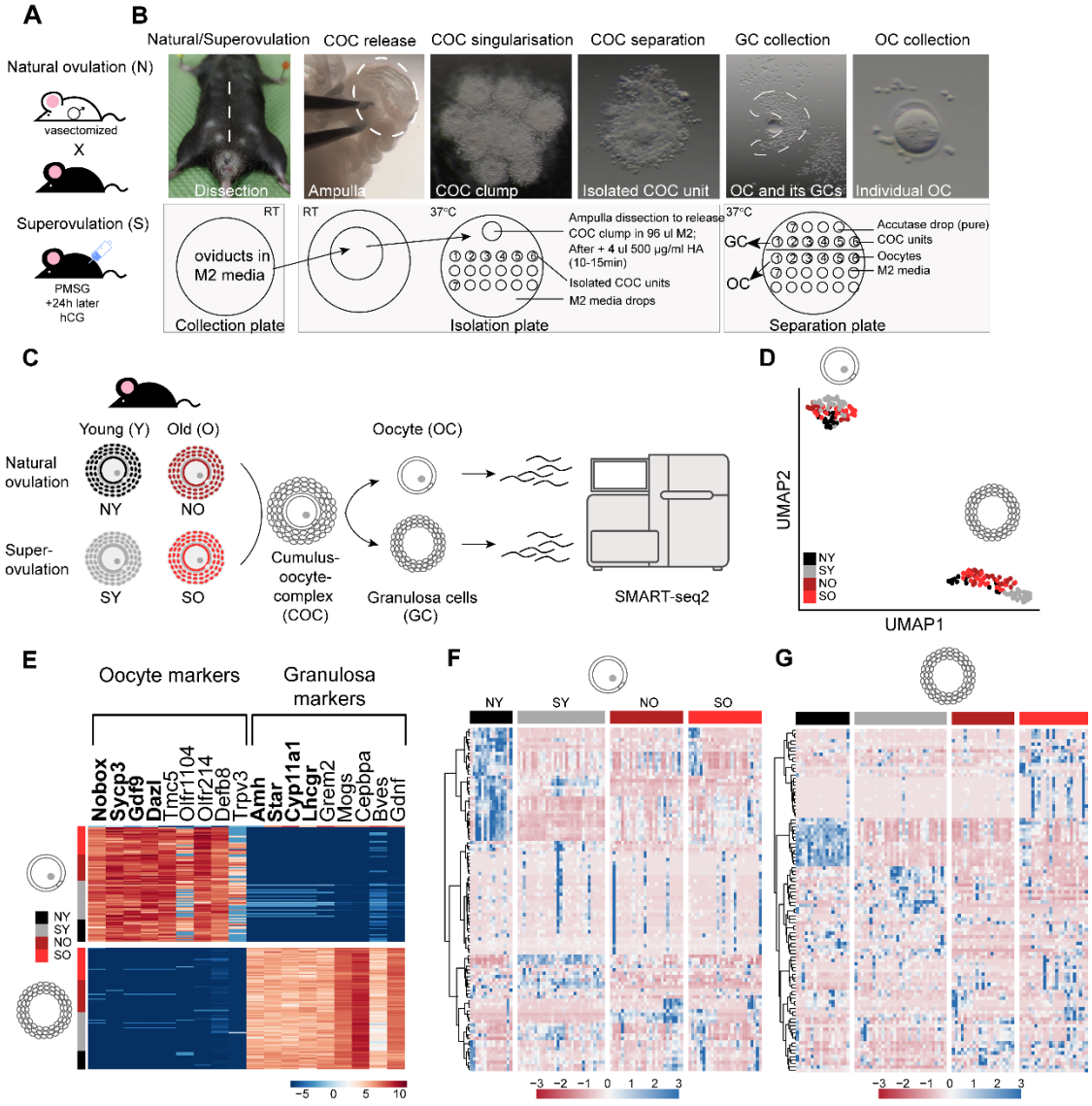

Figure 1. Study design for COC isolation after superovulation and ageing.

(A) Cartoon of natural and superovulation in mice. (B) Detailed protocol of COC isolation and OC/GC pair collection. (C) Cartoon for study design - collecting COCs from young naturally ovulated (NY, black) and superovulated (SY, grey), and old naturally ovulated (NO, dark red) and superovulated (SO, red) mice. Further COC is split into oocyte (OC) and granulosa cells (GCs) and RNA is prepared for sequencing using SMART-seq2 protocol. (D) Dimensionality reduction analysis Uniform Manifold Approximation and Projection (UMAP), cells from all four conditions shown in same colours as in C. (E) Cell-specific marker gene expression in collected OCs and GCs in all four conditions, genes are columns and cells are rows. (F, G) Heatmap showing Top100 variable genes, (genes are rows, and cells are columns) for oocytes (F) and granulosa cells (G). The figure is adapted from Daugelaite et al., 2023 (Biorxiv).

1.1.2. Superovulation perturbs COC gene expression

One hypothesis concerning superovulation is that forced maturation of follicles might expulse less mature oocytes. That immaturity should also be reflected in dysregulation of related pathways in both oocytes and granulosa cells.

To investigate a general effect of superovulation on COC transcriptomes, differential gene expression was computed using all available OC and GC transcriptomes in young mice. 3,519 genes of 22,181 genes detected (adjusted p-value < 0.05, 46% upregulated) were differentially expressed after superovulation in oocytes (Figure 2A, top panel) and 2,765 genes of 25,201 detected (adjusted p-value < 0.05, 40% upregulated) in granulosa cells (Figure 2B, top panel).

Overrepresentation (ORA) analysis was performed to evaluate functional pathways, first filtering the results by keywords, related to processes involved in oocyte development, folliculogenesis and hormonal regulation (Methods). In oocytes, many pathways involved in oocyte development were deregulated, including meiosis, mitochondrial metabolism, DNA damage, and hormonal response (Figure 2A, bottom panel). In granulosa cells, pathways regulating cell cycle, signalling, hormonal response and damage were also affected (Figure 2B, bottom panel). Overall, superovulation disrupts pathways required for successful COC development.

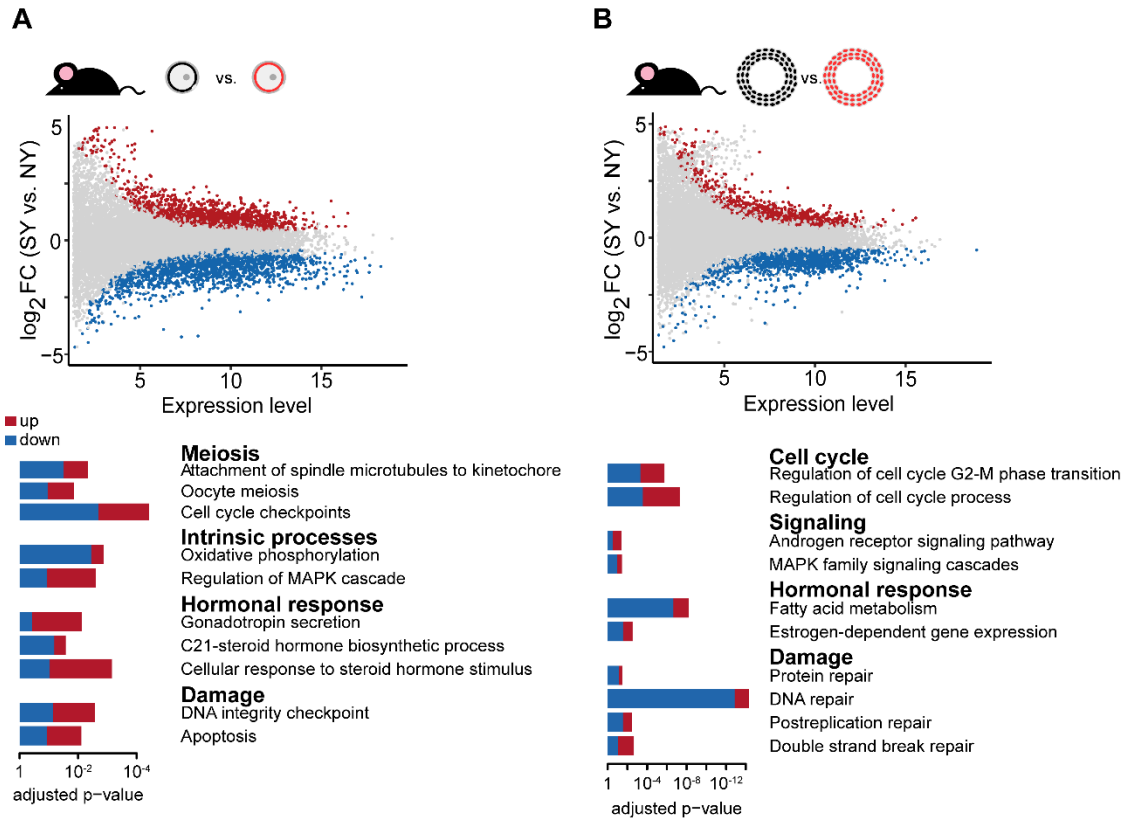

Figure 2. Gene expression comparison between young naturally ovulated and superovulated COCs.

(A, B) Top panels - Differentially expressed genes between naturally and superovulated COCs from young mice (n = 3 NY, 4 SY mice) in oocytes (A) and granulosa cells (B), upregulated genes are coloured in red, and downregulated are coloured in blue. Bottom panels - Selected enriched functional pathways in oocytes (A) and granulosa cells (B). The proportion of genes in the pathways are coloured based on 'SY compared to NY' reference, where upregulated in SY are marked in red and downregulated are marked in blue. The figure is adapted from Daugelaite et al., 2023 (Biorxiv).

1.1.3. Superovulation deregulates key COC maturation pathways

To investigate how specific mechanisms involved in regulating oocyte maturation are affected after superovulation, the expression of genes associated with three processes (cytoplasmic maturation, OC-GC communication, and spindle assembly) were compared between NY and SY COCs.

Cytoplasmic maturation was evaluated to assess whether superovulation disrupts the processes of re-polyadenylation, de-adenylation, and degradation of known transcripts (80,163–165). This evaluation compared a polyA-biased protocol (SMART-seq2) with a total RNA-seq protocol that uses random priming of transcripts (Methods). In case of re-polyadenylation, transcripts in mature oocytes would appear upregulated in SMART-seq2 and no difference would show in total RNA-seq (Figure 3A, re-polyadenylation). In turn, successful de-adenylation in mature oocytes would create a symmetric pattern (Figure 3A, de-adenylation). The degraded transcripts should appear as downregulated in mature oocytes in both protocols (Figure 3A, degradation).

To evaluate the differences in oocyte cytoplasmic maturation after superovulation, a transcriptome-wide study (165) was used as a reference for transcripts involved in oocyte maturation. Superovulation globally disrupted re-polyadenylation, de-adenylation and degradation of transcripts (Figure 3B).

To assess the role of specific genes, transcripts those involvement in oocyte maturation is proven were chosen for expression analysis (Figure 3C). Important for oocyte maturation, targets of re-polyadenylation (78,80,163,166,167), such as *Dazl*, *Cnot7* and *Btg4* were disrupted by superovulation. Other re-polyadenylation targets, for example, *Oosp1* and *Oosp3*, involved in meiotic progression and cell-cell signalling, and *Obox5* that acts as a transcription factor to control meiotic progression, were also disrupted (Figure 3C, re-polyadenylation). Superovulation affected the de-adenylation of transcripts, such as *Smc4*, chromosome condensation gene*, Taok2*, involved in cell cycle progression and response to external stimuli, as well as *Isyna1*, important for intracellular calcium level regulation and cell signalling. *Smc4* is typically de-adenylated during oocyte maturation (164), and *Taok2* and *Isyna1*, are identified as de-adenylated without degradation (165) (Figure 3C, de-adenylation). The degradation of transcripts, such as *Cpeb1, Nlrp14, Padi6, Zp2, and Wdr91* was perturbed by superovulation (Figure 3C, degradation). *Cpeb1* is the master regulator of maternal

mRNA translation (163), *Nlrp14* modulates oocyte's intracellular calcium levels (168), *Padi6* regulates cytoskeleton function and the formation of the meiotic spindle (169), *Zp2* is a key component of the zona pellucida, *Wdr91* transcripts are primarily found in immature oocytes (170). Overall, the targeted remodelling of these maternal transcripts during oocyte maturation is a critical regulatory mechanism that was disturbed after superovulation.

Next, the gene expression in cGMP pathway, essential for meiotic resumption, was checked for cell-cell communication. Before the LH surge, meiosis is arrested due to high cGMP concentrations (Figure 3D, upper panel). After LH surge, *Areg* is upregulated and *Esr2* and *Nrp2* are downregulated in granulosa cells, lowering the cGMP production that leads to meiosis resumption (171) (Figure 3D, lower panel). Superovulation dysregulated *Areg*, *Esr2* and *Nrp2* genes in granulosa cells compared to naturally ovulated (Figure 3D, lower panel). Out of these three genes, *Esr2* had a highest expression, which allowed me to validate its expression using Hybridization Chain Reaction (HCR), which is an imaging-based technique (Methods). In superovulated GCs, *Esr2* was significantly upregulated compared to naturally ovulated GCs (Figure 3E). This technique was not suitable to confidently determine *Areg* and *Npr2* expression because of their lower expression.

SAC is assembled in prometaphase I, when it attached to the kinetochore. Once microtubules are sufficiently attached to the chromosomes in metaphase I, the SAC proteins are detached and meiosis can progress to anaphase I (Figure 3F, left panel). In this dataset, SAC gene expression was also perturbed by superovulation (Figure 3F, right panel). Genes responsible for chromosome attachment to microtubules, *Mad2l1* and *Mad2l2*, were downregulated; *Bub1*, and *Bub1b*, important for correct chromosome segregation were upregulated. Together, this suggests a delayed anaphase onset in SY oocytes.

To conclude, superovulation perturbs oocyte and granulosa cell transcription, affecting critical maturation pathways.

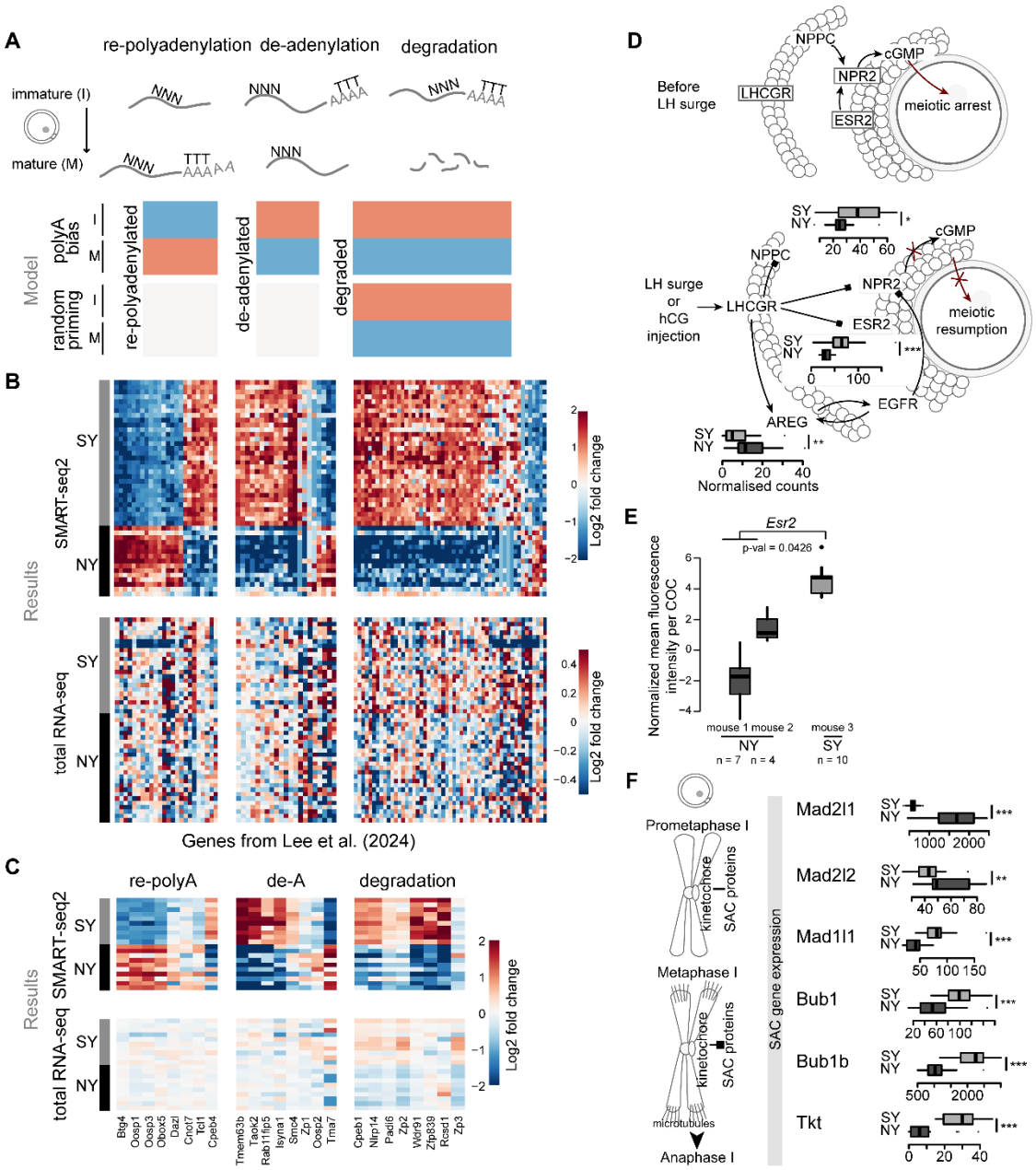

Figure 3. Superovulation perturbations of specific pathways involved in COC maturation.

(A) Top - Schematic drawing of transcript processing during maternal transcript remodelling during oocyte maturation (I – immature, M – mature oocyte). Bottom – the expected gene expression patterns of genes remodelled during oocyte maturation between polyA biased (SMART-seq2) and unbiased (total RNA-seq) protocols (red – upregulation, blue – downregulation, white – no change). (B) Gene expression comparison between naturally ovulated and superovulated oocytes using SMART-seq2 (n = 15 NY, 31 SY) and total RNA-seq (n = 25 NY, 22 SY) for genes from study of Lee et al. (165). The fold change was computed between NY and SY for each technology. Each row shows gene expression in single oocyte. (C) Gene expression comparison between naturally ovulated and superovulated (similar as in B). The fold change was computed between NY and SY for each technology. Each column is a selected gene, each row shows gene expression in single oocyte (randomly subsampled). (D) Schematic drawing of meiosis resumption process through cGMP cascade. Overlaid, bar plots show the gene expression of *Areg*, *Esr2* and *Npr2* that are in the cGMP pathway in

naturally (black bars) and superovulated (grey bars) granulosa cells (n = 18 NY, 31 SY GCs). Wilcoxon test p-value < 0.05 (*), 0.01 (**), 0.001 (***). (E) *Esr2* gene expression quantified from mean fluorescence intensity in granulosa cells (n = 11 NY, 10 SY GCs). Signal was normalized using a sample without *Esr2* probes, and background fluorescence is subtracted. (F) Left – schematic drawing of rough SAC assembly during meiosis I. Right - SAC gene expression in naturally and superovulated oocytes (n = 15 NY, 31 SY OCs). Wilcoxon test p-value < 0.05 (*), 0.01 (**), 0.001 (***). Centre line - median, box limits - first and third quartiles, whiskers - maximum and minimum or 1.5 times interquartile range if there were outliers, dots - outliers. The figure is adapted from Daugelaite et al., 2023 (Biorxiv).

1.1.4. Superovulation and ageing induce similar gene expression changes

After investigating effects of superovulation on COC transcriptomes, same questions arose for ageing. Interestingly, when comparing differentially expressed genes between naturally ovulated and superovulated cells, both OCs (Figure 4A) and GCs (Figure 4B) showed very small number of differentially expressed genes, without statistically significant differences. With a comparable number of replicates to the young mouse experiments, this analysis had sufficient statistical power to detect any differences in gene expression. The comparison of natural ageing (naturally ovulated young vs. old cells) and superovulation (naturally ovulated young vs. superovulated cells) showed that a common set of OC (Figure 4C) and GC (Figure 4D) genes were perturbed with a similar directionality by both processes. ORA analysis showed that shared differentially expressed genes were similar to those found after superovulation alone, including pathways involved in meiosis, estrogen response, oxidative phosphorylation and stress.

Cell-cell variability is a sign of ageing in FRT (172) and other cell types (173). To evaluate the cell-cell variability in COC ageing, differential Shannon entropy was calculated (Methods). Briefly, individual gene variability from gene expression was determined using Shannon entropy, where 0 means no variability and 1 represents high variability. Differential Shannon's entropy was then obtained by subtracting Shannon's entropy of one condition from the other condition. This measure therefore shows, whether gene expression had greater variability in one condition versus the other. In OCs, ageing increased cell-cell variability for numerous genes (Figure 4E). The superovulated OCs also showed a substantial increase in cell-cell variability (Figure 4E). In contrast, GC cell-cell variability increased during ageing but not in superovulation (Figure 4F).

Another mechanism is known to be involved in oocyte ageing is mitophagy, through selective degradation of damaged or dysfunctional mitochondria (136). Gene expression of mitophagy pathway genes showed that superovulation and ageing lead to similar perturbations, when compared to NY cells (Figure 4G).

The maternal remodelling could also be a reason for lower quality in older oocytes. Most genes in old OCs followed patterns as in superovulation (*see section 1.3. above*), but the gene expression was more variable (Figure 4H).

Overall, these results suggest that superovulation and ageing induce qualitatively comparable outcomes, affecting the same regulatory networks but to varying extents.

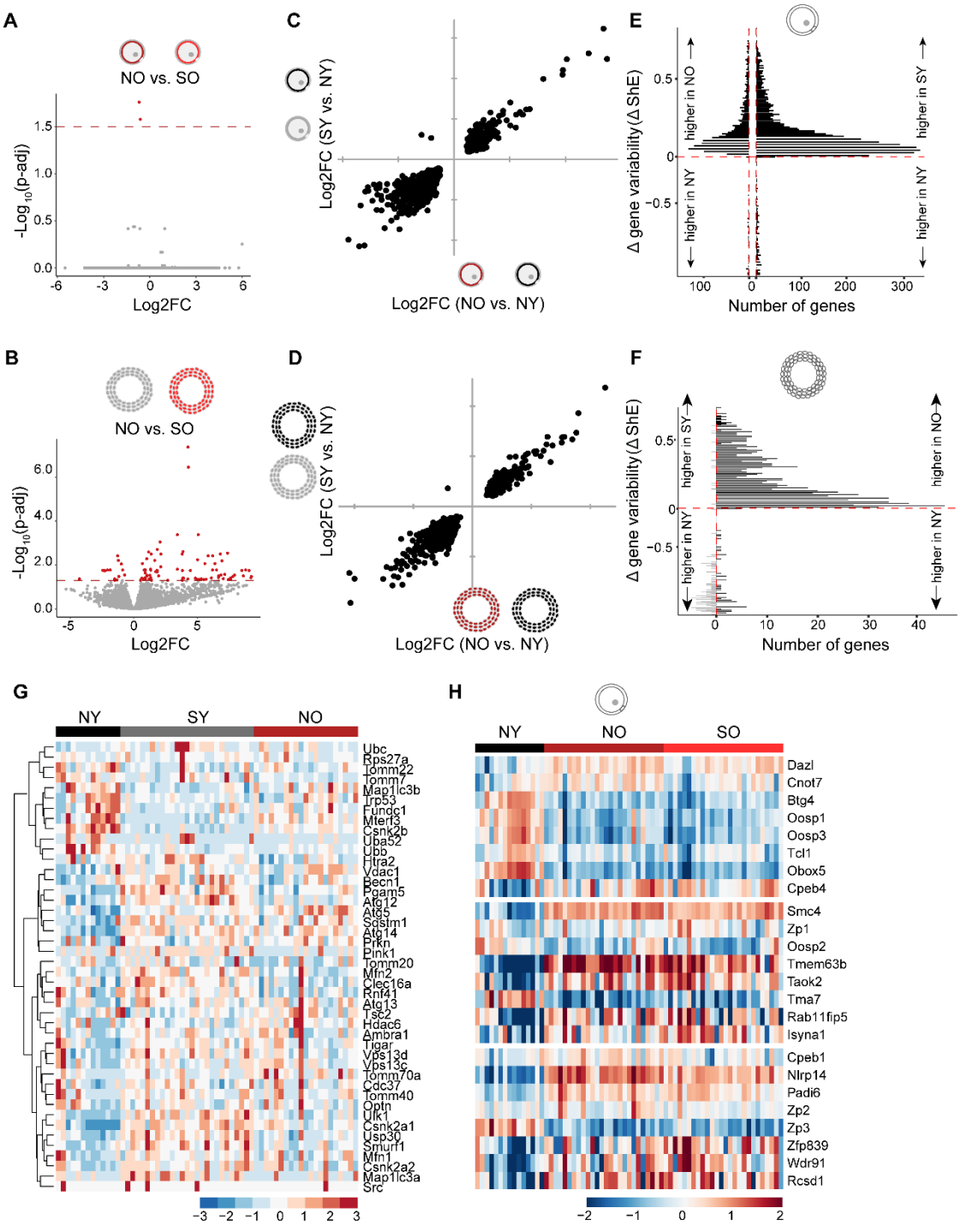

Figure 4. Comparison of COC gene expression after superovulation and ageing.

(A) Differential gene expression analysis of superovulated old (SO) versus naturally ovulated old (NO) oocytes. Area over the red line represents a significant expression change with threshold set at 1.5; therefore, significant differential genes are marked in red dots. (B)

Differential gene expression analysis of superovulated old (SO) versus naturally ovulated old (NO) granulosa cells. Area over the red line represents a significant expression change with threshold set at 1.5; therefore, significant differential genes are marked in red dots. (C) Log2 fold change of gene expression in superovulated young oocytes (SY) vs. naturally ovulated oocytes (NY) compared to Log2 fold change of gene expression in naturally ovulated old (NO) and young (NY) oocytes (n=3 NY, 4 SY, 3 NO mice). Only significantly expressed differential genes are represented (adjusted p-value < 0.05). (D) Log2 fold change of gene expression in superovulated young oocytes (SY) vs. naturally ovulated granulosa cells (NY) compared to Log2 fold change of gene expression in naturally ovulated old (NO) and young (NY) granulosa cells (n=3 NY, 4 SY, 3 NO mice). Only significantly expressed differential genes are represented (adjusted p-value < 0.05). (E) Differential Shannon entropy values as distribution of gene variability - NO (left) and SY (right) oocytes in comparison to NY oocytes. Higher Shannon entropy values represent increased gene expression variability. (F) Differential Shannon entropy values as distribution of gene variability - NO (right) and SY (left) granulosa cells in comparison to NY granulosa cells. Higher Shannon entropy values represent increased gene expression variability. (G) NY, SY, and NO cell expression of genes in mitophagy pathway (136). (H) NY, NO and SO oocyte gene expression of maternal remodelling genes from SMART-seq2 data. The Log2 fold change is computed between young and old groups. Each row is a gene, each column is gene expression in a single oocyte. The figure is adapted from Daugelaite et al., 2023 (Biorxiv).

1.1.5. Transcriptional effects of superovulation and ageing are not cumulative

The cumulative effects of superovulation and ageing on mouse COCs were examined by comparing all four COC conditions (Figure 5A).

To do so, the PCA of superovulated cells was computed, and followed by projection of old OCs (Figure 5B) and GCs (Figure 5C) onto it. The old cells fell between the extremities of NY and SY cells, suggesting that the impact of superovulation was diminished in old COCs. Old COCs had tendency of intermediate gene expression profile, also for genes involved in maternal remodelling, the SAC, and the cGMP pathway (Figure 5C). In sum, this showed that ageing and superovulation effects on gene expression were not additive.

To test the effect of age and superovulation relative to each other, the shifts relative to PC1 were quantified among all four conditions in both OCs (Figure 5F) and GCs (Figure 5G). Young COCs shifted strongly after superovulation, and but the shift was much weaker in old COCs. During ageing, the transcriptional changes differed between naturally ovulated and superovulated COCs. To summarize, experiments using only superovulated cells fail to accurately reflect the ageing effects observed in naturally ovulated COCs.

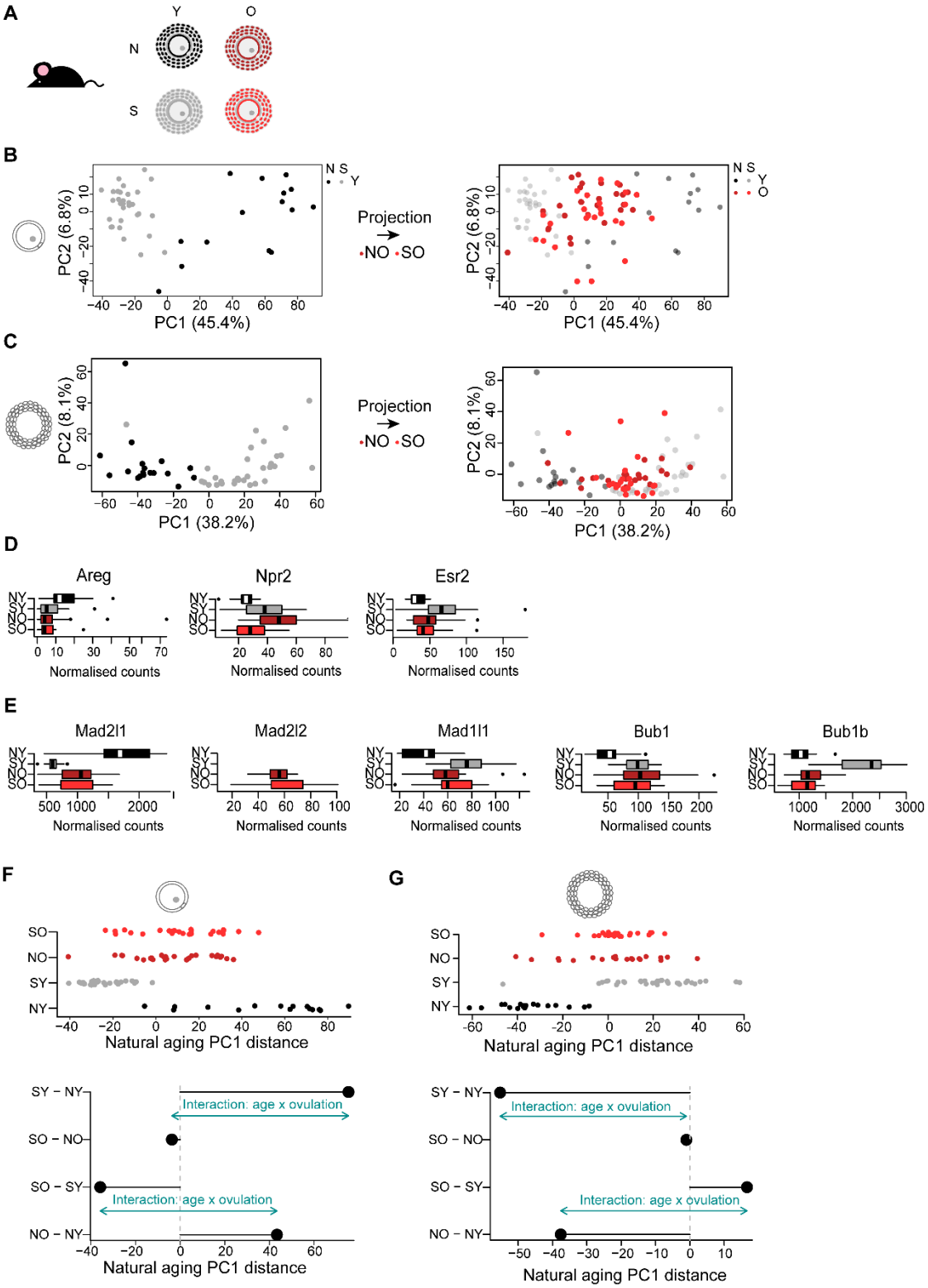

Figure 5. Relative impacts of superovulation and ageing effects.

(A) Schematic drawing of mice COCs in all four conditions: naturally ovulated young (NY, black), naturally ovulated old (NO, dark red), superovulated young (SY, grey), superovulated old (SO, red). (B) PCA of young oocytes based on differentially expressed genes between NY and SY (left, n = 15 NY and 31 SY OCs), where old oocytes are projected on this PCA (right, n = 26 NO and 26 SO OCs). (C) PCA of young granulosa cells based on differentially expressed genes between NY and SY (left, n = 15 NY and 31 SY GCs), where old granulosa cells are

projected on this PCA (right, n = 26 NO and 26 SO GCs). (D) NY, SY, NO and SO granulosa cell expression of genes involved in cGMP cascade. Centre line - median, box limits - first and third quartiles, whiskers - maximum and minimum or 1.5 times interquartile range if there were outliers, dots - outliers. (E) NY, SY, NO and SO oocyte SAC gene expression. Centre line - median, box limits - first and third quartiles, whiskers - maximum and minimum or 1.5 times interquartile range if there were outliers, dots - outliers. (F) Top - PC1 coordinates of oocytes in all four groups from PCA in Figure 5B. Bottom – PC1 shift quantification between groups. (G) Top - PC1 coordinates of granulosa cells in all four groups from PCA in Figure 5C. Bottom – PC1 shift quantification between groups. The figure is adapted from Daugelaite et al., 2023 (Biorxiv).

1.1.6. COC ageing is modestly conserved between mouse and human

As it is not possible to use naturally ovulated human samples, the COCs collected after hormonal treatments from human were used to compare the gene expression dysregulations in human granulosa cells and oocytes during ageing with the results obtained in mice.

First, human granulosa cells were collected from patients undergoing IVF, the RNA extracted and libraries prepared for bulk RNA-seq (Methods). The patients were distributed into younger (<31 years old, n = 4) and older (>38 years old, n = 4) age groups (Figure 6A). Because mural granulosa cells were collected during IVF procedure, the analysis strategy was adapted to account for differences in cell types (only cumulus granulosa cells in mice) by excluding genes with differential gene expression between human mural and cumulus cells (Methods). Second, the oocytes are not available for research in Germany, therefore, a dataset from already published study (174) was a source of gene expression data for oocytes in younger (<27 years old, n = 6) and older (>40 years old, n = 6) patients (Figure 6B).

In granulosa cells, the dysregulation of various signalling pathways, such as estrogen-dependent gene expression, were shared between human and mice (Figure 6C, Methods). There was a divergence in pathways involved in cell cycle regulation and fatty acid metabolism, among others. In oocytes, a similar analysis revealed that pathways in mitochondrial metabolism, oxidative stress response, and embryogenesis, responded similarly to ageing in both species (Figure 6D, Methods). Conservation of hormonal signalling and fertility pathways in COCs suggests that ageing might similarly affect the COC quality in human and mice.

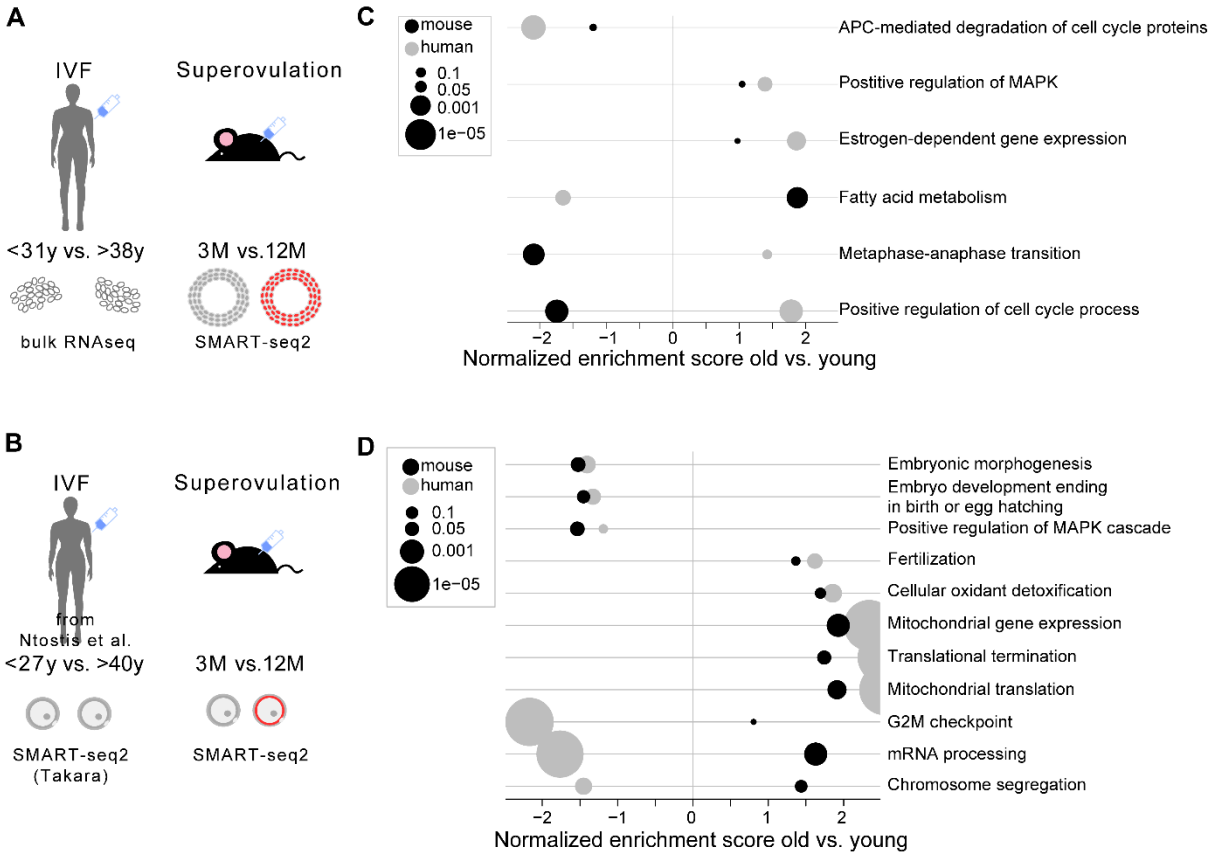

Figure 6. COC ageing comparison between human and mice.

(A) Schematic drawing of granulosa cell sample collection from IVF patients (left) and superovulated GCs from young and old mice (right). (B) Schematic drawing of publicly available study design for oocyte collection from IVF patients (left) and this study's superovulated OCs from young and old mice (right). (C) Overreprentation analysis of selected pathways in granulosa cells during ageing. The size of the circles shows adjusted p-values. (D) Overreprentation analysis of selected pathways in oocytes during ageing. The size of the circles shows adjusted p-values. The figure is adapted from Daugelaite et al., 2023 (Biorxiv).

1.2. Predicting Early Embryo Developmental Potential

In the second part of this project, the search of non-invasive methods of embryo quality prediction was focused on the idea that the communication between oocyte and its granulosa cells is vital for oocyte developmental potential. The approach was based on prospective, rather than retrospective study design, including targeted and controlled experimental set-up.

1.2.1. Superovulation perturbs oocyte-granulosa communication

To study cell-cell communication in oocytes and granulosa cells, the experiments were specifically designed to retain the information about OC-GC *in vivo* pairing. In these analyses, only paired data from OCs and GCs was used.

A cell-cell communication profile was constructed for each COC using the co-expression of ligand-receptor pairs (Methods, Figure 7A). Naturally ovulated COCs formed one group after hierarchical clustering, indicating uniform cell-cell communication. Surprisingly, superovulated COCs divided into two distinct groups (clusters S_N and S), with S_N more closely resembling the naturally ovulated COCs. These clusters were stable after subsampling and bootstrapping (Figure 7B).

In these clusters, several fertility-related ligand-receptor pairs were affected by superovulation, with stronger effects in S than S_N cluster (Figure 7A). In oocyte-to-oocyte communication by Fgf1-Fgfr1/2, fibroblast growth factors activate MAPK signalling cascade, partially induce extracellular signal-regulated protein kinase 2 (*Erk2*) phosphorylation and contribute towards meiosis re-initiation through Npr2 cascade (175). In oocyte-to-granulosa signalling, Bmp15-Bmpr1+2 are directly affected by gonadotropins and their mRNA levels should be lower in mature COCs (176), which was not the case for S group. In granulosa-to-oocyte signalling, Hspg2-Dag1 levels are important for oocyte quality and IVF outcomes. Lower perlecan (*Hspg2*) mRNA levels are associated with higher oocyte quality (177), as in N and, partially, S_N clusters. In granulosa-to-granulosa signalling, Wnt4-Fzd3+Lrp5/6, β-catenin canonical pathway is important for steroidogenesis in granulosa cells (178) and though particular timing of *Fzd3* expression after hCG injection is unclear, other Frizzled receptors, such as Fzd4, show a decrease protein amounts towards the ovulation.

The relative similarity between clusters S_N and N could also be observed in the PCA space (Figure 7C). These two clusters only appeared after superovulation in young mice, but not in naturally ovulated old mice, where samples have variable intermediate gene expression (Figure 7D). To better understand functional differences between the Sn and S groups, ORA analysis was performed and several pathways selected (Figure 7E). Pathways in cell cycle, several signalling cascades, responses to stress and hormones were more often upregulated in S cluster compared to S_N.

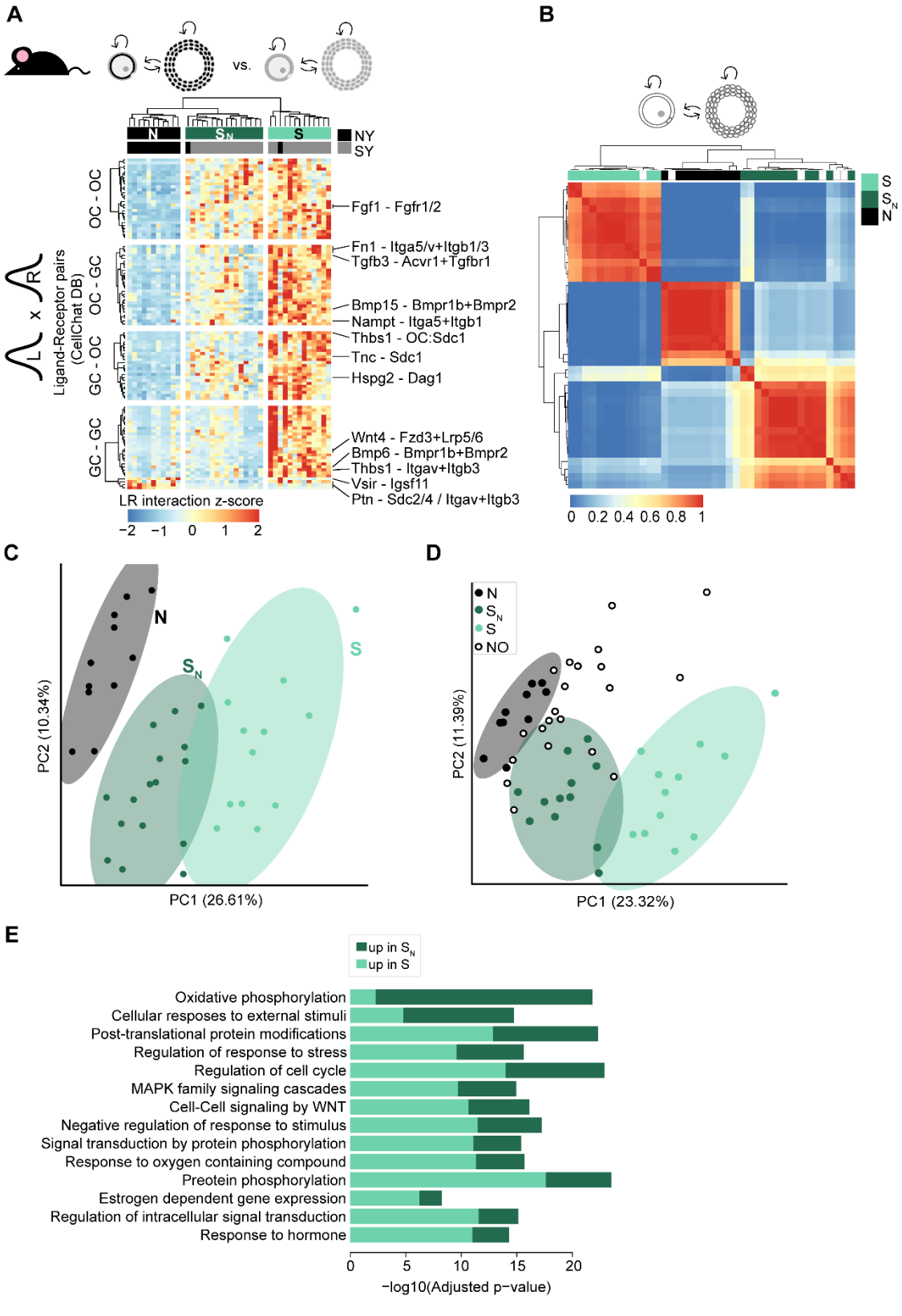

Figure 7. Cell-cell communication patterns after natural ovulation and superovulation.

(A) Ligand and receptor gene expressions are used to calculate cell-cell interaction scores between oocyte and its granulosa cells (OC-GC, GC-OC), as well as oocyte-oocyte (OC-OC) and granulosa-granulosa (GC-GC). Interaction scores are represented for ligand-receptor pairs (rows, z-scaled) in NY and SY COCs (columns, n = 13 NY, 27 SY OC-GC pairs). Only significantly different pairs between three clusters are shown (Kruskal-Wallis test, adjusted p-value < 0.05). Interaction scores are shown for ligand-receptor pairs (rows, z-scaled) in young natural and superovulated cells (columns, n = 13 NY, 27 SY OC-GC pairs) that displayed significant change between the three clusters (Kruskal-Wallis test adjusted p-value < 0.05). (B) Stability of the clusters are assessed by bootstrapping. The colour represents how often the two cells cluster together. (C) OC-GC interaction scores in PCA space for NY and SY (split into S_N and S) COCs. (D) OC-GC interaction scores in PCA space for NY, SY (split into S_N and S) and NO COCs. (E) Overrepresentation analysis of differentially expressed genes between S and S_N groups. Upregulated proportion of pathway genes in S_N is shown in dark green, upregulated in S in bright green. The figure is adapted from Daugelaite et al., 2023 (Biorxiv).

1.2.2. Transcription factor activity disruptions after superovulation reveal granulosa cell heterogeneity

To investigate TF activities in superovulated COCs, TFs upstream of dysregulated pathways were identified, and activity scores were calculated using target gene expression levels (Methods, Figures 8A and 8B). Transcription factors with insufficiently expressed direct target genes, like *Esr1* and *Esr2*, were excluded from the analysis. In oocytes, TF activity showed clustering into natural and superovulated groups without a notable substructure (Figure 8A). This is likely because of silenced transcription at meiosis II (79).

Superovulated granulosa cells formed two separate sub-clusters (clusters S_N and S, Figure 8B), as in cell-cell communication analysis (see section above). TFs showed activity in cell cycle, damage response, mostly active in N cluster, signalling, more active in both superovulated clusters, and hormonal response, with highest activity in S cluster (Figure 8C). A supplementary pathway activity analysis confirmed that S_N granulosa cells closely resembled normally ovulated cells in pathways related to replication and protein repair, MAPK and estrogen signalling, and showed intermediate activity in cell cycle control, DNA repair, and androgen receptor signalling (Methods, Figure 8D). Pathways related to fatty acid metabolism and double-strand break repair were more similar between S_N and S clusters compared to N.

To verify that gene expression differences were reflected in TF usage, the TF activity profiles were computed for old GCs. In the PCA space, the TF activity profiles for old granulosa cells were interspersed but aligned closer to cluster S_N than S (Figure 8E).

For further analyses, the consensus clusters for N, S_N, and S were defined by including the 34 out of 40 granulosa cell samples where cell-cell communication and TF activity analyses were consistent.

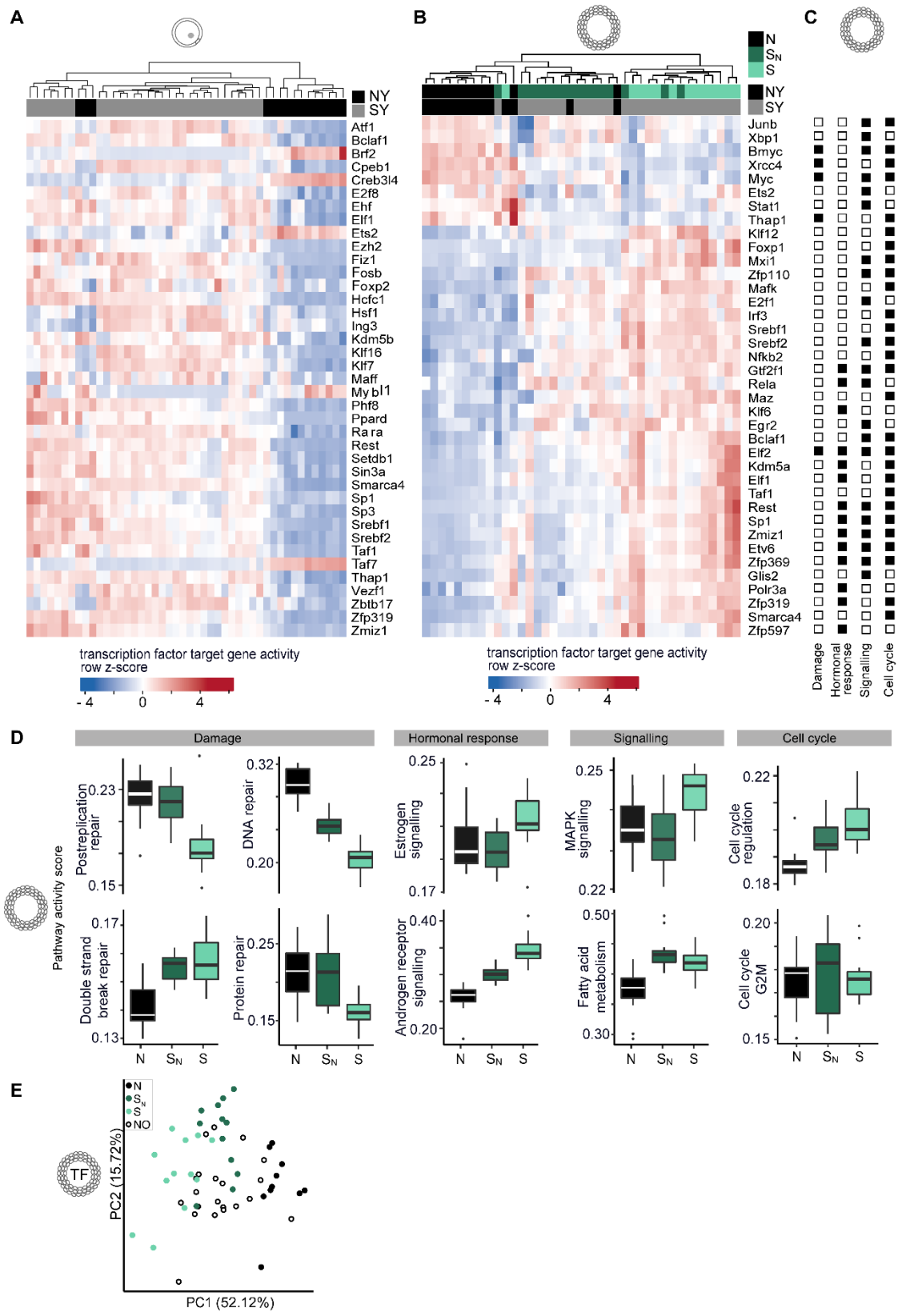

Figure 8. Transcription factor activity after natural and superovulation.

(A) Transcription factor (TF) activity scores for TFs associated with overrepresented pathways from Figure 2A. TFs with significantly different activity scores between superovulated and naturally ovulated young oocytes are represented (permutation test). (B) TF activity scores for TFs associated with overrepresented pathways from Figure 2B. TFs with significantly different

activity scores between superovulated and naturally ovulated young granulosa cells are represented (permutation test, n = 13 NY, 27 SY GCs). (C) TFs associated with overrepresented pathways from Figure 2B in superovulated granulosa cells. Filled squares show significant association with pathway category (damage, hormonal response, signalling, and cell cycle). (D) Activity scores of selected overrepresented pathways from Figure 2B in GCs. The activity scores are split by consensus clusters N, S_N and S (n = 10 N, 12 SN, 12S). Centre line represents median, box limits - first and third quartiles, whiskers show maximum and minimum or 1.5 times interquartile range in case of outliers, dots - outliers. (E) Activity scores of TFs in NY, SY and NO granulosa cells in PCA space. The figure is adapted from Daugelaite et al., 2023 (Biorxiv).

1.2.3. Development of targeted IVF experiment

To investigate whether the two granulosa clusters reflect different embryo development outcomes, I developed a targeted IVF assay to link granulosa cell transcriptional state to early embryo development (Methods, Figure 9A). Briefly, I took similar approach as in COC collection experiments, but instead of flash freezing the oocyte, I performed IVF on single oocytes and cultured single embryos until early morula (Figure 9B) and late blastocyst stages (Figure 9C), then collected and sequenced them. In parallel, I collected and sequenced the associated granulosa cells. I collected a substantial dataset of 219 COCs from 9 NY and 8 SY mice. The fertilization rate was 91.5% for naturally ovulated oocytes and 87.9% for superovulated oocytes, hence, the transcriptomes were analysed for the resulting 154 embryos.

A support-vector machine (SVM) classifier was trained using the consensus 34 granulosa cell replicates (see section above), achieving 83.3% accuracy on the test set (5/6 embryos correctly classified, Figure 9D). This classifier was then used to categorize granulosa cells from new IVF experiments into S_N, S, and "not assignable" (NA) (Methods, Figure 9A). Labels from the classified granulosa cells were then transferred to their corresponding embryos.

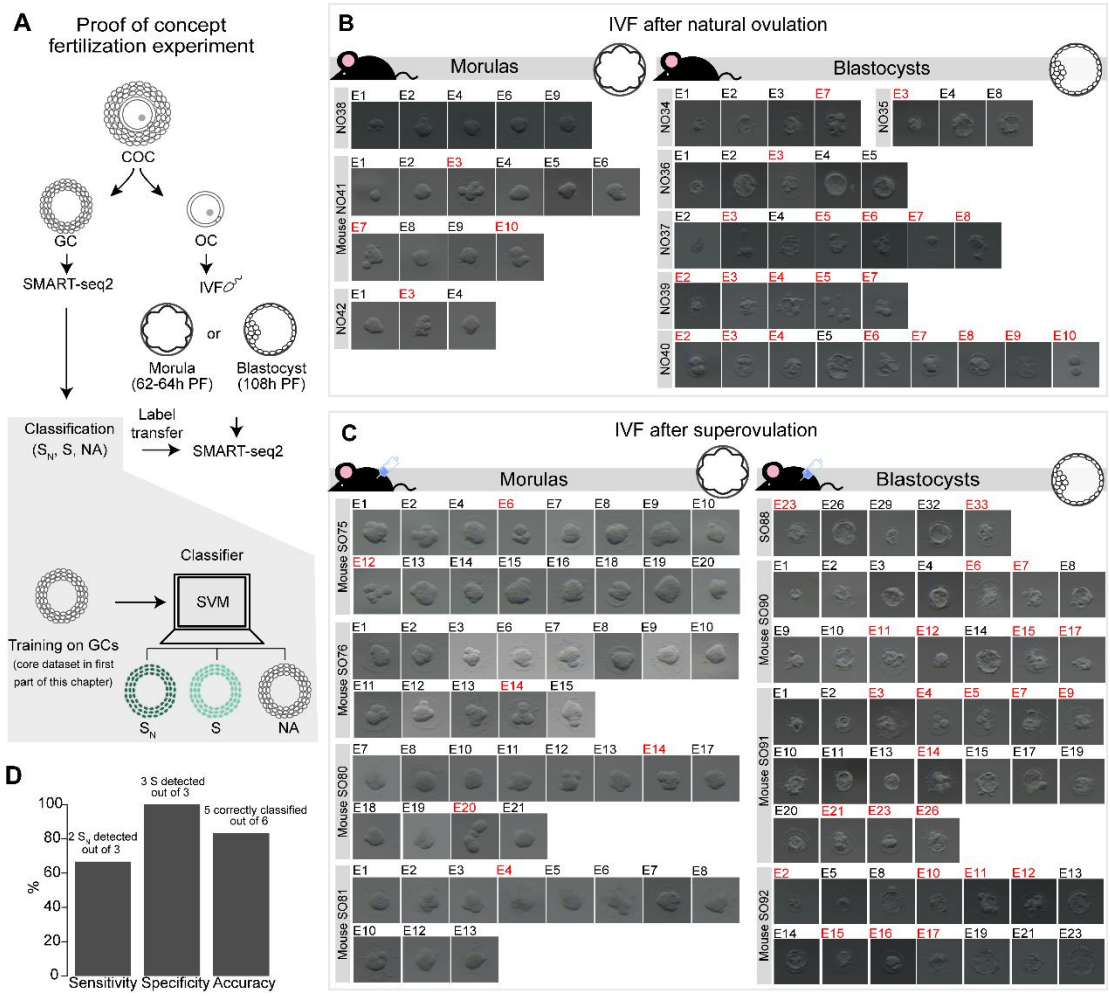

Figure 9. Targeted IVF assay and full embryonic dataset.

(A) Schematic representation of targeted IVF experiment where individual cumulus-oocyte-complexes (COCs) are digested into granulosa cell (GC) cloud and a single oocyte (OC). The granulosa cells are collected, libraries prepared using SMART-seq2 and then classified into S_N, S and NA classes by a previously trained support vector machine (SVM) classifier. The classifier is trained on granulosa cells from a separate experiment described in previous chapters. In parallel, the single oocytes are fertilized and cultured 62-64h post-fertilization (PF) until compacted morula stage or 108h PF until late blastocyst stage. The embryos are then collected and libraries prepared using the whole embryo by SMART-seq2. The classification labels from GCs are then transferred onto embryos. (B) Stereomicroscope photos of embryos at collection time-point of embryos derived from natural ovulation – morulas (left) and blastocysts (right). Each mouse is marked by labels starting with "NO" and each embryo is marked by labels starting with "E". Embryos marked in red arrested before reaching respective developmental stage. (C) Stereomicroscope photos of embryos at collection time-point of embryos derived from superovulation – morulas (left) and blastocysts (right). Each mouse is marked by labels starting with "SO" and each embryo is marked by labels starting with "E". Embryos marked in red arrested before reaching respective developmental stage. (D) SVM classifier's sensitivity, specificity and accuracy on the granulosa cell test set. The figure is adapted from Daugelaite et al., 2023 (Biorxiv).

1.2.4. Granulosa cells can predict early embryo trajectory

Further, each embryo was assessed to investigate its developmental trajectory, developmental arrest and copy number variation (CNV).

To closely investigate the developmental timing of these embryos, a developmental pseudotime reference was constructed by combining a previously published dataset of early embryonic development (179) with this study's morulas and blastocysts derived from natural ovulation (Figure 10A). Genes that correlated closely with developmental stages were selected (Figure 10B), and all embryos were ordered into a developmental trajectory (Methods). As expected (180), embryos from natural ovulation were the most advanced (Figure 10C). Embryos from superovulated oocytes showed clear separation, with S_N embryos being more advanced and closer to the natural group (Figure 10C). Several embryos did not develop to their respective developmental stages. For the 103 superovulated embryos, 14 arrested before reaching the 8-cell stage (Figure 9C, red marking), with 11 classified as S or NA (Figure 10D). The number of arrested embryos not statistically significant for the classification. Only three embryos showed aneuploidy detectable by gene expression data (Figure 10E), without a relationship with their classification.

To investigate whether SN and S classes can be discriminated by only a few markers, I tested gene expression by quantitative polymerase chain reaction (qPCR) of several selected genes from the SMV classifier. I performed a qPCR assay on granulosa cells from NY and SY mice on 12 target genes and used *Gapdh* as control (Figure 10F), out of which *Dync1h1*, *Hook3*, *Kmt2a*, *Lrp6*, *Phf20l*, *Vcan*, and *Zfp451* showed statistically significant differences between S_N and S granulosa cells.

Together, these results demonstrate that transcriptional signatures of granulosa cells can be used to non-invasively predict which pre-implantation embryos obtained after superovulation will resemble those obtained after natural ovulation. The initial transcriptional state of a COC seems to be reflected in the gene expression of derived embryos, despite the extensive genome remodelling during fertilization and ZGA.

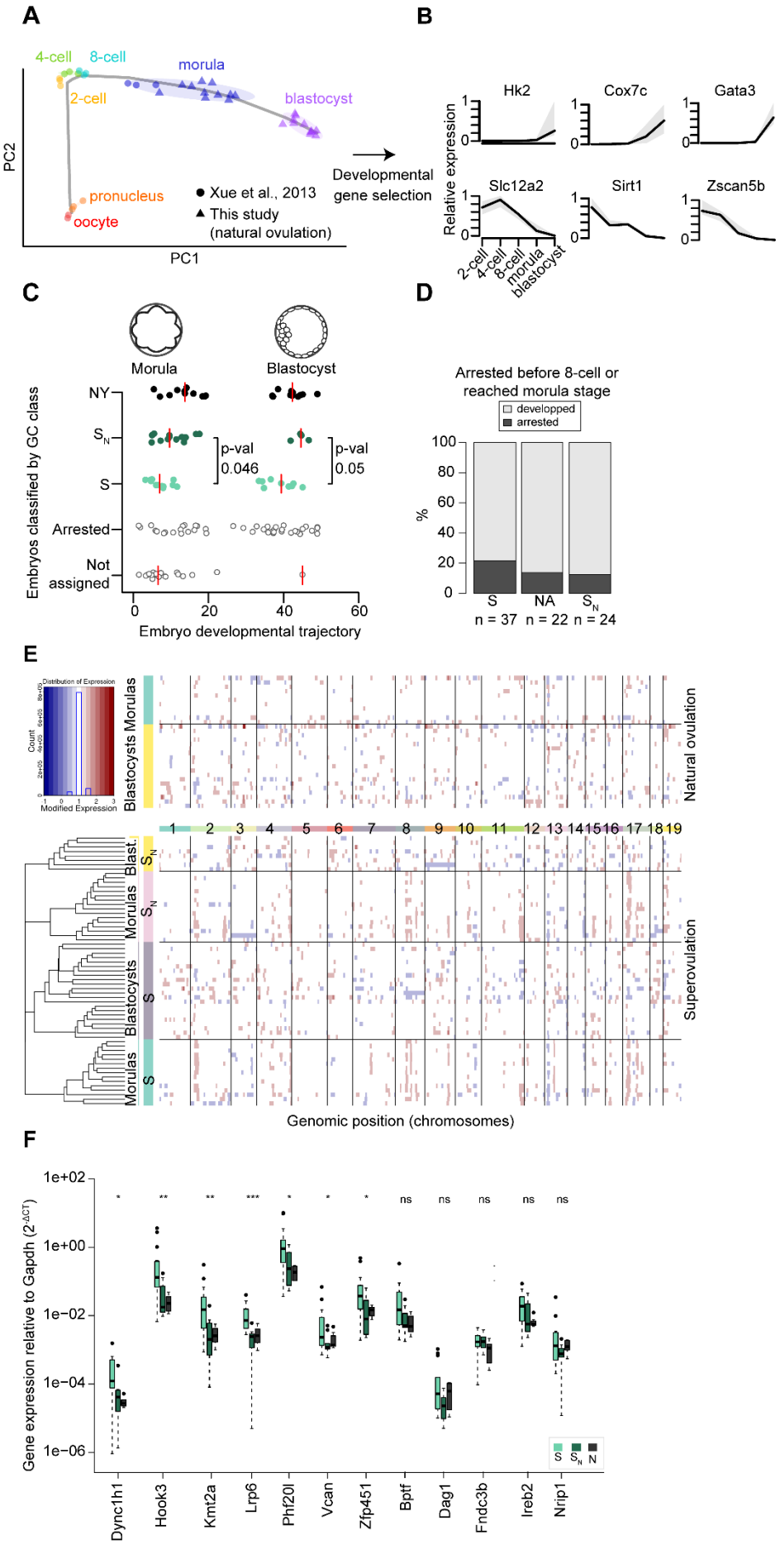
A
4-cell
8-cell
morula
2-cell
blastocyst
pronucleus
oocyte
PC2
PC1
Xue et al., 2013
This study
(natural ovulation)
Developmental
gene selection
B
Hk2
Cox7c
Gata3
Slc12a2
Sirt1
Zscan5b
Relative expression
2-cell
4-cell
8-cell
morula
blastocyst
C
Morula
Blastocyst
NY
S_N
S
Arrested
Not
assigned
p-val
0.046
p-val
0.05
Embryos classified by GC class
Embryo developmental trajectory
D
Arrested before 8-cell or
reached morula stage
developped
arrested
%
S
NA
S_N
n = 37 n = 22 n = 24
E
Distribution of Expression
Modified Expression
Blastocysts Morulas
Natural ovulation
Blast.
Morulas
Blastocysts
Morulas
Superovulation
Genomic position (chromosomes)
F
Gene expression relative to Gapdh (2^-ΔCT)
Dync1h1
Hook3
Kmt2a
Lrp6
Phf20l
Vcan
Zfp451
Bptf
Dag1
Fndc3b
Ireb2
Nrip1

Figure 10. Embryo developmental trajectory prediction from its granulosa cells.

(A) Embryo developmental pseudotime from oocyte to blastocyst based on data from Xue et al. (179) and this study. (B) Examples of developmental genes used for the pseudotime analysis. (C) Developmental pseudotime of embryos classified by their GC class. The pseudotime is calculated on developmental genes. Median is marked by red line; p-values are calculated using Wilcoxon test. (D) Percentage of embryos that stopped developing before morula stage in S_N and S groups vs. embryos that developed until morula stage. P-value is calculated using Fisher test and is not significant because of small embryo number. (E) inferCNV package is used to obtain whole genome copy number changes in embryos. Natural ovulation embryos are used as a reference (top panel) and superovulated embryos are represented as test (bottom panel). Only three embryos are aneuploid, without a clear link to their classification through GCs. (F) qPCR gene expression measurement of 12 chosen genes from classifier in superovulated and naturally ovulated young granulosa cells (n = 7 NY, 11 S_N and 23 S GCs). The p-value was calculated between S_N and S groups by Wilcoxon test, p-value < 0.05 (*), 0.01 (**), 0.001 (***). Centre line shows median, box limits - first and third quartiles, Whiskers represent the maximum and minimum values or 1.5 times the interquartile range, in case of outliers, dots - outliers. The figure is adapted from Daugelaite et al., 2023 (Biorxiv).

Discussion

The aim of this project was to dissect the impacts of superovulation and ageing on COCs using mouse as a model.

The research questions driving this investigation were:

- What molecular pathways are affected by superovulation in oocytes and granulosa cells? How is cell-cell communication affected?
- How do superovulation and natural ovulation compare in young and old mice? Are the impacts of superovulation and ageing on COCs transcriptomes additive and/or interactive?
- Can granulosa cell transcriptomes be used to predict the developmental outcome of associated oocytes?

To answer these questions, innovation in methodology was necessary. I adapted three main techniques: ovulation protocols, technique for COC isolation, and a targeted IVF for embryo trajectory prediction.

Standard superovulation protocols have mostly been developed for pre-pubertal mice but also work well in young adults. In contrast, there are much less studies that superovulate old mice as they yield much smaller amounts of oocytes than pre-pubertal mice (181). Nevertheless, it is still possible to superovulate older mice. Natural ovulation protocols have been used in young mice (182) but are extremely rare in old mice because ovulation is most often unsuccessful. I used the study from Ishikawa and Endo (183) who provide proof about natural ovulation in old mice and prove that ovulation is simply slower. I hence used that idea to naturally ovulate 12M old mice by delaying the COC collection by only couple of hours. I used the same approach for superovulating old mice and achieved only marginally lower amounts of retrieved COCs compared to young superovulated mice. This suggests that the ovarian reserve is still able to recruit follicles at 12M and that ovaries respond to hormonal stimulus for folliculogenesis. It is not known what causes this shift in ovulation timing, but slower metabolism, response to hormones, or changes in circadian rhythm could be contributing. It would be very interesting to study ovulation timing in IVF patients and whether older patients could profit from a delayed oocyte retrieval, instead of current standard of 36 hours after hCG injection, despite their age.

Many studies that tackle oocyte-granulosa cell communication through transcriptomics isolate immature follicles from the ovary, perform various *in vitro* maturation (IVM) experiments, or collect oocytes and GCs without retaining information about their pairing. Therefore, data about *in vivo* ovulated OC-GC pairs is missing. I adapted standard oocyte collection protocol, which use high concentration of hyaluronidase to clean the oocytes from granulosa cells. Instead, I used a very mild concentration that is enough to separate the COCs from one another. Inspired by COC collection protocol from whole ovaries used by Zhang et al. (159), I used Accutase, which is a mild cell culture enzyme mix, to further clean oocytes from GCs, while

working in individual drops of media. These simple, yet important, methodology changes allowed me to keep the *in vivo* information about OC-GC pairing, which was necessary for cell-cell communication analyses.

This technique also laid foundations for a targeted IVF experiment where I fertilized single oocytes while also collecting the associated granulosa cells. Studies that aim to predict embryo quality using GC transcriptomes mostly used the retrospective approach to correlate already known embryo developmental status to GC state. This contradicts the logic of preventive testing, as it is preferable to identify embryos with higher developmental potential before waiting for them to develop. My targeted IVF experiment offers a controlled, prospective study design, where GC status is transferred onto embryos, demonstrating how the GC transcriptional state remarkably follows embryo trajectory. One would hope that similar approaches could be tested in clinical settings, especially for patients undergoing ICSI where single oocytes are handled but their granulosa cells removed.

The relatively negative effect of superovulation on oocytes is known (184), and this study contributes by providing further proof about perturbations in specific molecular pathways, cell-cell communication and transcription factor activity. Results showed various deregulations in pathways related to oocyte maturation, including maternal transcript remodelling, which was not directly demonstrated before. Probably most unexpected was the finding that superovulated young granulosa cells split into two groups, where one group resembled natural ovulation more. Previously, clear transcriptional differences were shown between mural and cumulus granulosa cells in adults, and there was some proof about different GC waves during embryonic development. It would be intriguing to study the origin of these two groups of cumulus GCs further as they were only observed in younger mice.

The comparison between superovulation and ageing was surprising due to the significant similarity in transcriptional regulation, suggesting that these processes share underlying dysregulation mechanisms. However, the difference comes in the strength of perturbation, as old COCs tend to have intermediate transcriptomic profiles. Due to afore mentioned difficulties in naturally ovulating old mice, majority of studies make their conclusions about ageing from superovulated animals. By including naturally ovulated COCs as a reference, it was finally possible to test the additivity and interaction of superovulation and ageing. This 4-way comparison showed that superovulation and ageing are not completely independent processes – they interacted to perturb similar molecular pathways. They were also non-additive, meaning that the effect does not increase when using a superovulated old mouse instead of naturally ovulated mouse. Therefore, naturally ovulated COCs serve as a crucial reference for distinguishing the effects of ageing from superovulation and should be used in ageing studies as a standard.

In conclusion, I developed innovative techniques to analyse the functional interactions between oocytes and granulosa cells including predictions about embryo development. This research offers technical tools and novel scientific insights for enhancing IVF protocols and precisely studying female reproductive ageing.

Chapter 2
COC evolution in closely related mice species

The evidence of gamete evolution mostly come from studies of male but not female gametes. We know that sperm evolves faster than somatic tissues, and we tend to assume the same for oocytes. In the second research project of my thesis, the question is, how do oocytes evolve? Here, I use different mice species (*Mus musculus*, *Mus musculus castaneus*, *Mus spretus*, and *Mus caroli*, where evolutionary distances are relatively small – this allows a fine-grained comparison of evolutionary transcriptional divergence. In these species, there is limited number of studies investigating oocytes, and especially, in context of natural ovulation.

I completed the core experiments of this project but the data analysis is still ongoing, therefore, the results are preliminary.

Contribution acknowledgement

Perrine Lacour performed all bioinformatics analyses.

Anja Schneider and Marie Luise-Koch managed wild-derived mice colonies.

Animal caretakers checked vaginal plugs for naturally ovulated mice.

2. Results

2.1. Study design

To answer questions about gamete and somatic cell divergence, I employed four species of mice *Mus musculus* (C57Bl6/J), *Mus musculus castaneus* (CAST), *Mus spretus* (SPRET), and *Mus caroli* (CAR). These four species have diverged from each other 1, 2, and 3 million years ago, respectively (MYA). I then collected COCs from these mice after natural ovulation (N) and superovulation (S), retaining information about oocyte and surrounding GCs *in vivo* pairing (Figure 1A, Methods). This will allow comparative analyses of cell-cell communication and how different species react to external hormonal stimuli.

2.2. Reproduction characteristics of exotic mice

As seen in *Mus musculus* mice, ovulation depends on timing. For each species of wild-derived mice, I created strategies for correct ovulation timing by inducing ovulation and observing the COC expulsion. As a reference, in C57BL6/J superovulation is optimal at 14-16h after hCG injection and natural ovulation at 2-3h after the beginning of the light cycle (Methods). I determined the ovulation times for other species, as such:

- CAST mice superovulation was optimal at 18-19h post-hCG (for example, at 17h post-hCG there is lower number of COCs present in the oviduct, indicating that it is too early);
- CAST mice natural ovulation was optimal at 5-6h after beginning of the light cycle;
- SPRET superovulation worked well at 16-17h post hCG;
- SPRET natural ovulation at 2-4h after beginning of the light cycle;
- CAR superovulation was good at ~17h post hCG;
- Attempts to naturally ovulate CAR failed.

To evaluate the ovulation rates for each species, I calculated the average number of COCs found in oviducts after natural ovulation (Table 1). Natural ovulation rates were very similar to litter size after natural mating, suggesting that fertilization, implantation and further embryo development are efficient in these mice species.

Superovulation increased the ovulation rate in all species, where *Mus musculus* ovulates 2.7, *Mus castaneus* 2.5, *Mus spretus* 1.6 times more COCs than in the respective natural ovulations (Figure 1B). *Mus caroli* may ovulate 2.4 times more after superovulation than in natural conditions (calculated from litter size, instead of natural ovulation, Table 1). There is no data about litter sizes after superovulation available because these species were not used for breeding after superovulation. For further

experiments, I collected COCs, where 187 OCs and 200 GCs passed quality control (Table 2, *Mus musculus* dataset was used in Chapter 1).

Table 1. Ovulation rates and litters of four mice species.

	Natural ovulation			Natural mating			Superovulation		
Mouse species	Number of COCs in oviduct	Number of mice	Average ovulation rate	Total pup number	Total number of litters	Average pup number/ litter	Number of COCs in oviduct	Number of mice	Average ovulation rate
Mus musculus	101	14	7.2	542	128	4.2	288	15	19.2
Mus musculus castaneus	28	6	4.7	107	24	4.5	46	4	11.5
Mus spretus	20	4	5.0	123	23	5.3	48	6	8.0
Mus caroli	N/A	N/A	N/A	112	20	5.6	40	3	13.3

Table 2. Number of oocytes and granulosa cells that passed quality control.

	Natural ovulation		Superovulation	
Mouse species	Number of OCs	Number of GCs	Number of OCs	Number of GCs
Mus musculus	17	18	30	31
Mus musculus castaneus	24	27	38	37
Mus spretus	17	18	28	34
Mus caroli	N/A	N/A	33	35

2.3. Female gametes drive reproductive evolution

Oocytes and granulosa cells clearly separated by their transcription in the principal component analysis (PCA) space (Figure 1C), however, this separation was species-specific only for oocytes (Figure 1D). PC1 and PC2 dimensions explained most of the variation, but cell type and species-specific separations could also be observed in PC3/4 and PC4/5. When the same PCA was plotted excluding X-chromosome genes, the data points in the PCA did not change, therefore, X-chromosome genes do not drive the gamete divergence. In addition, the divergence of oocytes corresponded to the species divergence time (Figure 1E). To summarize, the preliminary results showed species-specific gamete but not somatic cell divergence.

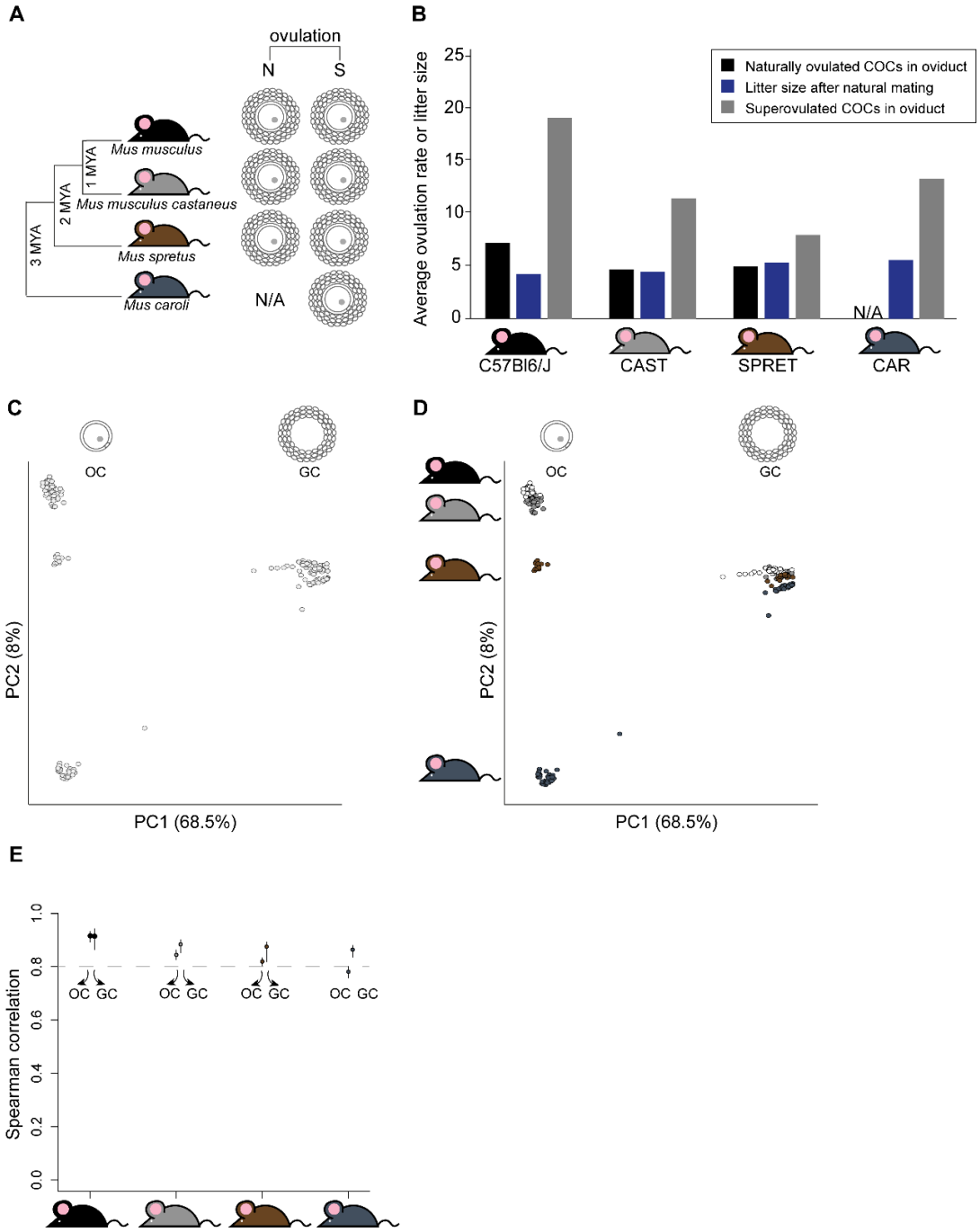

Figure 1. Oocyte and granulosa cell diversion in four closely related mice species.

(A) Schematic drawing of young mice COCs collected from *Mus musculus*, *Mus musculus castaneus*, *Mus spretus* and *Mus caroli* after natural ovulation (N) and superovulation (S). COCs from *Mus caroli* after natural ovulation were not retrieved (N/A). (B) Count of ovulated COCs in oviducts after natural ovulation (black column) and superovulation (grey column) as well as litter size (number of pups per litter) after natural breeding (blue column) in four species. (C) PCA space for all oocytes (OC) and all granulosa cells (GC) with clear separation by cell type. (D) PCA space for all OCs and all GCs coloured by mouse species: *Mus musculus* – black, *Mus musculus castaneus* – grey, *Mus spretus* – brown, *Mus caroli* – grey-blue. (E) Spearman's correlation coefficients between orthologous variable gene expression profiles in OCs and GCs between four mice species, colours are similar as in previous figures.

Discussion and Outlook

The preliminary results provide a promising basis for studying oocyte evolution, and suggest that oocytes drive evolution. In further work, many more questions will need to be explored. The first question is which genes drive this gamete divergence? From preliminary analysis showed the X-chromosome genes are not the main force driving the divergence. It maybe a set of developmental or oocyte-specific genes. There is currently little research on divergence in oocytes compared to sperm, but an example of positive selection were non-experimentally demonstrated for zona pellucida proteins (185). Cell-cell communication between oocyte and its granulosa cells is crucial for oocyte development, but does it play any role in evolution? It will be possible to analyse specific oocyte-granulosa pairs to study any possible relationship. Another question that arises is how changes in COC transcriptional state after hormonal stimulation are conserved between species. In Chapter 1, distant species – mouse and human – shared a modest conservation of pathways, but many similarly dysregulated pathways were related to hormone response. This dataset allows a more fine-grained analysis of conservation because species are closely related, cell types and experimental conditions are exactly the same.

From more technical perspective, it is the first time that these species were naturally ovulated, and there are very few studies that use superovulated *Mus caroli* (186). Species ovulation rate depends on genetic background (49), reflected in different ovulation rates and average litter sizes in these four mice species. As a limitation, the numbers of mice used for calculations are not very large and the ovulation rate could change when adding more mice into calculation. In addition, ovulation time-windows were optimized on a minimal number of mice possible, hence, when the ovulated COC number was satisfactory, I did not try to optimize further. The need to collect oocytes later than standard 48h is sometimes reported in older scientific papers but gets lost in the newer literature (186,187). The natural ovulation in *Mus caroli* failed because vaginal plugs did not show. It is possible that they dissolve faster than in other species, mice need an additional stimulus for mating or the vasectomized males were not interested in mating because of hormone loss. From colony management experience, *Mus caroli*, as other wild-derived species, take a little bit longer to mate, but they eventually have litters. One week of daily plug observation might not have been enough.

Overall, the dataset is ready for further analysis, which will focus on identifying genes that drive divergence, cell-cell communication and transcriptional response to hormonal stimulation.

Chapter 3

Ovarian cyclicity and ageing increase inflammation in lower reproductive tract organs

During estrous cycle, FRT rapidly clears inflammatory events and restore normal reproductive function. Fibroblasts are main source of inflammatory cytokine production and constitute ECM. During ageing, insufficient inflammation clearing and improper fibroblast homeostasis could lead to chronic inflammation and increased ECM production.

In the larger concept of this project, there were several major results:

- The upper (ovary, oviduct, uterus) and lower reproductive tract (cervix, vagina) differ in their composition and transcription;

- Fibroblasts shape inflammation during estrous cycle through cell-cell communication;

- Cyclicity contributes to the age-related accumulation of fibrosis and inflammation in the FRT.

In this chapter, I will only describe the results where I contributed directly. This project is now completed and the presented results are published:

“The cycling and aging mouse female reproductive tract at single-cell resolution” - *Cell* 187, 981–998. DOI: https://doi.org/10.1016/j.cell.2024.01.021

Ivana Winkler#, Alexander Tolkachov#, Fritjof Lammers$, Perrine Lacour$, **Klaudija Daugelaite**$, Nina Schneider, Marie-Luise Koch, Jasper Panten, Florian Grunschlager, Tanja Poth, Bianca Machado de Avila, Augusto Schneider, Simon Haas, Duncan T. Odom,* and Angela Goncalves*.

Contribution acknowledgement

Dr. Ivana Winkler and Perrine Lacour performed all bioinformatics analyses.

Dr. Alexander Tolkachov and Nina Schneider generated core scRNA-seq dataset for 3M, 18M and pregnant mice.

Nina Schneider and Marie-Luise Koch helped to generate scRNA-seq dataset for 9M, 12M, and 15M mice.

Dr. Bianca Machado de Avila and Dr. Augusto Schneider prepared VCD and related control samples.

Other contributions that are less relevant for this thesis are mentioned in the publication.

3. Results

3.1. Study design

Shortly, in the larger scope, this study compiled various types of data, with many analyses focusing on different phases of estrous cycle, including data from decidualized uteri in mice and human. I contributed data on FRT ageing and age-related fibrosis, so in this chapter, I will focus solely on the directly relevant results. Specifically, I provided scRNA-seq experimental data from FRT of 9M, 12M, 15M old mice in diestrus (~128,000 cells), complete spatial transcriptomics dataset (~34,000 covered spots) and coordinated chemically treated (VCD) sample import and processing (Figure 1 A-C).

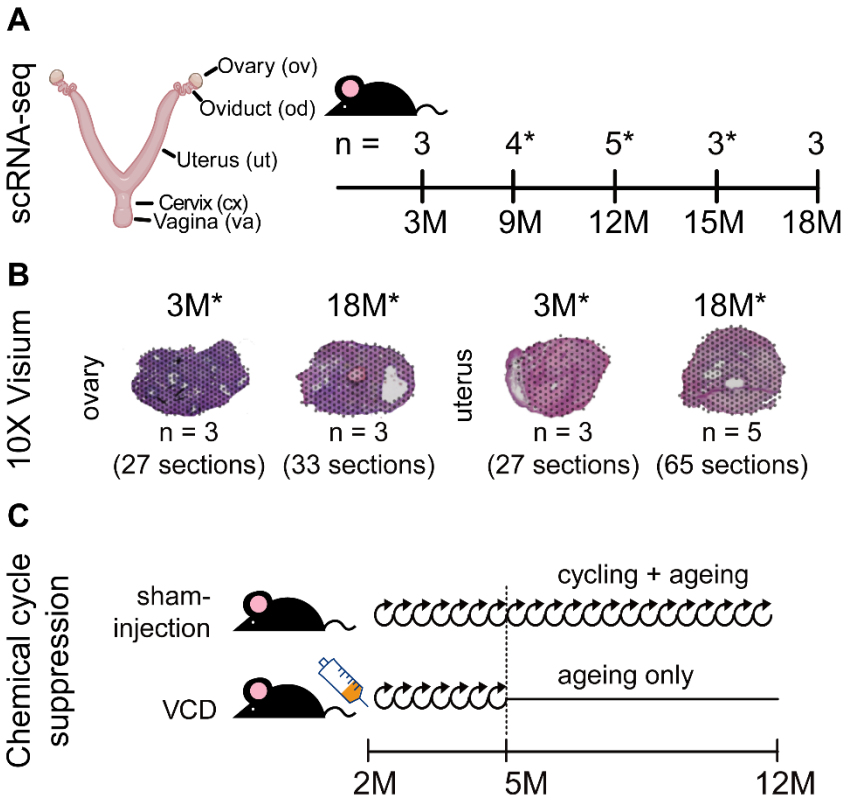

Figure 1. Graphical representation of experimental datasets used for analyses in Chapter 3.

(A) Single cell RNA sequencing dataset consisting of ovaries, oviducts, uteri, cervix and vagina collected from 3M, 9M, 12M, 15M and 18M old mice in diestrus, if cycling. Asterisks (*) mark timepoints where I contributed the data (~128.000 cells). (B) Spatial transcriptomics dataset of ovaries and uteri sections, collected from 3M and 18M old mice. Asterisks (*) mark timepoints where I contributed the data (152 sections, ~34,000 covered spots). (C) Experimental set-up for chemically inhibiting cycling in mice. Collaborators performed the experiment. This figure is adapted from Winkler et al., 2024 (Cell).

3.2. Inflammatory fibroblasts as primary source of inflammatory niches in ovaries and uteri

Immune cells are known to be largely responsible for inflammatory events. In FRT, the inflammation is resolved at each cycle, but there is a tendency of chronic inflammation over time. Fibroblasts contribute to inflammation by reacting to local microenvironment signals, secreting inflammatory factors and interacting with immune cells (188). Previous experiments on fibrosis accumulation in this project showed that intercellular collagen, indicating tissue fibrosis, accumulated during FRT ageing in the oviduct, uterus, and vagina (see Winkler et al., 2024).

To determine which cell types influence the fibroblast microenvironment in ovaries and uteri, I provided spatial transcriptomics experiments (Visium, 10X Genomics) to extend these analyses. I first optimized the permeabilization times for ovaries and uteri for this spatial transcriptomics technique and then processed the collected organs from 3M old mice in diestrus and 18M old acyclic mice (Methods). To identify gene expression profiles of various cell types in each Visium spot, the scRNA-seq was used to deconvolute the spatial data (Methods). Ovarian and uterine structures, including stroma, follicles and surface epithelia in ovaries (Figure 2A), stroma, luminal and glandular epithelia in uteri (Figure 2B), localized to expected areas in spatial transcriptomics experiments. Cell proportions were comparable in scRNA-seq and Visium slides, except underrepresentation of epithelial cells in scRNA-seq.

Linear mixed model was used to calculate which cell type best predict fibroblast inflammation, revealing that neighbouring stromal cells predicted inflammation more accurately than the activation or proportion of surrounding immune cells (Figure 2C). Fibroblast ECM remodelling was strongly predicted by adjacent fibroblast ECM activity (Figure 2D). In sum, fibroblast microenvironment shaped inflammation and ECM status in ageing ovaries and uteri.

To determine which cell type absorbs most of signals from inflammatory and ECM cytokines, calculation based on ligand counts was performed for each cell type (Methods). In uteri, fibroblasts used up the largest amount of inflammatory and ECM cytokines and, in ovaries, they had the second highest consumption of cytokines (Figure 2E). The spatial data was then used to enhance cell-cell interaction analysis, integrating physical proximity between cell types and adjusting communication scores by the proportion of ligand-receiving cell types (Methods). The results of spatial transcriptomics and scRNA-seq analyses were in overall agreement. In conclusion, fibroblasts predominantly utilized most of inflammatory and ECM cytokines.

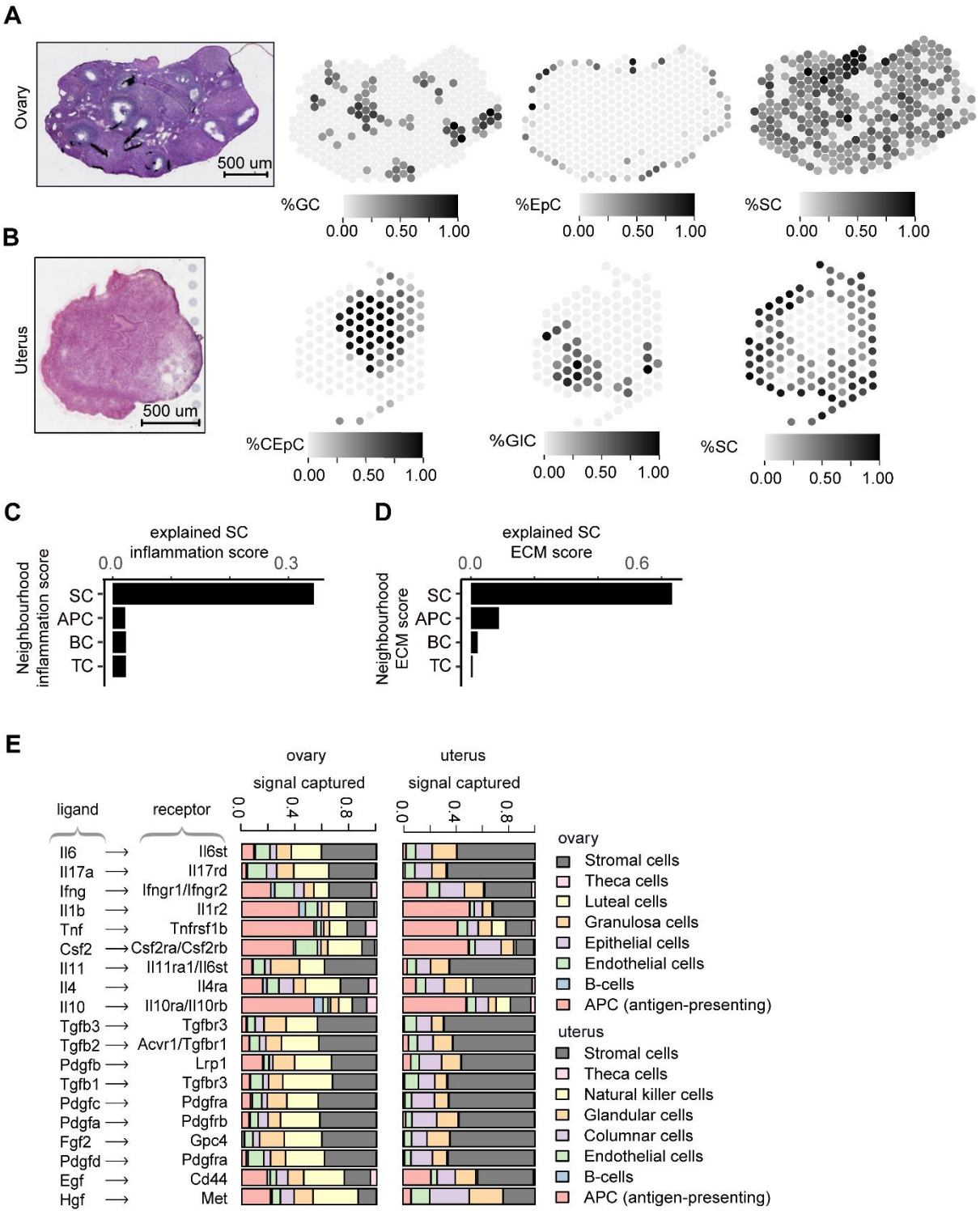

Figure 2. Fibroblast contribution to inflammation and ECM remodelling.

(A) H&E staining of ovary section from 3M old mouse (scale bar - 500 µm). Proportions of granulosa (GC), epithelial (EpC), and fibroblasts/stromal cells (SC) per spot. (B) H&E staining of uterus section from 3M old mouse (scale bar - 500 µm). Proportion of columnar epithelial (CEpC), glandular (GlC), and fibroblasts/stromal cells (SC) per spot. (C) Proportion of fibroblast/stroma cell inflammation scores in the ovary explained by inflammation scores of cell types in the neighbourhood. (D) Proportion of fibroblast/stroma cell (SC) ECM scores in the ovary explained by ECM scores of cell types in the neighbourhood. (E) Proportions of ligand

signal absorbed by different cell types in the ovary and uterus. Plots in this figure appear in Winkler et al. 2024 (Cell).

3.3. Age-related increase in fibroblast inflammation

scRNA-seq dataset was used to assess the extent and impact of inflammatory responses in ageing fibroblasts. The fibroblast inflammation was quantified in the upper FRT of mice aged 3, 9, 12, and 15 months, and 18M old acyclic mice using AUCell and a linear mixed model (Methods). The fibroblast inflammation in the lower FRT was measured only for 3M and 18M old mice. Ageing led to an increase in fibroblast inflammation across most reproductive organs, with the notable exception of the ovary (Figure 3A). The fibroblast inflammation varied between organs, and uterus and cervix showed most substantial increases. Next, the analysis distinguished whether the increase in inflammation stemmed from a specific subset of highly active fibroblasts or reflected a general increase of fibroblasts. In the uterus, the inflammation score distribution among fibroblasts was significantly different between young and old organs (Figure 3B). These distributions differed in shape, location, and size during ageing. This together suggests that both the expansion of inflammatory regions as well as increased inflammation of all fibroblasts drove the overall fibroblast inflammation in old mice.

Using spatial transcriptomics dataset, it was possible to interrogate how cell-cell communication affected the inflammation status in ageing fibroblasts. As ligand-receptor interactions in uterus showed increased inflammation activity, activated fibroblasts were analysed to determine if they form physical clusters with elevated inflammation in both ovary and uterus (Figure 3C). Briefly, inflammation activity scores were first calculated for each stromal cell (SC) spot in the ovary. Then, the scores were binarized into high (top 25%) and low inflammation, and spatial graphs were constructed by connecting neighbouring high-inflammation spots. Cluster coefficients were calculated to assess connectivity, revealing that cluster sizes significantly increased with age in uterus. This suggests that clusters of inflamed fibroblasts expand with age.

3.4. Both cycling and ageing contribute to fibrosis development in FRT

During the estrous cycle, the severity of age-related fibrosis in each FRT organ was linked to the intensity of ECM remodelling in fibroblasts (see Winkler et al., 2024). Each organ thus had a different predisposition to fibrosis development during ageing.

To decouple the effects of cyclicity and ageing on fibrosis development, a chemical treatment was used to prematurely terminate cycling in young mice (Methods, Figure 1C). 4-vinylcyclohexene diepoxide (VCD) was injected to 2M old mice, their acyclicity

confirmed at 5M, and reproductive organs collected at 12M, together with sham-injected control mice (Methods). The oviducts and uteri were then stained to evaluate fibrosis accumulation. I coordinated the sample import and prepared the samples for paraffin embedding and fibrosis staining, both performed by the Institute of Pathology in Heidelberg. The fibrosis in uteri was significantly reduced in old mice after VCD treatment, and a small but not significant reduction was observed in oviducts (Figure 3D). The control group, which cycled and aged, exhibited stronger fibrosis development. To summarize, fibrosis development was shaped by both cycling and ageing independently, through unresolved ECM remodelling.

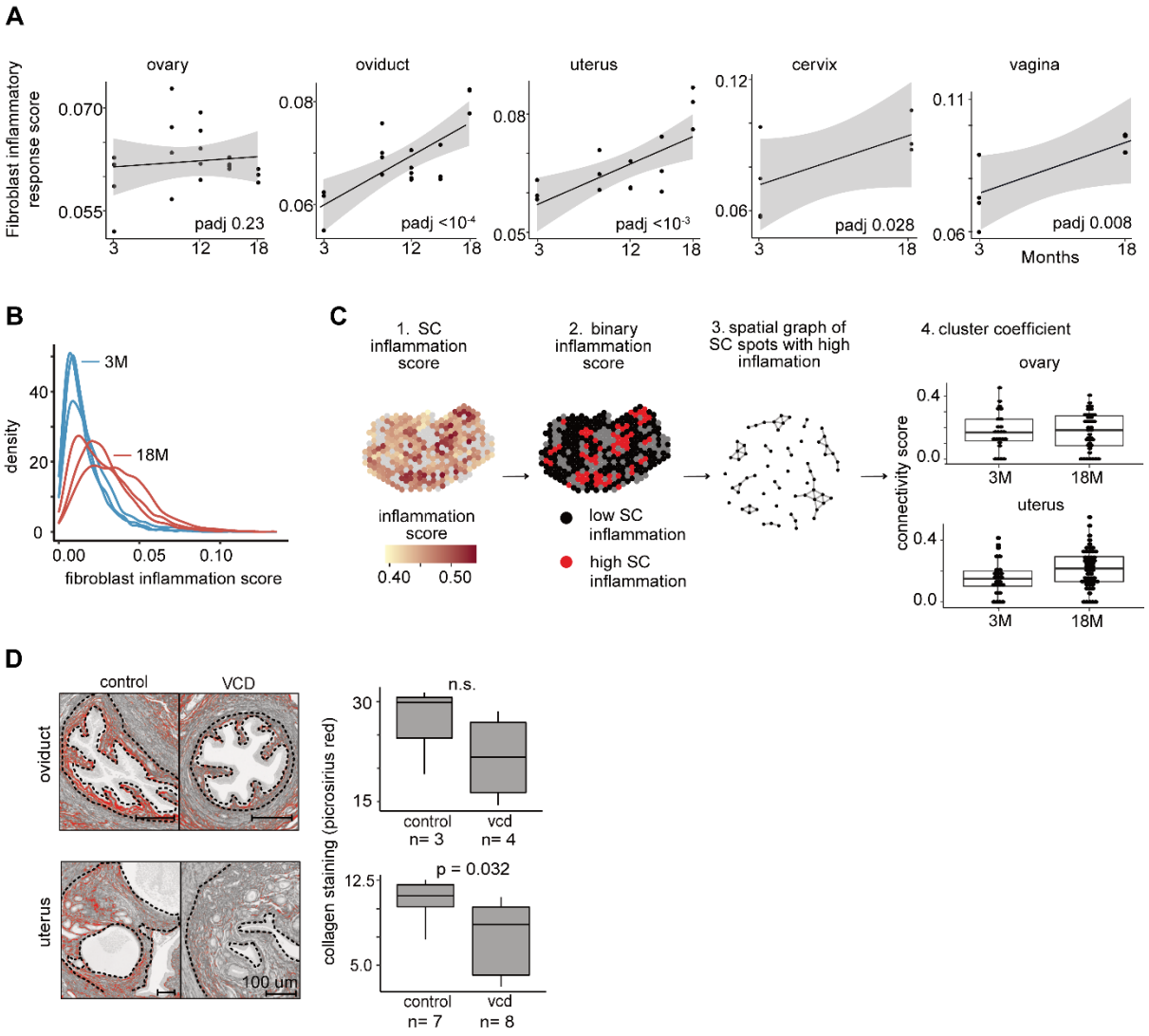

Figure 3. Ageing of FRT: fibroblast inflammation and fibrosis.

(A) Inflammatory gene activity scores averaged across all fibroblasts in ageing trajectory of FRT organs. Linear model predictions marked by black line and 95% confidence level interval by gray shading. (B) Uterus fibroblast inflammation scores shown as density plots for all young (blue) and old (red) mice biological replicates. (C) First, fibroblast (SC) inflammation score is calculated for every ovary and uterus section. Second, scores are binarized into high (top 25%) and low inflammation. Third, spatial graphs with high inflammation are constructed by connecting directly neighbouring spots. Lastly, connectivity scores are quantified for young

and old ovaries and uteri. (D) Collagen deposition in oviduct and uterus sections in control and VCD-treated mice (scale bars - 100 μm). Quantification of percentage area of stained collagen deposition in respective organs. Plots in this figure appear in Winkler et al. 2024 (Cell).

Discussion

This large-scale project interrogated most basic mechanisms of FRT function, from cyclicity and pregnancy to ageing. I contributed with a substantial amount of experimental data to help answering questions about FRT ageing, with focus on fibrosis and inflammation accumulation due to unresolved ECM remodelling.

Analyses of scRNA-seq in FRT organs during ageing showed that fibroblast inflammation affected FRT tissues in organ-specific manner. Interestingly, ovaries showed little inflammation, but uteri and cervix were extensively affected. The fibroblasts were identified as main source of inflammation during ageing. Further, using spatial transcriptomics experiments on ovaries and uteri, showing the local spread of the inflammation during ageing, that depends on local stromal cell niches. For the first time, the effects of cyclicity and ageing were decoupled using chemically-induced premature ovarian reserve exhaustion. This experiment revealed that fibrosis accumulation diminished during ageing when cyclicity ceased.

Collectively, these results are of utmost importance for better understanding FRT physiology and ageing.

Chapter 4

FRT transcriptional regulation and ageing after repeated superovulation

This project addresses a critical clinical issue: the impact of IVF on ovarian and other FRT tissue health. During IVF, women receive exogenous hormones to stimulate oocyte production, but the long-term consequences of these hormonal injections on tissue transcriptional regulation and morphology remain unclear. In this project, I use mice to model repeated superovulations and age the mice out to reduce different sources of variability and because current cohort of women who received IVF are not old enough yet. To bring the project closer to human cause, I will also use a small dataset of human granulosa cells from patients undergoing IVF. In previous chapter, I covered some aspects of FRT ageing, notably the fibrosis accumulation, inflammation status and their mechanisms. The prolonged use of oral contraceptives and parity both decrease the risk of ovarian cancer in women, suggesting a protective effect of ovulatory arrest. Here, the main hypothesis is that the repeated superovulation may accelerate FRT ageing, leading to damage and scarring similar to what occurs in older organs.

In this chapter, I focus more on ovarian ageing and how multiple hormonal stimulations affect the whole FRT. It contains powerful datasets of spatial transcriptomics of ovaries after repeated superovulation and single cell RNA sequencing of FRT throughout ageing and repeated superovulation. I have finalised the core datasets but the analyses are preliminary. I presented this project in a following conference:

The International PhD Student Cancer Conference

Cambridge, United Kingdom | July 2023

Talk *"Spatial transcriptomics of non-functional ovarian cysts in ageing mice"*

Contribution acknowledgement

Dr. Ivana Winkler and Perrine Lacour performed all bioinformatics analyses.

Dr. Alexander Tolkachov and Nina Schneider generated scRNA-seq datasets for 3M and 18M mice.

Dr. Julia Rehnitz and Ulrike Bender have kindly provided extracted RNA from human granulosa cells.

Nina Schneider generated scRNA-seq datasets for 9M, 12M, and 24M mice with me.

Lea Barthelme and Dr. Francesca Coraggio generated around half of spatial transcriptomics dataset.

Nina Schneider prepared bulk RNA sequencing libraries for human granulosa cells.

Marie Luise-Koch collected blood and assisted with organ collection from all mice.

William Wachter assisted with gDNA extractions from healthy and RSO mice ovaries.

Dr. Tanja Poth made all pathological evaluations.

Animal caretakers injected all mice (sham or hormones), except dose-response experiments.

4. Results

4.1. Study design

To build the core dataset for this project, I have created an injection plan for repeated superovulation (RSO), with following criteria i) standard dosage of gonadotropins (5IU of PMSG and 5IU of hCG), ii) injections administered for 5 times, iii) rest period, equivalent to one estrous cycle (5 days). I wrote the animal licence for this project and once approved by authorities, arranged intraperitoneal hormone injections for 80 mice. I had to repeat a few replicates and the whole timepoint of 12M due to technical issues of scRNA-seq protocol. I aged the RSO mice until 3M, 9M, 12M, and 18M. I selected these specific ages to represent key times for reproductive function: sexual immaturity (3-4 weeks), sexual maturity (10-14 weeks), the onset of reproductive decline (34-38 weeks), equivalent of menopause (46-52 weeks), and advanced reproductive age (70-76 weeks). I then collected their reproductive organs for either scRNA-seq or spatial transcriptomics (Visium); the samples were then processed and sequenced. Including controls from 37 untreated mice, this core dataset now consists of 178 scRNA-seq experiments, containing 892,645 cells (Figure 1A) and 37 Visium samples, presenting 472 ovary sections (Figure 1B).

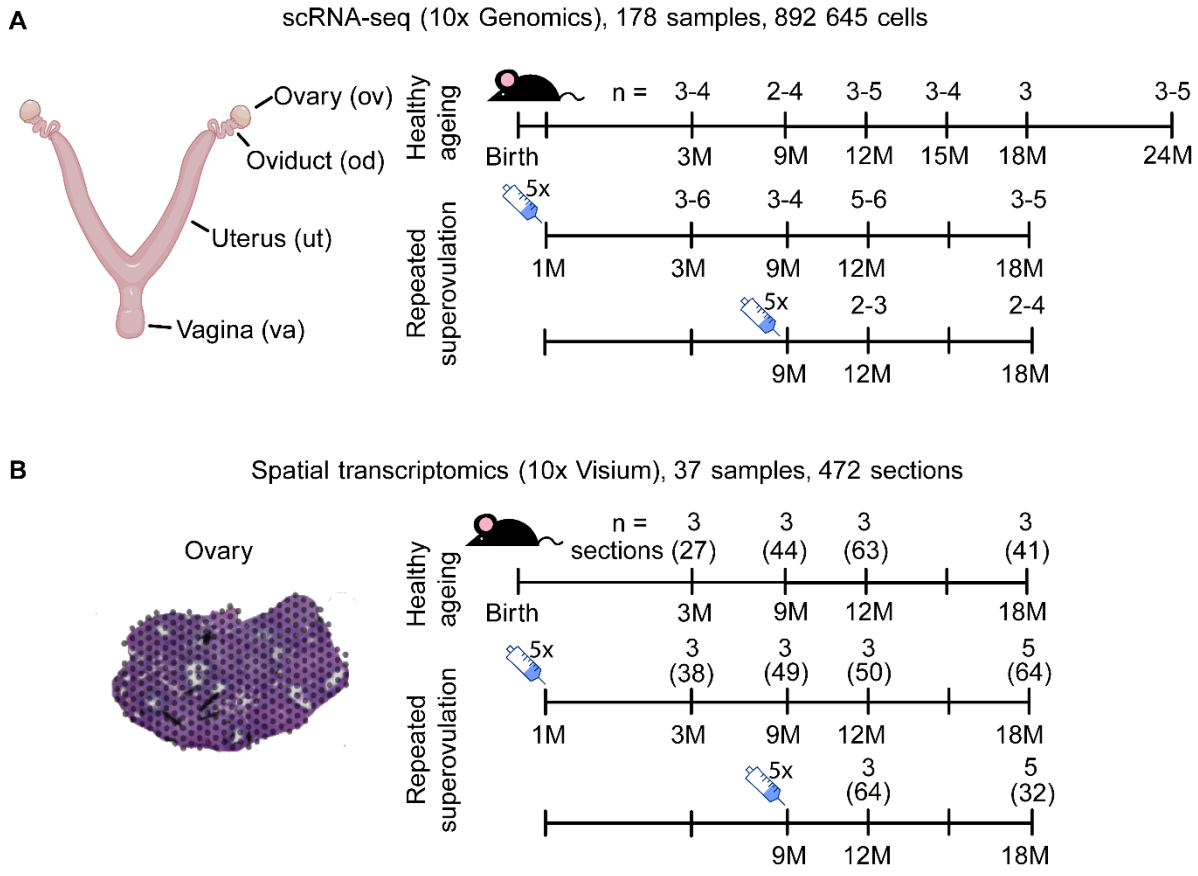

Figure 1. Core dataset of FRT healthy ageing and repeated superovulation.(A) Summary of samples processed using single cell RNA sequencing. Ovary, oviduct, uterus and vagina samples were collected for all mice. Control mice in healthy ageing timeline did not receive any injections. Repeated superovulation mice received 5 cycles of superovulation, starting at 4 weeks of age or at 9 months of age. 'n' marks mice number that passed quality control after sequencing, M means 'months. Healthy ageing scRNA-seq data is partially re-used from Chapter 3. (B) Summary of ovarian samples processed using Visium spatial transcriptomics. Control mice in healthy ageing timeline did not receive any injections. Repeated superovulation mice received 5 cycles of superovulation, starting at 4 weeks of age or at 9 months of age. 'n' marks mice number that passed quality control after sequencing, M means 'months. Figure created jointly with Dr. Ivana Winkler.

4.2. Ageing-associated changes in ovarian morphology and transcriptome

An obvious first question from this dataset is how does ageing affect ovarian transcriptome and what are related changes in the morphology? When processing mice tissues from different age-timepoints, I observed that ovaries first start accumulating lipofuscin (benign pigment) at 9M with increasing intensity during ageing. The ovarian atrophy was already prevalent from 12M but peaked between 18M and 24M. In addition, cysts, which are not follicles, started to appear around 12M and could be identified with certainty at 18M. As ovulation ceases between 12M and 18M, there were no visible antral follicles and corpus luteum left in 18M old ovaries. In parallel, pathologist Dr. Tanja Poth confirmed these observations in systematic analysis of hematoxylin eosin (H&E) stained tissue sections that I concurrently used for spatial transcriptomics experiments (Figure 2A).

Spatial transcriptomics is very useful to interrogate such heterogenous tissues as ovaries. Here, data from scRNA-seq helps to reinforce rather sparse spatial transcriptomics data to better quantify signals in cell populations. In preliminary results, clusters of young (3M) and old (18M) ovary samples were compared. The cell types were comparable between these two age time-points, demonstrating that spatial transcriptomics can detect all major cell types. However, when specifically comparing the cysts, they showed two distinct mutually exclusive transcriptomic signatures (Figure 2B), suggesting different cyst origins. First type of cysts predominantly expressed marker granulosa cell marker Inhibin Subunit Beta B (*Inhbb*) and the second type - Oviduct-specific glycoprotein 1 (*Ovgp1*). The epithelial cysts showed distinct localization and transcriptional signature that both differed from surface epithelial cells (Figure 2C). When epithelial cells from these cysts were subjected to differentially expressed gene analysis, the Ovgp1+ cysts showed overrepresentation of cancer-related pathways, such as p53 signalling, upregulation in KRAS signalling, epithelial-mesenchymal transition, among others (Figure 2D).

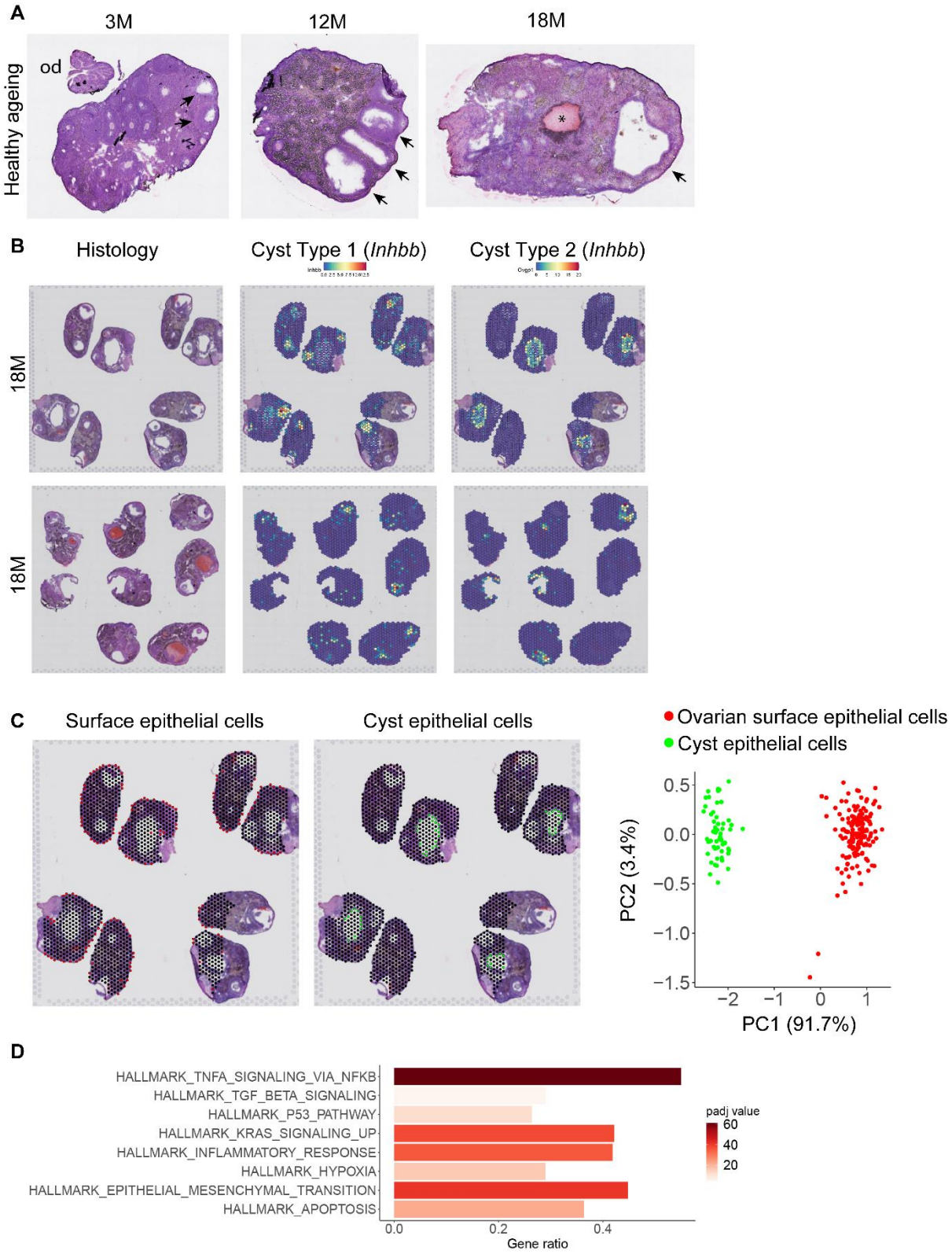

Figure 2. Morphology and transcriptional regulation during normal ovarian ageing.

(A) Examples of ovary section H&E staining during sample preparation for spatial transcriptomics. Cysts in older ovaries resemble antral and pre-ovulatory follicles in young ovaries (both marked by arrows); the follicles and cysts cannot be easily distinguished in mid-aged ovaries. Lipofuscin shows as brown inserts into stroma; haemorrhage is marked by *. (B)

Transcriptomically distinct and mutually exclusive cyst types differ by their markers, *Inhbb* and *Ovgp1*. Two examples shown from two different 18M old mice. (C) Cyst epithelial cells differ from surface epithelial cells, by localization (images from Visium slides) and transcriptionally (shown in PCA analysis). (D) Overrepresentation analysis for differentially expressed genes between epithelial cells in cysts and surface epithelia.

4.3. Morphology, physiology and transcriptomics of tissue ageing after repeated superovulation

The FRT tissues after RSO were often slightly larger, lumpy ovaries, bloated uteri, large vagina. In contrast, when looking at H&E staining, ovarian tissue morphology seemed largely similar to control ovaries. This similarity has not yet been confirmed by the pathologist, but it is planned.

When tracking the RSO mice estrous cycle by vaginal smears, I observed that the vaginal smears of 3M old mice resembled the proestrus/estrus-like stage over 7 consecutive days. I have tracked cycle for shorter period of time for other time-points, but very often RSO mice showed disrupted cycling even after 8 or 11 months past hormonal injections. It is important to note that it is very difficult to clearly evaluate in vaginal cytology RSO mice. It has been previously observed in rats that sex hormone injection in puberty would lead to persistent estrous (189). Ratio of high estrogen and low progesterone levels correlates to vaginal cornification, process that defines acyclicity in mice (190).

In addition to changes in cyclicity, I observed an increased incidence of intraperitoneal abnormal-looking growths in 18M RSO mice (~25% RSO vs. ~7% spontaneous occurrence without injection). These growths have been confirmed to be intestinal B-cell lymphomas by pathologist Dr. Tanja Poth. To control for injection bias, I then injected saline to pubertal (1M) and middle-aged (9M) mice (n=10 for each condition) and aged them until 18M. The middle-aged mice had 0% occurrence of intestinal growths by visual inspection, and sham-injected pubertal mice have not yet aged until 18M (due in November 2024).

One interesting hypothesis is that reproductive tissues age faster after RSO than during normal ageing. Do more ovulations also mean more tissue wounding and, hence, the more unresolved ECM remodelling? For this, scRNA-seq dataset will be useful to make predictions of FRT ageing in different cell types and organs, using machine learning. The preliminary results showed that age prediction significantly deviated from chronological age only in RSO ovaries but not in other FRT organs. To validate these bioinformatic age predictions, I extracted genomic DNA (gDNA) samples from ovaries of all timepoints in healthy aged and RSO mice (n=60) and DKFZ microarray core facility processed them for methylation array analysis (Methods). These samples are not yet analysed but will serve for construction of epigenetic ageing clock to validate bulk changes. Other transcriptomics analyses are yet to be done for these samples.

4.4. Uncoupling hormone dose and age

Briefly, the reasoning for looking at the hormonal dose-response per injection cycle is that IVF is most commonly performed in women aged 30-40, where ageing and repeated hormonal stimulation cumulatively affect outcomes. In older women, more IVF cycles are typically required for successful delivery. Does dose-response effect on whole FRT tissues (in mouse) and granulosa cells (in human) exist? What happens when hormonal injection is repeated? Do the gene expression changes accumulate or remain stable?

To answer these questions, I collected mice FRTs for scRNA-seq and ovaries for spatial transcriptomics after one to five cycles of superovulation at 3M of age (Figure 3A). scRNA-seq is done but I am still preparing the samples for spatial transcriptomics. In addition, through collaboration with clinician Dr. Julia Rehnitz (Frauenklinik, Heidelberg), I had access to extracted RNA from human granulosa cells that were collected from patients undergoing recurrent IVF cycles with up to 5 IVF cycles per person and one outlier with 11 cycles (Figure 3B). The RNA was then used to prepare libraries for bulk RNA sequencing and samples successfully sequenced (Methods). As these samples often come from the same patient, the variation stemming from genetic background will be strongly reduced. The analysis will take patient age at the time of IVF procedure into account.

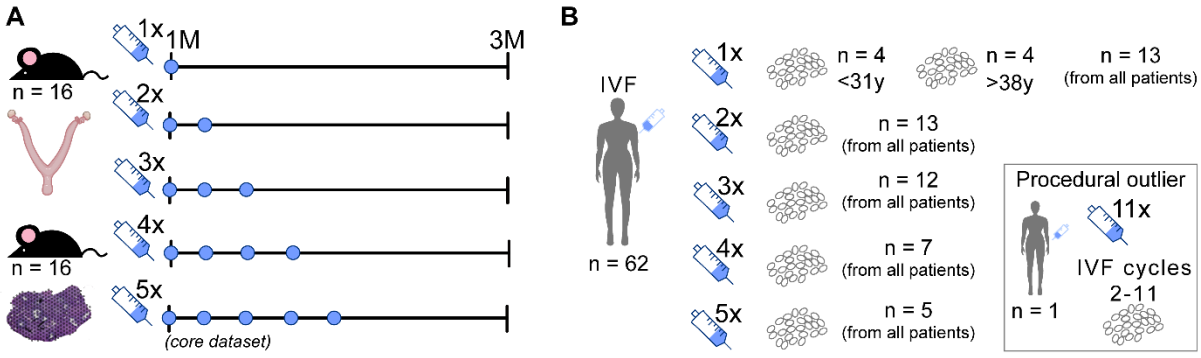

Figure 3. Schematic drawing of dose-response experiments in mice and human.

A) Reproductive tissues collected for single cell RNA sequencing were ovary, oviduct, uterus and vagina, and for spatial transcriptomics, only ovaries were processed. Specifically, both experiments contained 4 mice in each experimental group of 1-4 injections and 3-4 mice for 5 injections from the core dataset. All mice were killed at 3 months of age for organ collection. (B) Granulosa cell samples collected during IVF procedures at Frauenklinik. Samples after one injection will be used to construct age timeline for comparison of samples obtained after 2-5 injections, including adjusted patient age. Procedural outlier of granulosa cells after 2-11 injections will be used to study possible hormonal dosage plateau or additivity effects.

Discussion and Outlook

Most studies on IVF and hormonal stimulation focus on ART procedure efficiency and paediatric outcomes, not on maternal health risks. Once it was clear that hormonal overdose does not instantly induce cancer (158), long-term effects on FRT tissue physiology and regulation were poorly studied. It was shown in monkeys that hormonal stimulation protocols, similar to IVF, negatively affect ovary (191), uterus and mammary gland (192) gene expression and ultrastructure even a few years after the hormonal injections. In mice, adverse health effects and deregulations in ovaries were demonstrated (155). There are hints about the importance of perturbations when increasing the number of injections – decreasing oocyte numbers, abnormal mitochondrial distribution and copy number as well as worse embryo quality (157,193,194). However, these studies often lack large-scale transcriptional data and correctly adjusted ageing effects. In this transcriptomics-based project, there are several major axes, including many more scientific questions.

First, how do transcriptional changes correspond to tissue morphology? Many questions to answer in this axis, do cell proportions change similarly during ageing after RSO? Does increased cyclicity contribute to more severe fibrosis in FRT after RSO? And do cysts in RSO ovaries also show two types of cysts or is there preference for one type? Analyses of scRNA-seq and spatial transcriptomics datasets will help answer these questions.

Second, what are the long-term effects of several superovulations? Finishing the observations on sham-injected ageing RSO mice to control for intestinal tumours will reveal whether the tumour occurrence is driven by estrogen overdose. Observationally, cycle deregulations were more prevalent in mice injected in puberty (1M) than in mice that received injections at mid-age (9M). This may be because of different bodily hormonal constitution. Disbalances in estrogen-progesterone ratio can cause prolonged cyclicity similar to cycle of old mice (190). To investigate this, I have collected blood serum from all mice and I am planning to measure sex hormones using an ultra-sensitive mass-spectrometry-based assay.

Third, another important question is, do ovaries age faster after repeated hormonal injections? Here, data still needs deeper bioinformatics analyses as well as the analysis of methylation microarray samples to get more insights into the further direction.

Lastly, what is the relevance of hormonal dosage? The experiments on hormonal dosage will be especially interesting for patient cohorts. It is difficult to say whether the differences stemming from dosage will be large enough between IVF cycles. It will be possible to use the data from the mice to identify and compare more specific pathways or sets of genes.

Further work in this project will be focused on data analysis and use advanced bioinformatics tools, such as large-scale data integration and deconvolution, spatial transcriptomics analysis and artificial intelligence techniques to answer these questions.

General Conclusions

In this thesis, I have presented four scientific projects, where I lead three of them (Chapters 1, 2 and 4) and contributed as a second author to the last one (Chapter 3). During my thesis, I have established and adapted experimental methods to be able to address important scientific questions in Developmental Genomics.

In Chapter 1, I covered the main project that interrogates the relationship of oocytes and their granulosa cells in contexts of superovulation and ageing. The key findings of this project were that transcription and communication between oocytes and granulosa cells were disrupted after superovulation, revealing two types of superovulated granulosa cells. These transcriptional profiles of granulosa cells could be used to prospectively predict embryo developmental trajectories. In addition, comparison of naturally and superovulated old COCs allowed to show that superovulation and ageing interacted and affected similar sets of genes.

In Chapter 2, I described preliminary results of smaller but equally intriguing project which focusses on oocyte and granulosa cell evolution using COCs from wild-derived mice species. The first results are very promising – to my knowledge, it is the first direct evidence that oocytes drive gamete evolution. Further work will also focus on questions about what drives this evolution and how response to hormonal stimulation is conserved during evolution.

In Chapter 3, I narrated the main results of my contribution as a non-leading author, through collection of a significant proportion of data. This large data project focused on cyclicity and ageing of FRT organs, with focus on fibroblast role in chronic inflammation and ECM remodelling.

In Chapter 4, I explained the extensive efforts for a large data project which is focused on long-term consequences of multiple superovulations. It took 3 years to collect the organs from ageing mice and process the samples for scRNA-seq and spatial transcriptomics experiments. Further work will be focused on specific analyses interrogating FRT tissue health, ageing tendencies and transcriptional changes after repeated superovulations over time.

The technical and administrative achievements are often invisible in scientific projects. During this thesis, I was working closely with collaborators and technical assistants to achieve all these results. Some of my administrative achievements included writing and administering animal licenses, maintaining microscope, managing staff and data. On the technical side, I adapted standard oocyte handling techniques for tracked pair oocyte and granulosa cell isolation and modified standard protocols for single embryo IVF. I successfully naturally ovulated 12M old Bl6 mice and young wild-derived mouse species and shaped repeated superovulation protocol into its current form. In addition, I established a spatial transcriptomics workflow in our laboratory.

Overall, this thesis provides important scientific findings to Developmental Biology and Genomics fields, with many more results coming up.

Materials and methods

Methods were partially adapted from publications: Winkler et al., 2024 (Cell) and Daugelaite et al., 2023 (BioRxiv). Bioinformatics methods were provided by Perrine Lacour, Dr. Ivana Winkler and proofread by ChatGPT.

Experimental methods

Mice colonies

Chapter 1: Naturally ovulated or superovulated oocytes and granulosa cells were collected from 11-14 weeks (young) and 50-58 weeks (old) *Mus musculus* (C57BL/6J and C57BL/6Ly5.1) female mice. Around half of old mice had FRT pathologies and therefore could not ovulate. CD-1 vasectomized male mice were used for induction of ovulation in natural ovulation cohort; superovulated mice were not housed with vasectomized males.

Chapter 2: Naturally ovulated or superovulated oocytes and granulosa cells were collected from 11-15 weeks (young) *Mus musculus castaneus*, *Mus spretus*, and *Mus caroli* female mice. *Mus musculus* (C57BL/6J) dataset was collected in Chapter 1. Vasectomized male mice of respective species were used for induction of ovulation in natural ovulation cohort; superovulated mice were not housed with vasectomized males.

Chapter 3: FRT tissues were collected from healthy aged *Mus musculus* (C57BL/6J and C57BL/6Ly5.1) female mice at 3 months (M), 9M, 15M, and 18M of age. VCD experiment procedures were approved by the Ethics Committee of the Federal University of Pelotas (UFPel).

Chapter 4: FRT tissues were collected from healthy or repeatedly superovulated aged *Mus musculus* (C57BL/6J) at 3M, 9M, 18M, and 24M.

All chapters: Mice were kept at the DKFZ animal facility under controlled light-dark cycle (12h/12h, from 7:00 to 19:00) and had access to standard laboratory chow (Kliba 3437) and water *ad libitum*. All mice were virgins. C57BL/6J mice were purchased from Janvier (France) and allowed to adapt to animal facility conditions for at least 1 week. Wild-derived and C57BL/6Ly5.1 mice were bred in-house. All animal experiments were carried out according to governmental and institutional guidelines, approved internally (DKFZ-366) and by the local authority (Regierungspräsidium Karlsruhe, G-238/19, G- G-67/21). Each experimental group contained a minimum of three mice.

Natural ovulation and superovulation

Chapters 1 & 2

Mice were superovulated by intraperitoneal injection of 5 IU pregnant mare serum gonadotropin (PMSG - Pregmagon®) and 48 hours later a second injection of 5 IU human chorionic gonadotropin (hCG - Ovogest®) (146,195). The COCs were collected from ampullas: 14-16h post-hCG injection in young and 18-19h in old *Mus musculus*, 18-19h in *Mus musculus castaneus*, 16-17h in *Mus spretus*, and ~17h in *Mus caroli* (Methods Table 1). COCs were collected if oocytes had a uniform translucent cytoplasm, spherical shape and were surrounded by granulosa cells.

Methods Table 1. Ovulation timing after superovulation.

	Mus musculus (C57BL6)	*Mus musculus castaneus* (CAST/EiJ)	*Mus spretus* (SPRET/EiJ)	*Mus caroli* (CAROLI/EiJ)
Time of ovulation after hCG injection	Young: 13h50-15h50 after hCG Old: 18h15-19h10 after hCG	18h00-18h45 after hCG (e.g. 17h00 is rather early)	15h30-16h30 after hCG (e.g.17h45 is rather too late)	16h50-17h10 after hCG (e.g. 14h50 is too early)

For natural ovulation, mice were mated with vasectomized males in a 1:1 or 2:1 female-male ratio (Methods Table 2) shortly before the beginning of the dark cycle (182–184). Harem mating (2:1) is more efficient for wild-derived mice species, standard mating (1:1) is efficient enough for C57BL6/J mice. The C57BL/6 females were mated with vasectomized CD-1 males, *Mus musculus castaneus*, *Mus spretus* and *Mus caroli* were mated with males from their corresponding species. Next morning females presenting a copulatory plug were killed for COC collection: 2-3h after the beginning of the light cycle for *Mus musculus*, 5-6h for *Mus musculus castaneus* and 2-4h for *Mus spretus*, *Mus caroli* did not present copulatory plugs. Females without observable vaginal plugs were examined each morning for up to 2 weeks, often presenting plugs on the 3rd day and latest on 8th consecutive day. Males were allowed to rest for at least one day between successful sham-matings. Larissa Ziegler and Dr. Franciscus Van Der Hoeven performed vasectomy of males. Vasectomized CD-1 males were used instead of C57BL6/J because their mating performance is better.

Methods Table 2. Natural ovulation methodology and timing for 4 mouse species.

	Mus musculus (C57BL6/J)	*Mus musculus castaneus* (CAST/EiJ)	*Mus spretus* (SPRET/EiJ)	*Mus caroli* (CAROLI/EiJ)
Vasectomized male strain/species for mating	CD-1	CAST/EiJ	SPRET/EiJ	CAROLI/EiJ
Mating style	1:1 female - male	1:1 female - male or 2:1 females - male	1:1 female - male or 2:1 females - male	Tried all styles

Mating length	Mating over 3 consecutive days	Mating over 2 weeks	Mating over 2 weeks	Tried all lengths
Time of ovulation when plug observed	Around 8:00 – young; around 13:00 - old	Around 12:00-13:00	Around 09:00-11:00	Failed to observe plugs and ovulation

Repeated superovulation

Chapter 4

One cycle of superovulation consisted of 5IU PMSG and 48h later 5IU of hCG, as described above. Repeated superovulation consisted of 5 cycles of superovulation over five consecutive weeks, including 5 days of rest between injections. Young cohort of mice started receiving injections at age of 4 weeks; middle-age cohort received injections at 9M of age. Mice were killed for organ collection at 3M (10-14 weeks), 9M (34-38 weeks), 12M (46-52 weeks), and 18M (70-76 weeks). Sham-injected mice for specific control experiments received sterile saline (0.9% NaCl) injections instead of hormone solutions in a similar manner.

COC collection

Chapters 1 & 2

Mice were sacrificed by cervical dislocation and the oviducts dissected. Under the stereomicroscope (SteREO Discovery.V12, Zeiss) ampullas were torn to release the COCs into a 96 µl M2 media (M7167, Sigma) drop under mineral oil (69794, Sigma) at room temperature. Then, 4 µl of pre-heated 500 µg/ml hyaluronidase (H3884, Sigma) diluted in M2 media (final concentration in the drop 20 µg/ml) was added to separate the COCs into single units. The COCs were incubated for 10-20 min (shorter times are needed for COCs from wild-derived species) at 37°C and then mechanically separated into individual M2 drops using a 115-124 µm glass retransfer pipette (BioMedical Instruments). Individual COCs were washed in M2 once and incubated for less than 5 min with enzymatic mix Accutase (196) (A6964, Sigma) at 37°C to further separate the granulosa cells from the oocytes. Once separated, small bulk of GCs were collected from these individual drops using a mouth pipette pre-filled with Dulbecco's phosphate-buffered saline (DPBS, 59321C, Sigma). Oocytes were washed once with M2 media and thoroughly with DPBS before collection. Cells were immediately flash frozen in liquid nitrogen in individual 0.2ml thin wall PCR tubes (731-0679, VWR) and stored at -80°C until further use. The media in the mouth pipette was changed between micromanipulations of singularized COCs, granulosa cells and oocytes to ensure sample specificity.

In vitro fertilisation assay

Chapter 1

Young C57BL6/J mice were superovulated and COCs singularized as described above. Granulosa cells were immediately flash frozen and paired oocytes were divided into individual drops of CARD media (Cosmobiousa) under mineral oil (Vitrolife) for fertilization. The oocytes were incubated at 37°C, 5% CO_2 for 30-40 min prior to fertilisation (197). Frozen (198) *Mus musculus* (C57BL6/J) male sperm was obtained from the DKFZ Transgenic Service. Sperm straws contained 6.41-10.6 x 10^6/ml progressive spermatozoids with 7.75-14 x 10^6/ml motility. The sperm straws were thawed and capacitated in Fertiup media (Cosmobiousa) for 30 min prior fertilisation. Fertilisation was achieved by combining 2.5 µl of activated sperm with 20 µl CARD media drops containing a single oocyte and incubated at 37°C, 5% CO_2 for 3 hours. Further, oocytes were individually washed in Human Tubal Fluid (HTF) media drops and transferred to 20 µl HFT drops for overnight culture. After 24 hours, the fertilisation rate was evaluated and 2-cell stage embryos were transferred to G1+ media (Vitrolife) for further development. Early morula stage embryos were collected based on an observation window of 62 to 64h post-fertilisation. For collection, the embryos were washed in DPBS and flash frozen in similar manner as oocytes.

Oocyte, granulosa cell and embryo sample sequencing (SMART-seq2)

Chapters 1 & 2

Oocyte and granulosa cell samples were processed for full-length cytoplasmic RNA amplification using a slightly modified SMART-seq2 protocol (Picelli et al. 2014). Libraries for next generation sequencing were prepared using Nextera XT DNA library Prep Kit (Illumina). Briefly, cells were lysed with 0.2% Triton X-100 (Sigma Aldrich) and reverse transcription was facilitated by Maxima-H Minus Reverse Transcriptase (Thermo Fisher). Amplification of complementary deoxyribonucleic acid (cDNA) was achieved with 17 PCR cycles for oocytes, 20 cycles for granulosa cells, and 16-17 cycles for embryos. 1 ng of cDNA was used as template for library preparation, then tagmented, double indexed and amplified with 11 PCR cycles. Prior to sequencing libraries were multiplexed into a single pool. Quality control for sample preparation was performed using 4200 TapeStation hsD5000 tapes (Agilent), and Qubit 4 fluorometer High Sensitivity dsDNA assays (Thermo Fisher). Samples which failed cDNA amplification were excluded. Oocyte and granulosa samples were sequenced on NextSeq550 (Illumina) using Single-Ended 75bp High-Output kits at the DKFZ Open Sequencing Lab. All samples from IVF experiments were sequenced on a Novaseq6000 at the Institute of Clinical Molecular Biology (IKMB), Kiel, Germany.

Total RNA sequencing for oocytes

Chapter 1

Oocytes from naturally and superovulated mice were collected and COCs singularized as described above. SMARTer Stranded Total RNA - Low Input Mammalian (Takara) kit was used for lysis, cDNA amplification and library preparation with 10 cycles for

PCR-1 and 16 cycles for PCR-2. Samples were sequenced as recommended by the manufacturer on Novaseq6000 with paired-end sequencing at IKMB.

qPCR for classifier marker genes in granulosa cells

Chapter 1

12 target genes used by the granulosa cell-embryo classifier were tested using qPCR to validate gene expression differences between S and S_N clusters. qPCR primers were manufactured by Sigma-Aldrich and designed using IDT PrimerQuest Tool from sequences in the NCBI nucleotide database (Methods Table 3). PowerUp SYBR Master Mix with 500 nM final concentration for forward and reverse primers and ~1 ng of cDNA was used to prepare qPCR reactions. 54 granulosa samples were analyzed in duplicates using Fast cycling mode on a QuantStudio 5 Real-Time PCR System with 384-well block (Thermo Fisher) as recommended by the manufacturer.

Methods Table 3. qPCR primer sequences.

Gene name	Forward sequence	Reverse sequence
Kmt2a	GGAGCGAGAGAAGGAGAATAAG	CCGACCCACAGGATACAAAG
Dync1h1	ACCTAACGGTGTTGTCTTGG	GACTCTCTGTGTGCCGTATTT
Lrp6	GAAGATGGGAGGGTAGCAATAC	GGGAAGCCCACCAGATAAAG
Ireb2	CTCACCCAGAAACAGTGAACTA	GGAGGCAGAATCACAAGATACA
Hook3	TGGCATTAGCAAGGGATGAG	CCTGGTTAGAAGGCACAGAAA
Fndc3b	GAGATCACGGATGGAACTTCTG	GCCTGGTTTCAAATGGGTAAAG
Bptf	CTGGGACAAGAAGGGAAGTATC	GCCTCCTCTTATCATGGTCTTC
Zfp451	GGTGACACGTTTCTCCAACTA	GACGCACTGCTAAGGAAAGA
Nrip1	CTTTCCTATCTGGGTCAACATCTC	TGCTAAGTGGCCCTGTTATTC
Phf20l1	TCAGAAGTCACAGGGAGTAGAA	ACTACTTTGGAGGTGGGATTTG
Vcan	AGTGGAGGAGGAAGGTATGT	GCTTCGGGATGGGTAGTATATG
Dag1	TCCCACTTCAGATGGTTGTG	GGAGAGATGGCTCAGTGTTAAG
GAPDH	GTGGCAAAGTGGAGATTGTTG	CGTTGAATTTGCCGTGAGTG

Vaginal smears for estrous cycle staging

Chapters 3 & 4

Vaginal smears were used to evaluate estrous cycle stage over a few consecutive days or at time of death as previously described (199). Briefly, cells from vaginal fluid were collected by washing vaginal entry with PBS, the solution spread onto microscopy slides and air-dried. The slides were then stained with 0.1% crystal violet solution (Sigma-Aldrich 61135) for 1 minute, rinsed in water for 1 minute and air-dried. Estrous stage was evaluated by cellular composition of the smear (199) under the stereoscope (ZEISS, Discovery.V12).

Single cell RNA sequencing for mouse FRT

Chapters 3 & 4

Mice were dissected to collect reproductive tract, organs were separated into ovaries, oviducts, uteri, cervix and vagina, cleaned from the fat and cut into smaller pieces. Tissue preparations were first digested in 600µL 0,25% trypsin in HBSS at 37°C with gentle shaking for 30 min. The samples were further digested with 600µL of additional enzyme mix of Collagenase I (1.25 mg/ml), II (0.5 mg/ml), IV (0.5 mg/ml), and Hyaluronidase (0.1 mg/ml) in HBSS for more 2 hours. 600µL HBSS with 10% FBS was added to quench the enzymatic reaction. The cell suspensions were then strained through 40µm strainer (Greiner Bio One) to remove undigested tissue and debris. Straining excluded large cells, such as oocytes and smooth muscle cells. The samples were centrifuged at 350g for 8 min at 4°C, supernatant removed and cells resuspended in PBS with 0,04% BSA, 1 mM EDTA and propidium iodide (PI) was added to final concentration of 1 µg/ml prior to FACS. FACS was performed at DKFZ Flow Cytometry Core facility on FACSAria II and FACSAria Fusion (BD Biosciences) with 85µm nozzle. Live cells were sorted by excluding PI-positive cells, doublets were excluded by SSC width and SSC area ratio. Around 70,000 cells were sorted into 1.5 ml Eppendorf tubes containing 0.04% BSA and 1mM EDTA in PBS sorting media. Samples were kept on ice while sorting and further processed for scRNA-seq as soon as possible.

Cell suspensions were loaded onto ChromiumTM Single Cell Chip B (Chromium Single Cell 3' Reagent Kits v3.0) for 3M and 18M experiments or Chip G (Reagent Kit v3.1) for 9M, 12M, and 15M experiments in Chapter 3. All experiments in Chapter 4 were done using Chip G and chemistry v.3.1. Reverse transcription and library construction were carried out according to the manufacturer's recommendations. All FRT samples, except 3M and 18M timepoints, and all RSO samples were paired-end sequenced on a Novaseq6000 at the IKMB, Kiel, Germany. FRT samples from 3M and 18M old mice were paired-end sequenced on a Novaseq6000 at the DKFZ Next-Generation Sequencing core facility.

VCD treatment

Chapter 3

C57BL/6 mice in VCD group were intraperitoneally injected with 160 mg/kg 4-vinylcyclohexene diepoxide diluted in sesame oil (VCD; Sigma-Aldrich) at 60 days of age. Mice received injections for 20 consecutive days. Sham-injected mice group received only sesame oil injections. The cyclicity was evaluated by vaginal cytology for 5 consecutive days at 5M of age. VCD group was confirmed as acyclic. Mice were killed at 12M of age to collect oviducts and uteri, which were preserved in 10% paraformaldehyde solution. Bianca Machado de Avila and Augusto Schneider in Brazil performed this experiment.

Fibrosis staining and quantification

Chapter 3

After fixation in 10% buffered formalin, control and VCD-treated oviducts and uteri were dehydrated, embedded in paraffin, and cut into 4 µm sections. For the staining, tissues were deparaffinised using xylene, rehydrated in ethanol and distilled water and incubated in Picrosirius Red solution for 1 hour. Then the tissues were washed twice with acetic acid water, dehydrated with ethanol and cleared with xylene. This staining was performed by staff at the Institute of Pathology, Heidelberg.

Whole tissue images of samples were acquired by the Aperio AT2 slide scanner (Leica) at 40x resolution. ImageJ software was used to quantify percentage of fibrotic area by setting a signal threshold in stroma-containing regions. RGB images were split into three channels and the quantification was performed on the green channel. Regions of interest were drawn around stroma areas and collagen accumulations were defined as percentage of area with positive signal. The quantification was performed by Dr. Ivana Winkler.

Spatial transcriptomics for mouse FRT

Chapters 3 & 4

Mice were dissected to collect FRT and organs embedded in biopsy cryomolds (Tissue Tek) using optimum cutting temperature matrix (O.C.T., Tissue Tek) and a bath of pre-cooled (-60-70^{o}C) isopentane (Sigma) on dry ice. The samples were stored until further use at -80^{o}C, wrapped into parafilm. Blocks were cut using cryomicrotome (CM3050S, Leica), head temperature set at -10^{o}C and 10 µm thick tissue sections placed on Visium Spatial Gene Expression Slides (10X Genomics). Optimized Hematoxylin and Eosin (H&E) staining times were used for ovaries (hematoxylin - 5 min, 30s blueing agent and 1 min eosin) and uteri (hematoxylin – 7 min, 30s blueing agent and 2 min eosin). The images of tissues were taken by Nikon Eclipse Ti inverted microscope equipped with 20X Apo Air Ph1 DM objective and DS-Ri2 color camera. Tissue permeabilization times for ovaries (18 min) and uteri (24 min) were optimized using Visium Spatial Tissue Optimization kit (10X Genomics). Reverse transcription and library construction were carried out according to the manufacturer's recommendations, using Dual Index

Kit TT Set A for indexing. Samples were sequenced on NovaSeq6000 at the IKMB, Kiel, Germany.

gDNA extraction and DNA methylation microarrays for mouse ovaries

Chapter 4

Around 20 tissue sections (10 µm thick) were sectioned using cryomicrotome as above and placed into pre-chilled round-bottom 2 ml Eppendorf tubes. Samples were stored at -80°C until processing. To extract genomic DNA, AllPrep DNA/RNA Micro kit (Qiagen) was followed as recommended by the manufacturer in the handbook section "Simultaneous Purification of Genomic DNA and Total RNA from Microdissected Cryosections". gDNA samples ranging from 150 ng to 1 µg were then processed on Infinium Mouse Methylation BeadChips (Illumina) by DKFZ Microarray core facility.

Bulk RNA sequencing of human granulosa cells

Chapters 1 & 4

Controlled ovarian stimulation was performed depending on the individual patient's situation using long GnRH agonist protocol or the GnRH antagonist protocol as previously described (200). Granulosa cells were retrieved from follicular fluid after transvaginal ultrasound-guided follicle puncture for IVF procedure (201). Briefly, the fluid was transferred to 14-ml tubes (Cook Medical, Bloomington, IN, USA), incubated at 37°C, and then moved to a 100-mm culture dish on a heated table at 37°C. Mural granulosa cells were identified under a stereomicroscope (SMZ1500, Nikon), washed in Sydney IVF fertilization medium, and 2.5 µl of cells were transferred to tubes pre-filled RNAlater for storage at 4°C. Granulosa cell samples were centrifuged at 5000×g for 5 min, the supernatant discarded and total RNA isolated using TRIzol (Life Technologies) according to the manufacturer's instructions. Samples were stored at -80°C until further use. Further, RNA was cleaned from DNA with DNA-free™ DNA Removal Kit (Invitrogen) and ~1 µg of RNA was used to construct libraries with Truseq Stranded mRNA kit (Illumina) and barcoded with IDT for Illumina-TruSeq DNA and RNA UD Indexes. 65 granulosa cell samples were sequenced on Nextseq2000 (Illumina) with 100bp paired-end sequencing at DKFZ, Heidelberg, Germany.

All patient procedures were were carried out at the Universitäts-Frauenklinik, Heidelberg, Germany and approved by the local ethical committee of the University of Heidelberg, Germany (S-602/2013). All participating patients signed informed written consent and completed clinical questionnaires. Only samples from normal responders undergoing IVF due to male or idiopathic subfertility were included.

Bioinformatics methods (collaboration)

Quality control for sequenced samples

Chapters 1 & 2

Sequencing alignment files were demultiplexed by the DKFZ Genomics and Proteomics Core Facility. Adapters were trimmed, and reads aligned to the mm10 genome (GRCm38) using STAR (v.2.7.0f). Gene-barcode count matrices were analysed using R (v.4.0.0) and Seurat (v.4.0.3). Samples were retained if they had over 5000 reads, more than 1000 detected genes, and less than 5% mitochondrial reads. Mislabelled samples were identified through cell-type-specific marker gene expression, resulting in the removal and resequencing of 10 samples (Chapter 1 only). Raw count tables for all replicates were merged and normalized using Seurat's SCTransform function. PCA was computed on the top 3000 variable genes, and UMAP was computed on the first 30 principal components.

Chapters 3 & 4

For scRNA-seq sequencing, raw reads were processed using Cellranger analysis pipeline. The "cellranger count" command was used to generate filtered and raw matrices. Reads were aligned to the mouse genome (mm10). To exclude low quality cells, an adaptive filtering threshold approach was used based on high mitochondrial RNA content, count depth, and too high numbers of genes per barcode. Filtering was based on the median absolute deviation (MAD) from the median value of each metric across all cells, performed using the Scater package. Counts were normalized using the ScTransform and doublet scores assessed by doubletCluster and doubletCells functions from the Scran package.

Differential gene expression (DGE)

Chapter 1

DESeq2 (202) and a pseudo-bulk approach were used to do DGE analysis (v.1.28.1). SCT-corrected counts (adjusted for sequencing depth) for each mouse were aggregated by cell type and used as input for DESeq2. Effects of superovulation and age were modelled with an interaction term between them.

Overrepresentation analysis

Chapters 1 and 3

Overrepresentation analysis (ORA) was conducted using a hypergeometric test with gene sets from the MsigDB pathway collection (Hallmarks, KEGG, Reactome, GO Biological Process). P-values were adjusted using the Benjamini-Hochberg procedure.

Cell-cell communication analysis

Chapter 1

For each follicle, OC-GC interaction scores were computed using the CellChat ligand-receptor database (203), factoring in gene expression. Gene counts were normalized with the SCnorm method, and only the top 100 most expressed ligand and receptor genes were analysed. Interaction scores were calculated by multiplying the ligand expression in the sender cell with the receptor expression in the receiver cell. For multi-subunit receptors, the least expressed subunit was used. Communication was evaluated for OC-GC pairs in both directions, as well as for autocrine signalling within OCs and GCs.

Chapter 3

Cellular communication to fibroblasts was quantified by multiplying ligand expression in various cell types with receptor expression in fibroblasts, using ligand-receptor pairs from CellChat (203) and CelltalkDB (204). Average expression values across all estrous cycles were used, with the minimum expressed subunit considered for multi-subunit receptors. Communication scores were compared across reproductive organs using a permutation test, and statistical significance was determined by comparing expression ratios to a null distribution, with multiple testing correction via the Benjamini-Hochberg procedure. For selected ligand-receptor pairs, likely ligand sources were identified by calculating z-scores based on total ligand expression across cell types. The focus was on pairs related to inflammation and ECM, considering their functional roles.

Transcription factor activity analysis

Chapter 1

Single-Cell Regulatory Network Inference and Clustering (SCENIC) (205) (v. 1.2.4) was applied to perform granulosa cell regulatory network analysis. Using SCT-normalized gene expression data, gene co-expression networks were identified via GENIE3, enriched transcription factor motifs were scored with RcisTarget, and regulon activity scores were calculated via AUCell. To evaluate overlap between regulons and pathways significantly dysregulated by superovulation, a Jaccard index was used to quantify the overlap between regulon target genes and pathway genes. The enrichment was assessed using a hypergeometric test. Hierarchical clustering of transcription factors was performed using Euclidean distances and the complete clustering method.

Chapter 3

pySCENIC (v.0.12.1) was used for computing regulatory network analysis in fibroblasts, utilizing SCT-normalized gene expression data from specific cell subsets: fibroblasts from all organs across cycle phases, fibroblasts in diestrus and aged

samples. Gene co-expression networks were determined using grnboost2, transcription factor motifs were predicted with the ctx function, and regulon activity scores were calculated via AUCell. Regulon activity across FRT organs or with ageing was assessed by comparing activity scores to null distributions obtained through 1000 label permutations, with multiple testing correction performed via the Benjamini-Hochberg procedure.

Transcription factors related to inflammation and ECM were selected based on the overlap and enrichment of target genes with those of selected ligands from the NicheNet database. Classification of transcription factors as fibrosis- and/or inflammation-associated was based on enrichment scores of target genes in inflammation (Hallmark collection) and ECM organization (Reactome collection) pathways. Overlap between target genes and pathway genes was quantified using the Jaccard index, and enrichment was assessed with a hypergeometric test.

Pathway activity scoring

Chapter 1

Scoring of pathway activity was done through AUCell package (205) (v. 1.10.0) by calculating an enrichment score of each gene set within the top 20% most expressed genes in each cell. The gene sets were the same as in ORA.

Chapter 3

Gene set activity was scored using the AUCell R package (v.1.10.0), assessing whether specific gene sets were enriched within the top 5% or 10% of expressed genes per cell. The gene sets used matched those in the ORA analysis. To score the activity of inflammatory and ECM-related genes, the “Hallmark_inflammatory_response” and “Reactome_extracellular_matrix_organization” pathways were used. For scoring ligand-target gene activity in fibroblasts, the NicheNet ligand-target model (v.1.1.1) was used to identify predicted targets. AUCell scores were computed for each cell and averaged across conditions for each population, with cycle phase scores weighted according to phase duration. A mixed generalized linear regression model with a random intercept was applied to test the significance of activity score changes across the estrous cycle, using the glmmTMB package (v.1.1.5). P-values were corrected using the Benjamini-Hochberg procedure.

To estimate the fibroblast inflammation rate in the different FRT organs, a linear mixed model was fit at the cell level including age, organ and the interaction of age and organ as fixed effects, and individual (mouse) as a varying intercept random effect.

Transcriptional heterogeneity analysis

Chapters 1 and 3

Differential Shannon Entropy (dShE) was utilized to evaluate differences in transcriptional heterogeneity between young and old naturally ovulated COCs, and

superovulated and naturally ovulated young COCs (Chapter 1). In addition, dShE was used to assess the differences in transcriptional heterogeneity between young (diestrus) and old cell populations (Chapter 3). dShE was calculated with the EntropyExplorer (206) package (v.1.1). Multiple testing correction was applied using the Benjamini-Hochberg procedure.

IVF analysis

Chapter 1

Two support vector machines were trained to classify granulosa cells from the IVF experiment into S_N and S groups. The consensus S_N and S clusters of granulosa cells from the original experiment served as the training and test sets, using the `caret` package (v.6.0-94) with a linear kernel for classification.

The first classifier utilized regulons identified via SCENIC. Only transcription factors regulating pathways altered by superovulation were included. These regulons were scored on raw counts of young superovulated granulosa cells using AUCell with the top 2000 genes, and these scores were input for training. Further refinement of transcription factor selection involved identifying those with significantly different activity scores between the S_N and S groups using a generalized linear mixed model with random intercept. The model, fitted under a beta distribution using the `glmmTMB` package (v.1.1.7), used activity scores as the dependent variable and group labels as the independent variable, with sample label as a random effect. Features with an adjusted p-value < 0.05 were selected for classifier training.

The second classifier identified DEGs between the S_N and S groups using DESeq2, accounting for the mouse of origin. DEGs meeting specific thresholds (baseMean >50, adjusted p-value <0.01, and absolute log2 fold change >0.7) were used to compute a PCA, with PC 1 effectively separating the SN and S groups. Genes with loadings above 0.09 (top 50%) were selected for classifier training. Prior to training, features with near-zero variance, correlation, or linear dependency were removed. A genetic algorithm performed the final feature selection, and adaptive resampling tuned the cost hyperparameter.

Granulosa cells from the IVF experiment were classified using both the transcription factor and DEG-trained classifiers. Cells with differing classification labels between the two classifiers were marked as “not assignable.”

Copy number variations in the embryos were detected using the InferCNV package (v.1.17.0), with S_N-classified embryos as the control group. Differentially expressed genes between S_N and S embryos were calculated by fitting a negative binomial generalized linear model using the MASS package, with multiple testing correction via the Benjamini-Hochberg procedure.

Embryonic pseudotime analysis

Chapter 1

Sequencing data from Xue et al. (179) was processed as described above. Raw count tables were merged with count tables of our naturally ovulated embryos. Counts were normalized using the Seurat SCTransform function. Genes associated with early embryonic development were selected based on three criteria: 1) the gene must be among the top 3000 highly variable genes identified by Seurat; 2) the Spearman correlation between the gene's expression and embryonic stage (ranging from 2-cell to blastocyst) had to be above 0.85 (with an adjusted p-value < 0.01); 3) the gene needed to exhibit an absolute log2 fold change greater than 1 between the 8-cell and morula stages, as well as between morula and blastocyst stages, in the same direction as the overall correlation. Pseudotime trajectories for embryos were calculated using Slingshot (207) (v.1.6.1). Dimensionality reduction was performed via PCA, utilizing the full covariance matrix rather than clustering. Principal curves were fitted using the Slingshot function.

Total RNA-seq analysis

Chapter 1

Sequencing raw alignment files were demultiplexed by the DKFZ Genomics and Proteomics Core Facility. The sequencing reads were aligned to the mm10 genome using the Cogent NGS Analysis Pipeline (CogentAP, Takara Bio, v.1.5.1). Gene-barcode count matrices were analysed using R (v.4.0.0) and Seurat (v.4.0.3). Samples were retained if more than 5000 genes were detected and if ribosomal and mitochondrial reads were below 18% and 2.5%, respectively. Cell-type-specific marker gene expression was verified to rule out granulosa cell contamination.

Raw counts from all replicates were merged and corrected using the SCTransform function from Seurat. Genes of interest linked to maternal transcriptome remodelling were identified based on existing literature. Log2 fold changes were calculated for each gene in each sample using the average expression of the gene in the opposite ovulation group (natural ovulation as the reference for superovulated samples and vice versa).

For transcriptome-wide analysis, a dataset from Lee et al. (165) was used. Genes were considered impacted by one of the three processes if they met specific criteria for differences between the GV and MII groups: 1) a geometric mean tail length change exceeding 20 nucleotides with an adjusted p-value under 0.001, representing at least 70% of the maximum tail length, and 2) at least 50 reads in the stage with the highest expression (GV if degraded, MII if re-polyadenylated). Additionally, for deadenylated groups, the natural log ratio of read counts between MII and GV had to be positive or below -2 for the "stable" and "degraded" groups, respectively, based on Lee et al.'s classification.

Human granulosa cell data analysis

Chapter 1

Sequencing alignment files were demultiplexed by the DKFZ Genomics and Proteomics Core Facility. Reads were aligned to the 1KGRef_PhiX genome (hs37d5 with an added PhiX contig) using STAR (v.2.5.3a) and the DKFZ RNAseqWorkflow pipeline (v.1.3.0). Gene-barcode count matrices were analyzed in R (v.4.0.0), with samples filtered by mitochondrial read percentage (below 18%, 80th percentile) to ensure quality. Differential gene expression (DGE) analysis was performed using DESeq2 (v.1.28.1) with age group as a predictor (<31 or >38 years). Gene set enrichment was assessed using fgsea (v.1.14.0) with Hallmarks, Reactome, and GO Biological Process pathways. An additional analysis, excluding top differentially expressed genes between cumulus and mural granulosa cells (52), showed minimal impact on the results. Please note the human granulosa cell samples in Chapter 4 have not yet been analysed.

Spatial transcriptomics analysis

Chapter 3

Raw sequencing reads were processed with spaceranger (v1.3.1, 10X Genomics). To estimate gene expression for each cell type in every spot, DestVI (v1.0.3) along with the corresponding tissue single-cell reference was used. Cell proportions per spot were thresholded using DestVI utilities (v0.1) and manually adjusted based on tissue architecture inferred from histology images.

To explore spatial niches of inflamed stromal cells in young uteri and ovaries, a mixed linear generalized model with a random intercept was applied, using inflammation activity scores (via AUCell) as the dependent variable. The model was fitted using the lme4 package (v1.1-27.1), with variance explained measured by marginal R-squared values from the MuMIn package (v1.47.5).

To assess clustering of highly inflamed stromal cells, cluster coefficients were calculated. Stromal cell spots were defined based on a minimum estimated proportion of stromal cells and their gene expression imputed via DestVI. Inflammation scores were binarized, and spatial graphs of stromal cell spots with high inflammation were constructed, with global cluster coefficients calculated using iGraph (v1.5.0).

To extend initial scRNA-seq findings, cell-to-cell communication analysis based on spatial data was performed. Ligand-receptor interaction scores were calculated for each neighbourhood, considering the diffusion of ligand molecules across adjacent spots. Scores were computed by multiplying ligand expression by receptor expression in fibroblasts, weighted by the proportion of signal captured by each cell type within the neighbourhood.

Data and code availability

Sequencing data is publicly available in BioStudies Arrayexpress database for following datasets.

Chapter 1:

Oocyte and granulosa cell pairs using SMART-seq2: E-MTAB-13479;

Embryos and paired granulosa cells using SMART-seq2: E-MTAB-13480;

Oocyte total RNA sequencing (Chapter 1): E-MTAB-13474;

Human granulosa cell bulk RNA sequencing (Chapter 1): E-MTAB-13496.

Chapter 3:

Mouse FRT tissues across estrous cycle and ageing using 10x scRNA-seq : E-MTAB-11491, E-MTAB-12889;

Young and old mouse ovaries and uterus using 10x Visium: E-MTAB-12105.

Code used in this thesis is publicly available in these Github repositories:

https://github.com/goncalves-lab/follicle_project (Chapter 1);

https://github.com/goncalves-lab/estrus_cycle_study (Chapter 3).

Reference list

1. Kutschera U, Levit GS, Hossfeld U. Ernst Haeckel (1834–1919): The German Darwin and his impact on modern biology. Theory in Biosciences. 2019.
2. Raudenska M, Vicar T, Gumulec J, Masarik M. Johann Gregor Mendel: the victory of statistics over human imagination. Vol. 31, European Journal of Human Genetics. 2023.
3. Hopwood N. Inclusion and exclusion in the history of developmental biology. Dev. 2019;146(7).
4. Lohmann I. The birth of evo-devo. Vol. 24, Nature Reviews Molecular Cell Biology. 2023.
5. Tickle C, Urrutia AO. Perspectives on the history of evo-devo and the contemporary research landscape in the genomics era. Philos Trans R Soc B Biol Sci. 2017;372(1713).
6. Steptoe PC, Edwards RG. Birth after the reimplantation of a human embryo. Vol. 2, Lancet. 1978.
7. Fishel S, Hadjantonakis AK, Plusa B, Rienzi L, Yamanaka Y, Suwińska A, et al. Breakthroughs and challenges of modern developmental biology and reproductive medicine. Int J Dev Biol. 2019;63(3–5).
8. St Johnston D. The Renaissance of Developmental Biology. PLoS Biol. 2015;13(5).
9. Dai X, Shen L. Advances and Trends in Omics Technology Development. Vol. 9, Frontiers in Medicine. 2022.
10. Snead AA, Clark RD. The Biological Hierarchy, Time, and Temporal 'Omics in Evolutionary Biology: A Perspective. Vol. 62, Integrative and Comparative Biology. 2022.
11. Bressan D, Battistoni G, Hannon GJ. The dawn of spatial omics. Vol. 381, Science. 2023.
12. Gao F, Huang K, Xing Y. Artificial Intelligence in Omics. Vol. 20, Genomics, Proteomics and Bioinformatics. 2022.
13. He X, Liu X, Zuo F, Shi H, Jing J. Artificial intelligence-based multi-omics analysis fuels cancer precision medicine. Vol. 88, Seminars in Cancer Biology. 2023.
14. Ball P. Most advanced synthetic human embryos yet spark controversy. Vol. 618, Nature. 2023.
15. Smith K. Women's health research lacks funding — these charts show how. Nature. 2023;617(7959).
16. Waterston RH, Lindblad-Toh K, Birney E, Rogers J, Abril JF, Agarwal P, et al. Initial sequencing and comparative analysis of the mouse genome. Nature. 2002;420(6915).
17. Breschi A, Gingeras TR, Guigó R. Comparative transcriptomics in human and mouse. Vol. 18, Nature Reviews Genetics. 2017.
18. Keane TM, Goodstadt L, Danecek P, White MA, Wong K, Yalcin B, et al. Mouse genomic variation and its effect on phenotypes and gene regulation. Nature. 2011;
19. Mattioli K, Oliveros W, Gerhardinger C, Andergassen D, Maass PG, Rinn JL, et al. Cis and trans effects differentially contribute to the evolution of promoters and enhancers. Genome Biol. 2020;21(1).
20. Goncalves A, Leigh-Brown S, Thybert D, Stefflova K, Turro E, Flicek P, et al. Extensive compensatory cis-trans regulation in the evolution of mouse gene expression. Genome Res. 2012;22(12).
21. Orr HA, Masly JP, Presgraves DC. Speciation genes. Vol. 14, Current Opinion in Genetics and Development. 2004.
22. Johnson NA. Hybrid incompatibility genes: Remnants of a genomic battlefield? Vol. 26, Trends

in Genetics. 2010.

23. Eckardt S, McLaughlin KJ, Willenbring H. Mouse chimeras as a system to investigate development, cell and tissue function, disease mechanisms and organ regeneration. Vol. 10, Cell Cycle. 2011.

24. Gert KRB, Panser K, Surm J, Steinmetz BS, Schleiffer A, Jovine L, et al. Divergent molecular signatures in fish Bouncer proteins define cross-fertilization boundaries. Nat Commun. 2023;14(1).

25. El Yakoubi W, Akera T. Condensin dysfunction is a reproductive isolating barrier in mice. Nature. 2023;623(7986).

26. Wolfner MF. The gifts that keep on giving: Physiological functions and evolutionary dynamics of male seminal proteins in Drosophila. In: Heredity. 2002.

27. McDonough-Goldstein CE, Borziak K, Pitnick S, Dorus S. Drosophila female reproductive tract gene expression reveals coordinated mating responses and rapidly evolving tissue-specific genes. G3 Genes, Genomes, Genet. 2021;11(3).

28. Wolfner MF, Suarez SS, Dorus S. Suspension of hostility: Positive interactions between spermatozoa and female reproductive tracts. Vol. 11, Andrology. 2023.

29. Bedford JM. Sperm capacitation and fertilization in mammals. Biol Reprod Suppl. 1970;2.

30. Sebkova N, Cerna M, Ded L, Peknicova J, Dvorakova-Hortova K. The slower the better: How sperm capacitation and acrosome reaction is modified in the presence of estrogens. Reproduction. 2012;143(3).

31. Byers SL, Wiles M V., Dunn SL, Taft RA. Mouse estrous cycle identification tool and images. PLoS One. 2012;

32. Bertolin K, Murphy BD. Reproductive Tract Changes During the Mouse Estrous Cycle. In: The Guide to Investigation of Mouse Pregnancy. 2014.

33. Snell GD. Biology of the Laboratory Mouse. 1941;1(1):55–88. Available from: http://repositorio.unan.edu.ni/2986/1/5624.pdf

34. Coss D. Regulation of reproduction via tight control of gonadotropin hormone levels. Mol Cell Endocrinol. 2018;

35. Hoffmann HM. Determination of Reproductive Competence by Confirming Pubertal Onset and Performing a Fertility Assay in Mice and Rats. J Vis Exp. 2018;(140).

36. Yaw AM, Duong T V., Nguyen D, Hoffmann HM. Circadian rhythms in the mouse reproductive axis during the estrous cycle and pregnancy. J Neurosci Res. 2021;99(1).

37. Odom DT, Dowell RD, Jacobsen ES, Gordon W, Danford TW, MacIsaac KD, et al. Tissue-specific transcriptional regulation has diverged significantly between human and mouse. Nat Genet. 2007;39(6).

38. Cunha GR, Sinclair A, Ricke WA, Robboy SJ, Cao M, Baskin LS. Reproductive tract biology: Of mice and men. Vol. 110, Differentiation. 2019.

39. Dutta S, Sengupta P. Men and mice: Relating their ages. Vol. 152, Life Sciences. 2016.

40. Winkler I, Goncalves A. Do mammals have menopause? Cell. 2023 Oct;186(22):4729–33.

41. Wilhelm D, Palmer S, Koopman P. Sex determination and gonadal development in mammals. Vol. 87, Physiological Reviews. 2007.

42. Fukuda K, Muraoka M, Kato Y, Saga Y. Decoding the transcriptome of pre-granulosa cells during the formation of primordial follicles in the mouse. Biol Reprod. 2021;105(1).

43. Garcia-Alonso L, Lorenzi V, Mazzeo CI, Alves-Lopes JP, Roberts K, Sancho-Serra C, et al. Single-cell roadmap of human gonadal development. Nature. 2022;607(7919).

44. Niu W, Spradling AC. Two distinct pathways of pregranulosa cell differentiation support follicle formation in the mouse ovary. Proc Natl Acad Sci U S A. 2020;117(33).

45. Saitou M, Yamaji M. Primordial germ cells in mice. Cold Spring Harb Perspect Biol. 2012;4(11).

46. Soygur B, Laird DJ. Ovary Development: Insights From a Three-Dimensional Imaging Revolution. Vol. 9, Frontiers in Cell and Developmental Biology. 2021.

47. Liu C, Peng J, Matzuk MM, Yao HHC. Lineage specification of ovarian theca cells requires multicellular interactions via oocyte and granulosa cells. Nat Commun. 2015;6.

48. Nef S, Parada LF. Hormones in male sexual development. Vol. 14, Genes and Development. 2000.

49. Spearow JL. Major genes control hormone-induced ovulation rate in mice. J Reprod Fertil. 1988;

50. Spearow JL, Barkley M. Genetic Control of Hormone-Induced Ovulation Rate in Mice1. Biol Reprod. 1999;

51. Baerwald AR, Adams GP, Pierson RA. Ovarian antral folliculogenesis during the human menstrual cycle: A review. Vol. 18, Human Reproduction Update. 2012.

52. Papler TB, Bokal EV, Maver A, Kopitar AN, Lovrečić L. Transcriptomic analysis and meta-analysis of human granulosa and cumulus cells. PLoS One. 2015;10(8).

53. Luisi S, Florio P, Reis FM, Petraglia F. Inhibins in female and male reproductive physiology: Role in gametogenesis, conception, implantation and early pregnancy. Vol. 11, Human Reproduction Update. 2005.

54. Young JM, McNeilly AS. Theca: The forgotten cell of the ovarian follicle. Reproduction. 2010.

55. Matsuda F, Inoue N, Manabe N, Ohkura S. Follicular growth and atresia in mammalian ovaries: Regulation by survival and death of granulosa cells. Vol. 58, Journal of Reproduction and Development. 2012.

56. Care AS, Diener KR, Jasper MJ, Brown HM, Ingman W V., Robertson SA. Macrophages regulate corpus luteum development during embryo implantation in mice. J Clin Invest. 2013 Aug 1;123(8):3472–87.

57. Stewart CA, Behringer RR. Mouse oviduct development. Results Probl Cell Differ. 2012;55.

58. Wang S, Larina I V. In vivo dynamic 3D imaging of oocytes and embryos in the mouse oviduct. Cell Rep. 2021;36(2).

59. Ford MJ, Harwalkar K, Pacis AS, Maunsell H, Wang YC, Badescu D, et al. Oviduct epithelial cells constitute two developmentally distinct lineages that are spatially separated along the distal-proximal axis. Cell Rep. 2021;36(10).

60. Harwalkar K, Ford MJ, Teng K, Yamanaka N, Yang B, Burtscher I, et al. Anatomical and cellular heterogeneity in the mouse oviduct - Its potential roles in reproduction and preimplantation development. Biol Reprod. 2021;104(6).

61. Lengyel E. Ovarian cancer development and metastasis. Vol. 177, American Journal of Pathology. 2010.

62. Sosa-Stanley JN, Peterson DC. Anatomy, Abdomen and Pelvis, Uterus. StatPearls. 2018.

63. Das A, Mantena SR, Kannan A, Evans DB, Bagchi MK, Bagchi IC. De novo synthesis of estrogen in pregnant uterus is critical for stromal decidualization and angiogenesis. Proc Natl Acad Sci U S A. 2009;106(30).

64. Malik M, Roh M, England SK. Uterine contractions in rodent models and humans. Vol. 231, Acta Physiologica. 2021.

65. Katz DF. Human cervical mucus: Research update. Am J Obstet Gynecol. 1991;165(6).

66. Grover A, Pandey D. Anatomy and physiology of cervix. In: Colposcopy of Female Genital Tract. 2017.

67. Lee SK, Kim CJ, Kim D-J, Kang J. Immune Cells in the Female Reproductive Tract. Immune Netw. 2015;15(1).

68. Fortune JE. The early stages of follicular development: Activation of primordial follicles and growth of preantral follicles. Anim Reprod Sci. 2003;78(3–4).

69. Chen Y, Yang W, Shi X, Zhang C, Song G, Huang D. The Factors and Pathways Regulating the Activation of Mammalian Primordial Follicles in vivo. Vol. 8, Frontiers in Cell and Developmental Biology. 2020.

70. Richard S, Anderson NJ, Zhou Y, Pankhurst MW. Mouse primary follicles experience slow growth rates after activation and progressive increases that influence the duration of the primary follicle phase†. Biol Reprod. 2023;109(5).

71. Morton AJ, Candelaria JI, McDonnell SP, Zgodzay DP, Denicol AC. Review: Roles of follicle-stimulating hormone in preantral folliculogenesis of domestic animals: what can we learn from model species and where do we go from here? Vol. 17, Animal. 2023.

72. Sánchez F, Adriaenssens T, Romero S, Smitz J. Different follicle-stimulating hormone exposure regimens during antral follicle growth alter gene expression in the cumulus-oocyte complex in mice. Biol Reprod. 2010;83(4).

73. Kawashima I, Kawamura K. Regulation of follicle growth through hormonal factors and mechanical cues mediated by Hippo signaling pathway. Vol. 64, Systems Biology in Reproductive Medicine. 2018.

74. Zuccotti M, Ponce RH, Boiani M, Guizzardi S, Govoni P, Scandroglio R, et al. The analysis of chromatin organisation allows selection of mouse antral oocytes competent for development to blastocyst. Zygote. 2002;10(1).

75. Bouniol-Baly C, Hamraoui L, Guibert J, Beaujean N, Szöllösi MS, Debey P. Differential transcriptional activity associated with chromatin configuration in fully grown mouse germinal vesicle oocytes. Biol Reprod. 1999;60(3).

76. Bennabi I, Terret ME, Verlhac MH. Meiotic spindle assembly and chromosome segregation in oocytes. J Cell Biol. 2016;215(5).

77. McAinsh AD, Kops GJPL. Principles and dynamics of spindle assembly checkpoint signalling. Vol. 24, Nature Reviews Molecular Cell Biology. 2023.

78. Reyes JM, Ross PJ. Cytoplasmic polyadenylation in mammalian oocyte maturation. Vol. 7, Wiley Interdisciplinary Reviews: RNA. 2016.

79. Su YQ, Sugiura K, Woo Y, Wigglesworth K, Kamdar S, Affourtit J, et al. Selective degradation of transcripts during meiotic maturation of mouse oocytes. Dev Biol. 2007;

80. Yang CR, Rajkovic G, Daldello EM, Luong XG, Chen J, Conti M. The RNA-binding protein DAZL functions as repressor and activator of mRNA translation during oocyte maturation. Nat Commun. 2020;11(1).

81. Martins JPS, Liu X, Oke A, Arora R, Franciosi F, Viville S, et al. DAZL and CPEB1 regulate mRNA translation synergistically during oocyte maturation. J Cell Sci. 2016;129(6).

82. Sha QQ, Dai XX, Dang Y, Tang F, Liu J, Zhang YL, et al. A MAPK cascade couples maternal mRNA translation and degradation to meiotic cell cycle progression in mouse oocytes. Dev. 2017;144(3).

83. Yu C, Ji SY, Sha QQ, Dang Y, Zhou JJ, Zhang YL, et al. BTG4 is a meiotic cell cycle-coupled maternal-zygotic-transition licensing factor in oocytes. Nat Struct Mol Biol. 2016;23(5).

84. Sha Q, Yu J, Guo J, Dai X, Jiang J, Zhang Y, et al. CNOT 6L couples the selective degradation of maternal transcripts to meiotic cell cycle progression in mouse oocyte . EMBO J.

2018;37(24).

85. Dai XX, Jiang ZY, Wu YW, Sha QQ, Liu Y, Ding JY, et al. CNOT6/6L-mediated mRNA degradation in ovarian granulosa cells is a key mechanism of gonadotropin-triggered follicle development. Cell Rep. 2021;37(7).

86. Robker RL, Hennebold JD, Russell DL. Coordination of ovulation and oocyte maturation: A good egg at the right time. Vol. 159, Endocrinology. 2018.

87. Su YQ, Sugiura K, Eppig JJ. Mouse oocyte control of granulosa cell development and function: Paracrine regulation of cumulus cell metabolism. Vol. 27, Seminars in Reproductive Medicine. 2009.

88. Gilula NB, Epstein ML, Beers WH. Cell-to-cell communication and ovulation. A study of the cumulus-oocyte complex. J Cell Biol [Internet]. 1978 Jul 1;78(1):58–75. Available from: https://doi.org/10.1083/jcb.78.1.58

89. Crozet F, Letort G, Bulteau R, Silva C Da, Eichmuller A, Tortorelli AF, et al. Filopodia-like protrusions of adjacent somatic cells shape the developmental potential of oocytes. Life Sci Alliance. 2023;6(6).

90. Wu X, Matzuk MM. GDF-9 and BMP-15: Oocyte organizers. Vol. 3, Reviews in Endocrine and Metabolic Disorders. 2002.

91. Driancourt MA, Reynaud K, Cortvrindt R, Smitz J. Roles of KIT and KIT LIGAND in ovarian function. Vol. 5, Reviews of Reproduction. 2000.

92. Thomas FH, Vanderhyden BC. Oocyte-granulosa cell interactions during mouse follicular development: Regulation of kit ligand expression and its role in oocyte growth. Vol. 4, Reproductive Biology and Endocrinology. 2006.

93. Thomas FH, Ethier JF, Shimasaki S, Vanderhyden BC. Follicle-stimulating hormone regulates oocyte growth by modulation of expression of oocyte and granulosa cell factors. Endocrinology. 2005;146(2).

94. Joyce IM, Clark AT, Pendola FL, Eppig JJ. Comparison of recombinant growth differentiation factor-9 and oocyte regulation of KIT ligand messenger ribonucleic acid expression in mouse ovarian follicles. Biol Reprod. 2000;63(6).

95. Wigglesworth K, Lee KB, O'Brien MJ, Peng J, Matzuk MM, Eppig JJ. Bidirectional communication between oocytes and ovarian follicular somatic cells is required for meiotic arrest of mammalian oocytes. Proc Natl Acad Sci U S A. 2013;

96. Zhang M, Su YQ, Sugiura K, Wigglesworth K, Xia G, Eppig JJ. Estradiol promotes and maintains cumulus cell expression of natriuretic peptide receptor 2 (NPR2) and meiotic arrest in mouse oocytes in vitro. Endocrinology. 2011;152(11).

97. Oliver R, Basit H. Embryology, Fertilization. StatPearls. 2020.

98. Svoboda P, Franke V, Schultz RM. Sculpting the Transcriptome During the Oocyte-to-Embryo Transition in Mouse. In: Current Topics in Developmental Biology. 2015.

99. Vastenhouw NL, Cao WX, Lipshitz HD. The maternal-to-zygotic transition revisited. Vol. 146, Development (Cambridge, England). 2019.

100. Goodenough U, Heitman J. Origins of eukaryotic sexual reproduction. Cold Spring Harb Perspect Biol. 2014;6(3).

101. Wilkins AS, Holliday R. The evolution of meiosis from mitosis. Vol. 181, Genetics. 2009.

102. Turner LM, Hoekstra HE. Causes and consequences of the evolution of reproductive proteins. Vol. 52, International Journal of Developmental Biology. 2008.

103. Murat F, Mbengue N, Winge SB, Trefzer T, Leushkin E, Sepp M, et al. The molecular evolution of spermatogenesis across mammals. Nature. 2023;613(7943).

104. Trost N, Mbengue N, Kaessmann H. The molecular evolution of mammalian spermatogenesis. Cells Dev. 2023;175.

105. Larson EL, Vanderpool D, Keeble S, Zhou M, Sarver BAJ, Smith AD, et al. Contrasting levels of molecular evolution on the mouse X chromosome. Genetics. 2016;203(4).

106. López-Otín C, Blasco MA, Partridge L, Serrano M, Kroemer G. The hallmarks of aging. Cell. 2013.

107. Wallace WHB, Kelsey TW. Human ovarian reserve from conception to the menopause. PLoS One. 2010;

108. Park SU, Walsh L, Berkowitz KM. Mechanisms of ovarian aging. Vol. 162, Reproduction. 2021.

109. Parkening TA, Collins TJ, Smith ER. Plasma and pituitary concentrations of LH, FSH, and Prolactin in aging C57BL/6 mice at various times of the estrous cycle. Neurobiol Aging. 1982;3(1).

110. Liu Y, Kong F, Wang W, Xin J, Zhang S, Chen J, et al. Low estrogen level in aged mice leads to abnormal oogenesis affecting the quality of surrounded nucleolus-type immature oocytes. Reprod Fertil Dev. 2022;34(15).

111. Shirasuna K, Iwata H. Effect of aging on the female reproductive function. Contracept Reprod Med. 2017;2(1).

112. Zhou F, Shi LB, Zhang SY. Ovarian fibrosis: A phenomenon of concern. Vol. 130, Chinese Medical Journal. 2017.

113. Landry DA, Vaishnav HT, Vanderhyden BC. The significance of ovarian fibrosis. Oncotarget. 2020;11(47).

114. Sköld C, Corvigno S, Dahlstrand H, Enblad G, Mezheyeuski A, Sundström-Poromaa I, et al. Association between parity and pregnancy-associated tumor features in high-grade serous ovarian cancer. Cancer Causes Control. 2024;

115. Chatzidaki EE, Powell S, Dequeker BJH, Gassler J, Silva MCC, Tachibana K. Ovulation suppression protects against chromosomal abnormalities in mouse eggs at advanced maternal age. Curr Biol. 2021;31(18).

116. Komatsu M, Fujita H. Electron-microscopic studies on the development and aging of the oviduct epithelium of mice. Anat Embryol (Berl). 1978;152(3).

117. Tinelli A, Andjić M, Morciano A, Pecorella G, Malvasi A, D'Amato A, et al. Uterine Aging and Reproduction: Dealing with a Puzzle Biologic Topic. Vol. 25, International Journal of Molecular Sciences. 2024.

118. Woods L, Perez-Garcia V, Kieckbusch J, Wang X, Demayo F, Colucci F, et al. Decidualisation and placentation defects are a major cause of age-related reproductive decline. Nat Commun. 2017;8(1).

119. Siegel RL, Miller KD, Jemal A. Cancer statistics, 2020. CA Cancer J Clin. 2020;70(1).

120. Hansen KR, Knowlton NS, Thyer AC, Charleston JS, Soules MR, Klein NA. A new model of reproductive aging: The decline in ovarian non-growing follicle number from birth to menopause. Hum Reprod. 2008;

121. Navot D, Bergh RA, Williams MA, Garrisi GJ, Guzman I, Sandler B, et al. Poor oocyte quality rather than implantation failure as a cause of age-related decline in female fertility. Lancet. 1991;337(8754).

122. Grøndahl ML, Yding Andersen C, Bogstad J, Nielsen FC, Meinertz H, Borup R. Gene expression profiles of single human mature oocytes in relation to age. Hum Reprod. 2010;25(4).

123. Llonch S, Barragán M, Nieto P, Mallol A, Elosua-Bayes M, Lorden P, et al. Single human oocyte

transcriptome analysis reveals distinct maturation stage-dependent pathways impacted by age. Aging Cell. 2021;

124. Steiner AZ, Pritchard D, Stanczyk FZ, Kesner JS, Meadows JW, Herring AH, et al. Association between biomarkers of ovarian reserve and infertility among older women of reproductive age. JAMA - J Am Med Assoc. 2017;318(14).

125. Merriman JA, Jennings PC, Mclaughlin EA, Jones KT. Effect of aging on superovulation efficiency, aneuploidy rates, and sister chromatid cohesion in mice aged up to 15 months. Biol Reprod. 2012;86(2).

126. Pan H, Ma P, Zhu W, Schultz RM. Age-associated increase in aneuploidy and changes in gene expression in mouse eggs. Dev Biol. 2008;

127. Hamatani T, Falco G, Carter MG, Akutsu H, Stagg CA, Sharov AA, et al. Age-associated alteration of gene expression patterns in mouse oocytes. Hum Mol Genet. 2004;

128. Khurana P, Smyth NR, Sheth B, Velazquez MA, Eckert JJ, Fleming TP. Advanced maternal age perturbs mouse embryo development and alters the phenotype of derived embryonic stem cells. J Dev Orig Health Dis. 2022 Jun 1;13(3):395–405.

129. Lane S, Kauppi L. Meiotic spindle assembly checkpoint and aneuploidy in males versus females. Vol. 76, Cellular and Molecular Life Sciences. 2019.

130. Blengini CS, Nguyen AL, Aboelenain M, Schindler K. Age-dependent integrity of the meiotic spindle assembly checkpoint in females requires Aurora kinase B. Aging Cell. 2021;20(11).

131. Bennabi I, Crozet F, Nikalayevich E, Chaigne A, Letort G, Manil-Ségalen M, et al. Artificially decreasing cortical tension generates aneuploidy in mouse oocytes. Nat Commun. 2020;11(1).

132. Nikalayevich E, Letort G, de Labbey G, Todisco E, Shihabi A, Turlier H, et al. Aberrant cortex contractions impact mammalian oocyte quality. Dev Cell. 2024;59(7).

133. Mihajlović AI, Haverfield J, FitzHarris G. Distinct classes of lagging chromosome underpin age-related oocyte aneuploidy in mouse. Dev Cell. 2021;56(16).

134. Pasquariello R, Ermisch AF, Silva E, McCormick S, Logsdon D, Barfield JP, et al. Alterations in oocyte mitochondrial number and function are related to spindle defects and occur with maternal aging in mice and humans. Biol Reprod. 2019;100(4).

135. Cox RT, Poulton J, Williams SA. The role of mitophagy during oocyte aging in human, mouse, and Drosophila: implications for oocyte quality and mitochondrial disease. Vol. 2, Reproduction and Fertility. 2021.

136. Zhang Y, Bai J, Cui Z, Li Y, Gao Q, Miao Y, et al. Polyamine metabolite spermidine rejuvenates oocyte quality by enhancing mitophagy during female reproductive aging. Nat Aging. 2023;3(11).

137. Vander Borght M, Wyns C. Fertility and infertility: Definition and epidemiology. Vol. 62, Clinical Biochemistry. 2018.

138. Niederberger C, Pellicer A, Cohen J, Gardner DK, Palermo GD, O'Neill CL, et al. Forty years of IVF. Vol. 110, Fertility and Sterility. 2018.

139. Wyns C, De Geyter C, Calhaz-Jorge C, Kupka MS, Motrenko T, Smeenk J, et al. ART in Europe, 2017: Results generated from European registries by ESHRE. Hum Reprod Open. 2021;2021(3).

140. Sunderam S, Kissin DM, Zhang Y, Jewett A, Boulet SL, Warner L, et al. Assisted Reproductive Technology Surveillance — United States, 2018. MMWR Surveill Summ. 2022;71(4).

141. Malizia BA, Hacker MR, Penzias AS. Cumulative Live-Birth Rates after In Vitro Fertilization. N Engl J Med. 2009;360(3).

142. Baker VL, Brown MB, Luke B, Smith GW, Ireland JJ. Gonadotropin dose is negatively

correlated with live birth rate: Analysis of more than 650,000 assisted reproductive technology cycles. In: Fertility and Sterility. 2015.

143. Kumar P, Sait SF, Sharma A, Kumar M. Ovarian hyperstimulation syndrome. Vol. 4, Journal of Human Reproductive Sciences. 2011.

144. Alper MM, Fauser BC. Ovarian stimulation protocols for IVF: is more better than less? Vol. 34, Reproductive BioMedicine Online. 2017.

145. Pacchiarotti A, Selman H, Valeri C, Napoletano S, Sbracia M, Antonini G, et al. Ovarian Stimulation Protocol in IVF: An Up-to-Date Review of the Literature. Curr Pharm Biotechnol. 2016;17(4).

146. Luo C, Zuñiga J, Edison E, Palla S, Dong W, Parker-Thornburg J. Superovulation strategies for 6 commonly used mouse strains. J Am Assoc Lab Anim Sci. 2011;

147. Gardner DK, Balaban B. Assessment of human embryo development using morphological criteria in an era of time-lapse, algorithms and “OMICS”: Is looking good still important? Vol. 22, Molecular Human Reproduction. 2016.

148. Kakourou G, Mamas T, Vrettou C, Traeger-Synodinos J. An Update on Non-invasive Approaches for Genetic Testing of the Preimplantation Embryo. Curr Genomics. 2022;23(5).

149. Theilgaard Lassen J, Fly Kragh M, Rimestad J, Nygård Johansen M, Berntsen J. Development and validation of deep learning based embryo selection across multiple days of transfer. Sci Rep. 2023;13(1).

150. Fluks M, Collier R, Walewska A, Bruce AW, Ajduk A. How great thou ART: biomechanical properties of oocytes and embryos as indicators of quality in assisted reproductive technologies. Vol. 12, Frontiers in Cell and Developmental Biology. 2024.

151. Wyse BA, Fuchs Weizman N, Kadish S, Balakier H, Sangaralingam M, Librach CL. Transcriptomics of cumulus cells – a window into oocyte maturation in humans. J Ovarian Res [Internet]. 2020;13(1):93. Available from: https://doi.org/10.1186/s13048-020-00696-7

152. Uyar A, Torrealday S, Seli E. Cumulus and granulosa cell markers of oocyte and embryo quality. In: Fertility and Sterility. 2013.

153. Scarica C. Improving oocyte and embryo competence assessment through granulosa cells transcriptome analysis. Curr Trends Clin Embriol. 2016;3(1):12.

154. Smith ADAC, Tilling K, Nelson SM, Lawlor DA. Live-birth rate associated with repeat in vitro fertilization treatment cycles. JAMA - J Am Med Assoc. 2015;314(24).

155. Zhang J, Lai Z, Shi L, Tian Y, Luo A, Xu Z, et al. Repeated superovulation increases the risk of osteoporosis and cardiovascular diseases by accelerating ovarian aging in mice. Aging (Albany NY). 2018;

156. Park SJ, Kim TS, Kim JM, Chang KT, Lee HS, Lee DS. Repeated superovulation via PMSG/hCG administration induces 2-Cys peroxiredoxins expression and overoxidation in the reproductive tracts of female mice. Mol Cells. 2015;

157. Tang S Bin, Yang LL, Zhang TT, Wang Q, Yin S, Luo SM, et al. Multiple superovulations alter histone modifications in mouse early embryos. Reproduction. 2019;157(6).

158. Rizzuto I, Behrens RF, Smith LA. Risk of ovarian cancer in women treated with ovarian stimulating drugs for infertility. Vol. 2019, Cochrane Database of Systematic Reviews. 2019.

159. Zhang Y, Yan Z, Qin Q, Nisenblat V, Chang HM, Yu Y, et al. Transcriptome Landscape of Human Folliculogenesis Reveals Oocyte and Granulosa Cell Interactions. Mol Cell. 2018;72(6):1021-1034.e4.

160. Assou S, Anahory T, Pantesco V, Le Carrour T, Pellestor F, Klein B, et al. The human cumulus-oocyte complex gene-expression profile. Hum Reprod. 2006;

161. Rajkovic A, Pangas SA, Ballow D, Suzumori N, Matzuk MM. NOBOX deficiency disrupts early folliculogenesis and oocyte-specific gene expression. Science (80-). 2004;305(5687).

162. Bullejos M, Koopman P. Germ cells enter meiosis in a rostro-caudal wave during development of the mouse ovary. Mol Reprod Dev. 2004;68(4).

163. Chen J, Melton C, Suh N, Oh JS, Horner K, Xie F, et al. Genome-wide analysis of translation reveals a critical role for deleted in azoospermia-like (Dazl) at the oocyte-to-zygote transition. Genes Dev. 2011;25(7).

164. Luong XG, Daldello EM, Rajkovic G, Yang CR, Conti M. Genome-wide analysis reveals a switch in the translational program upon oocyte meiotic resumption. Nucleic Acids Res. 2020;48(6).

165. Lee K, Cho K, Morey R, Cook-Andersen H. An extended wave of global mRNA deadenylation sets up a switch in translation regulation across the mammalian oocyte-to-embryo transition. Cell Rep. 2024;43(2).

166. Tora L, Vincent SD. What defines the maternal transcriptome? Vol. 49, Biochemical Society Transactions. 2021.

167. Liu Y, Zhao H, Shao F, Zhang Y, Nie H, Zhang J, et al. Remodeling of maternal mRNA through poly(A) tail orchestrates human oocyte-to-embryo transition. Nat Struct Mol Biol. 2023;30(2).

168. Meng TG, Guo JN, Zhu L, Yin Y, Wang F, Han ZM, et al. NLRP14 Safeguards Calcium Homeostasis via Regulating the K27 Ubiquitination of Nclx in Oocyte-to-Embryo Transition. Adv Sci. 2023;10(27).

169. Jentoft IMA, Bäuerlein FJB, Welp LM, Cooper BH, Petrovic A, So C, et al. Mammalian oocytes store proteins for the early embryo on cytoplasmic lattices. Cell. 2023;186(24).

170. Zhao ZH, Meng TG, Li A, Schatten H, Wang ZB, Sun QY. RNA-Seq transcriptome reveals different molecular responses during human and mouse oocyte maturation and fertilization. BMC Genomics. 2020;21(1).

171. Strączyńska P, Papis K, Morawiec E, Czerwiński M, Gajewski Z, Olejek A, et al. Signaling mechanisms and their regulation during in vivo or in vitro maturation of mammalian oocytes. Vol. 20, Reproductive Biology and Endocrinology. 2022.

172. Winkler I, Tolkachov A, Lammers F, Lacour P, Daugelaite K, Schneider N, et al. The cycling and aging mouse female reproductive tract at single-cell resolution. Cell. 2024;187(4).

173. Kimmel JC, Penland L, Rubinstein ND, Hendrickson DG, Kelley DR, Rosenthal AZ. Murine single-cell RNA-seq reveals cell-identity- And tissue-specific trajectories of aging. Genome Res. 2019;

174. Ntostis P, Iles D, Kokkali G, Vaxevanoglou T, Kanavakis E, Pantou A, et al. The impact of maternal age on gene expression during the GV to MII transition in euploid human oocytes. Hum Reprod. 2022;37(1).

175. Cailliau K, Browaeys-Poly E, Vilain JP. Fibroblast growth factors 1 and 2 differently activate MAP kinase in Xenopus oocytes expressing fibroblast growth factor receptors 1 and 4. Biochim Biophys Acta - Mol Cell Res. 2001;1538(2–3).

176. Guéripel X, Brun V, Gougeon A. Oocyte bone morphogenetic protein 15, but not growth differentiation factor 9, is increased during gonadotropin-induced follicular development in the immature mouse and is associated with cumulus oophorus expansion. Biol Reprod. 2006;75(6).

177. Ma Y, Jin J, Tong X, Yang W, Ren P, Dai Y, et al. ADAMTS1 and HSPG2 mRNA levels in cumulus cells are related to human oocyte quality and controlled ovarian hyperstimulation outcomes. J Assist Reprod Genet. 2020;37(3).

178. Hernandez Gifford JA. The role of WNT signaling in adult ovarian folliculogenesis. Reproduction. 2015;150(4).

179. Xue Z, Huang K, Cai C, Cai L, Jiang CY, Feng Y, et al. Genetic programs in human and mouse

early embryos revealed by single-cell RNA sequencing. Nature. 2013;500(7464).

180. Van Der Auwera I, D'Hooghe T. Superovulation of female mice delays embryonic and fetal development. Hum Reprod. 2001;16(6).

181. Gosden RG, Laing SC, Flurkey K, Finch CE. Graafian follicle growth and replacement in anovulatory ovaries of aging C57BL/6J mice. J Reprod Fertil. 1983;

182. Wang Y, Ock SA, Chian RC. Effect of gonadotrophin stimulation on mouse oocyte quality and subsequent embryonic development in vitro. Reprod Biomed Online. 2006;

183. Ishikawa H, Endo A. Prolongation of duration of ovulation in ageing mice. J Reprod Fertil. 1996;

184. Lee M, Ahn J Il, Lee AR, Ko DW, Yang WS, Lee G, et al. Adverse effect of superovulation treatment on maturation, function and ultrastructural integrity of murine oocytes. Mol Cells. 2017;

185. Swanson WJ, Yang Z, Wolfner MF, Aquadro CF. Positive Darwinian selection drives the evolution of several female reproductive proteins in mammals. Proc Natl Acad Sci U S A. 2001;98(5).

186. Lambert H. Role of sperm-surface glycoproteins in gamete recognition in two mouse species. J Reprod Fertil. 1984;70(1).

187. Martín-Coello J, González R, Crespo C, Gomendio M, Roldan ERS. Superovulation and in vitro oocyte maturation in three species of mice (Mus musculus, Mus spretus and Mus spicilegus). Theriogenology. 2008;70(6).

188. Davidson S, Coles M, Thomas T, Kollias G, Ludewig B, Turley S, et al. Fibroblasts as immune regulators in infection, inflammation and cancer. Vol. 21, Nature Reviews Immunology. 2021.

189. Finch CE, Mobbs C V., Felicio LS, Nelson JF. Ovarian and steroidal influences on neuroendocrine aging processes in female rodents. Endocr Rev. 1984;5(4).

190. Nelson JF, Felicio LS, Osterburg HH, Finch CE. Altered profiles of estradiol and progesterone associated with prolonged estrous cycles and persistent vaginal cornification in aging C57BL/6J mice. Biol Reprod. 1981;24(4).

191. Dong G, Guo Y, Cao H, Zhou T, Zhou Z, Sha J, et al. Long-term effects of repeated superovulation on ovarian structure and function in rhesus monkeys. Fertil Steril. 2014;102(5).

192. Yan P, Xu J, Zeng Y, Dong G, Cao H, Zheng M, et al. Long-term effects of repeated superovulation on the uterus and mammary gland in rhesus monkeys. J Assist Reprod Genet. 2017;34(4).

193. Xie JK, Wang Q, Zhang TT, Yin S, Zhang CL, Ge ZJ. Repeated superovulation may affect mitochondrial functions of cumulus cells in mice. Sci Rep. 2016;6.

194. Kalthur G, Salian SR, Nair R, Mathew J, Adiga SK, Kalthur SG, et al. Distribution pattern of cytoplasmic organelles, spindle integrity, oxidative stress, octamer-binding transcription factor 4 (Oct4) expression and developmental potential of oocytes following multiple superovulation. Reprod Fertil Dev. 2016;28(12).

195. Pangas SA, Li X, Robertson EJ, Matzuk MM. Premature luteinization and cumulus cell defects in ovarian-specific Smad4 knockout mice. Mol Endocrinol. 2006;

196. Zhang Y, Yan Z, Qin Q, Nisenblat V, Chang HM, Yu Y, et al. Transcriptome Landscape of Human Folliculogenesis Reveals Oocyte and Granulosa Cell Interactions. Mol Cell. 2018;

197. Wigger M, Tröder SE, Zevnik B. A simple and economic protocol for efficient in vitro fertilization using cryopreserved mouse sperm. PLoS One. 2021;16(10 October).

198. Nakagata N. Cryopreservation of mouse spermatozoa. Mamm Genome. 2000;11(7).

199. Cora MC, Kooistra L, Travlos G. Vaginal Cytology of the Laboratory Rat and Mouse: Review

and Criteria for the Staging of the Estrous Cycle Using Stained Vaginal Smears. Toxicol Pathol. 2015 Aug;43(6):776–93.

200. Rehnitz J, Alcoba DD, Brum IS, Dietrich JE, Youness B, Hinderhofer K, et al. FMR1 expression in human granulosa cells increases with exon 1 CGG repeat length depending on ovarian reserve. Reprod Biol Endocrinol. 2018;16(1).

201. Rehnitz J, Capp E, Messmer B, Nguyen XP, Germeyer A, Freis A, et al. Fmr1 and akt/mtor signaling in human granulosa cells: Functional interaction and impact on ovarian response. J Clin Med. 2021;10(17).

202. Love MI, Huber W, Anders S. Moderated estimation of fold change and dispersion for RNA-seq data with DESeq2. Genome Biol. 2014;

203. Jin S, Guerrero-Juarez CF, Zhang L, Chang I, Ramos R, Kuan CH, et al. Inference and analysis of cell-cell communication using CellChat. Nat Commun. 2021;12(1).

204. Shao X, Liao J, Li C, Lu X, Cheng J, Fan X. CellTalkDB: A manually curated database of ligand-receptor interactions in humans and mice. Brief Bioinform. 2021;22(4).

205. Aibar S, González-Blas CB, Moerman T, Huynh-Thu VA, Imrichova H, Hulselmans G, et al. SCENIC: Single-cell regulatory network inference and clustering. Nat Methods. 2017;

206. Wang K, Phillips CA, Saxton AM, Langston MA. EntropyExplorer: An R package for computing and comparing differential Shannon entropy, differential coefficient of variation and differential expression. BMC Res Notes. 2015;8(1).

207. Street K, Risso D, Fletcher RB, Das D, Ngai J, Yosef N, et al. Slingshot: Cell lineage and pseudotime inference for single-cell transcriptomics. BMC Genomics. 2018;19(1).